UNIVERSITÀ DI PARMA

UNIVERSITA' DEGLI STUDI DI PARMA

PhD in Drugs, Biomolecules and Health Products

XXXI Cycle

Design, synthesis and optimization of inhibitors of enzymes involved in the sulfur assimilation pathway in Gram negative Bacteria

Coordinator of the PhD program:

Prof. Marco Mor

Supervisor:

Prof. Gabriele Costantino

Co-supervisor:

Dr. Marco Pieroni

PhD Candidate:

Joana Rita Pinto de Magalhães

Years: 2015/2018

Publications:

- Annunziato G., Pieroni M., Benoni R., Campanini B., Pertinhez T.A., Pecchini C., Bruno A., Magalhães J., Bettati S., Franko N., Mozzarelli A., Costantino G.; Cyclopropane-1,2-dicarboxylic acids as new tools for the biophysical investigation of O-acetylserine sulfhydrylases by fluorimetric methods and saturation transfer difference (STD) NMR. Journal of enzyme inhibition and medicinal chemistry (2016). (doi: 10.1080/14756366.2016.1218486)

- Magalhães J., Annunziato G., Franko N., Pieroni M., Campanini B., Bruno A., Costantino G.; Integration of Enhanced Sampling Methods with Saturation Transfer Difference Experiments to Identify Protein Druggable Pockets; Journal of Chemical information and Modeling (2018). (doi: 10.1021/acs.jcim.7b00733)

- Magalhães J., Franko N., Annunziato G., Welch M., Dolan S.K., Bruno A., Mozzarelli A., Armao S., Jirgensons A., Pieroni M., Costantino G., Campanini B.; Discovery of novel fragments inhibiting O-acetylserine sulphhydrylase by combining scaffold hopping and ligand–based drug design; Journal of enzyme inhibition and medicinal chemistry (2018). (doi: 10.1080/14756366.2018.1512596)

- Magalhaes J., Franko N., Annunziato G., Pieroni M., Benoni R., Nikitjuka A., Mozzarelli A., Bettati S., karawajczyk A., Jirgensons A., Campanini B., Costantino G.; Refining the Structure−Activity Relationships of 2-Phenylcyclopropane Carboxylic Acids as Inhibitors of O-Acetylserine Sulfhydrylase Isoforms; Journal of enzyme inhibition and medicinal chemistry (2018). (doi: 10.1080/14756366.2018.1518959)

Acknowledgments

I would like to thank Professor Gabriele Costantino for giving me the opportunity to be part of such a challenging project both personally and professionally. This PhD allowed me to experience different cultures and work environments. I haven't only developed my skills as a medicinal chemist, I consider that today I should be able to easily adapt to different environments and ways of work.

I would also like to thank Marco Pieroni for being there for me during the spiral of feelings that this PhD allowed me to experience. The fact that you always had your door open to listen to me and give me advices allowed me to put in perspective the downsides of the work. I want to thank you as well for stimulating my project management skills, even though sometimes I felt it was too much, now I know I am able to take all the necessary actions to make a scientific project move forward.

I want to thank my lab colleagues Laura Pavone and Miriam Girardini. You were great and I am absolute sure I wouldn't have arrived to the end without you. Thank you so much for all the tips, help and even the ability to understand my italian-portuguese! You were not only good lab colleagues, you are also great friends!

I would like to thank my colleague Giannamaria Annunziato as well. In the beginning your help with NMR, contract, lab utilities and all the information I needed was precious. I am also very grateful for the stimulating discussions that we had about the project during these three years.

I want to thank as well my supervisors, Päivi Tammela and Aigars Jirgensons and all my lab colleagues from Latvia and Finland, you were very helpful and

made my stay very pleasant both personally and professionally. I would also like to thank Anna karawajczyk for her help in arranging everything for my stay in Germany and for your help during my actual stay.
After thanking the supervisors, I would also like to thank my fellow ESRs Silvia Stotani, Viviana Gatta and Konstantinos Grammatoglou. Konsta you were great, all the information you gave me when I moved to Latvia allowed me to have such a smooth transition. Viviana you are a great friend and an awesome lab colleague, always ready to help. Silvia, my weekends in Dortmund just wouldn't have been the same without you!

I want to thank as well to all the people that allowed me to develop this research topic: Nina Franko, Vanesa Garrido, Barbara Campanini, Andrea Mozzarelli, Antonio Felici, Sara Flisi, Clotilde Cabassi, Agostino Bruno, Elisa Azzali and Sabrina Tassini you are a part of this work too, and all of this wouldn't have been possible without your active collaboration!

In the end I want to thank to my family, especially my mother for all the support during these three years. All in all, three years isn't a lot of time but unfortunately during these three years we suffer a huge loss and faced quite hard challenges. Living all of this apart from you was particularly tough and I am very grateful for your understanding, unconditional support and motivation every day. Thank you so much for teaching me that if we work hard we will always achieve a result, it may not be what we desired but still it is a piece of the history that assembles the book!

Thank you all!

Abstract

Worldwide emergence of resistant bacteria is endangering the efficacy of antibiotics, which have saved millions of lives and transformed medicine. After years of success in treating bacterial infections, the lack of new drug development in the field poses bacteria once again as life threatening conditions. ESKAPE pathogens (*Enterococcus faecium*, *Staphylococcus aureus*, *Klebsiella pneumoniae*, *Acinetobacter baumannii*, *Pseudomonas aeruginosa* and *Enterobacter* species) and in particular their Gram negative representatives have been causing high morbidity and mortality among critically ill patients and those requiring invasive devices or surgeries.

The lack of new antibacterials and the restless spread of antibacterial resistance represent one of the most challenging public health threats of the XXI century, and make urgent to find new ways to fight bacterial infections.

Reduction of virulence and decrease in the onset of antibiotic resistance have already been associated with mutations on the genes that codify cysteine biosynthetic enzymes. Therefore, in an attempt to reduce bacterial fitness and infectivity, we have explored the approach of shutting-down cysteine biosynthesis in bacteria through inhibition of the enzymes that catalyze the last steps of the biosynthetic pathway: O-Acetylserine sulfhydrylase (OASS) and Serine Acetyltransferase (SAT).

I have taken the cue from 1-(4-methylbenzyl)-2-phenylcyclopropanecarboxylic acid, an previously reported OASS inhibitor, which, despite binding the enzyme at nanomolar concentration, failed to show any antibacterial activity likely due to permeability issues. Thus four different approaches were taken: (i) a medicinal chemistry campaign aiming at increase the permeability of the previously identified hit was started; (ii) a scaffold hopping was performed in order to skip the cyclopropane scaffold and identify a compound able to cross Gram negative cell wall; (iii) explore

the closed conformation of the enzyme through funnel metadynamics and STD NMR to explore tolerability to derivatization and obtain analogues with diverse pharmacokinetic properties; (iv) incorporate in the structure of the nanomolar enzyme binder a siderophore to try to promote uptake trough a trojan-horse strategy.

The aim of our medicinal chemistry campaign was to obtain several derivatives with different pharmacokinetic properties from the parent compound. The design was based on the available literature, being aware that established rules to enhance permeability in Gram negative bacteria have not been defined yet. Even though major changes in the lipophilic character of the inhibitors were performed, a few derivatives were able to mantain the nanomolar binding affinity to the enzyme.

Scaffold hopping approach resulted in the identification of a fragment that offers noticeable space for further chemical optimization and that presents better pharmacological properties than the original hit.

Funnel metadynamics combined with STD NMR allowed identification of a point of derivatization of the hit that presents high tolerability towards lipophilic and hydrophilic groups. This way, expansion of the series towards compounds with very different physicochemical characteristics can be done without impairing the activity of the parent compound.

The result of inclusion of a siderophore in the parent compound is still under investigation.

To identify SAT inhibitors, a virtual screening of an in house and three commercial focused chemical libraries were performed. Concerning the virtual screening of the in house library, a low micromolar enzyme binder was identified but once again permeability emerged as the main cause for the lack of activity in bacteria. On the other hand, the virtual screening of the commercial focused libraries led to the identification of a hit compound

endowed with good in vitro and in cell activity, that is currently object of study to validate its use as antibacterial adjuvant.

List of Abbreviations

WHO: World Health Organization

HTS: High throughput screening

MDR: Multidrug Resistant

MRSA: Methicillin resistant *Staphylococcus aureus*

MIC: Minimal inhibitory concentration

OM: Outer membrane

APS: adenosine 5'-phosphosulfate

PAPS: phosphoadenoside 5'-phosphosulfate

OAS: O-acetylserine

OASS: O-acetylserine sulfhydrylase

StOASS: *S. typhimurium* O-acetylserine sulfhydrylase

SAT: Serine acetyltransferase

NAS: N-acetylserine

PLP: Pyridoxal 5'-phosphate

PBP: penicillin binding protein

PG: peptidoglycan

EcSAT: *E. coli* serine acetyltransferase

LPS: Lipopolysaccharide

StSAT: *S. typhimurium* serine acetyltransferase

DME: dimethoxyethane

DMF: Dimethylformamide

DCM: Dichloromethane

HiSAT: *H. influenzae* serine acetyltransferase

VS: virtual screening

rt: room temperature

HATU: 1-[Bis(dimethylamino)methylene]-1H-1,2,3-triazolo[4,5-b]pyridinium 3-oxid hexafluorophosphate

CDI: 1,1'-Carbonyldiimidazole

RM: reaction mixture

Cpd: compound

eq: equivalent

PAβN: L-Phe-L-Arg-β-naphthalamide

EDGs: electron donor groups

LE: ligand efficiency

FBDD: fragment based drug discovery

Mtb: *Mycobacterium tuberculosis*

List of schemes

List of Figures

List of Tables

Index

1. Introduction

1.1. Antibacterial discovery

Fighting bacterial infections has always been a concern of mankind and whenever antibacterial compounds weren't available, that was done using mercury salts and herbs. The first antibacterial drug discovery program started in the 20th century with the screening of compounds from the dye industry, which allowed the discovery of salvarsan by Paul Ehrlich **(1, Fig. 1)** in 1910. The systematic screening approach employed by Ehrlich was also applied by the pharmaceutical industry, and other so-called "sulfa drugs", like protonsil **(2, Fig. 1)**, were successfully discovered. Nevertheless, antibacterial drug discovery revolution started in 1928 when Sir Alexander Fleming discovered penicillin, **(3, Fig. 1)** from *Penicillium notatum*. Even though several researchers had already observed antibacterial properties of penicillin, it was Fleming's persistence and commitment to get chemists involved in solving issues like purification and stability of penicillin that allowed its purification and testing, in 1940, by Howard Florey and Ernest Chain. The same purification procedures were employed to allow mass production and distribution of penicillin by the year of 1945. [1]–[3] Later on, the identification of the mechanism of action of sulfa drugs as inhibitors of folate biosynthesis pathway paved the way to target screening and lead optimization programs of the pyrimidine class of antibacterials, which resulted in the discovery of trimethoprim **(4, Fig. 1)** at the beginning of the 1960's. [2]

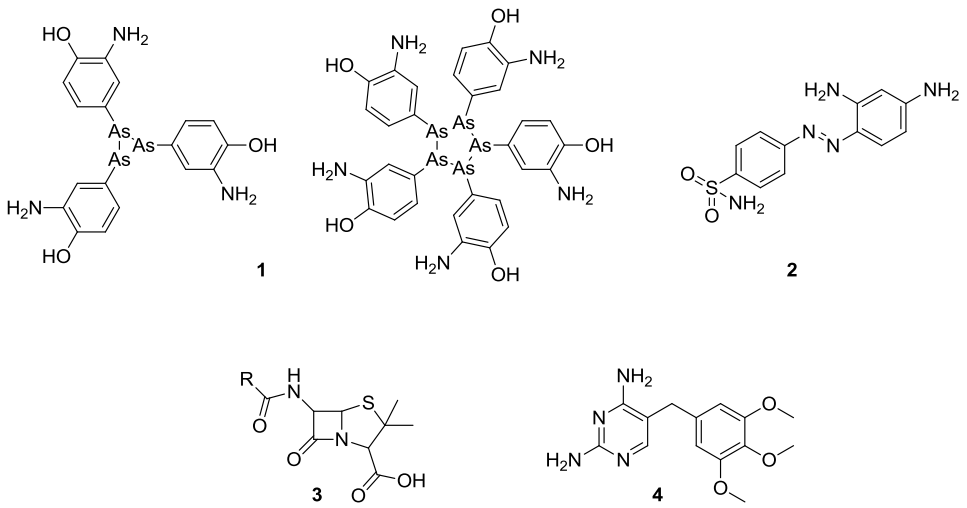

Figure 1 - Chemical structure of Salvarsan **(1)**, Protonsil **(2)**, Penicillins **(3)** and Trimethoprim **(4)**. Salvarsan is a mixture of two arsenium compounds and in the chemical structure of compound **3**, the R group represents the point of diversity of the structure of penicillins.

Between 1950 and 1970, in the so-called "golden-age" of antibacterial drug discovery, the empirical screening of microbial natural products fermentation provided the major part of antibacterial classes currently used for the treatment of infections **(Fig. 2)**. [1], [2]

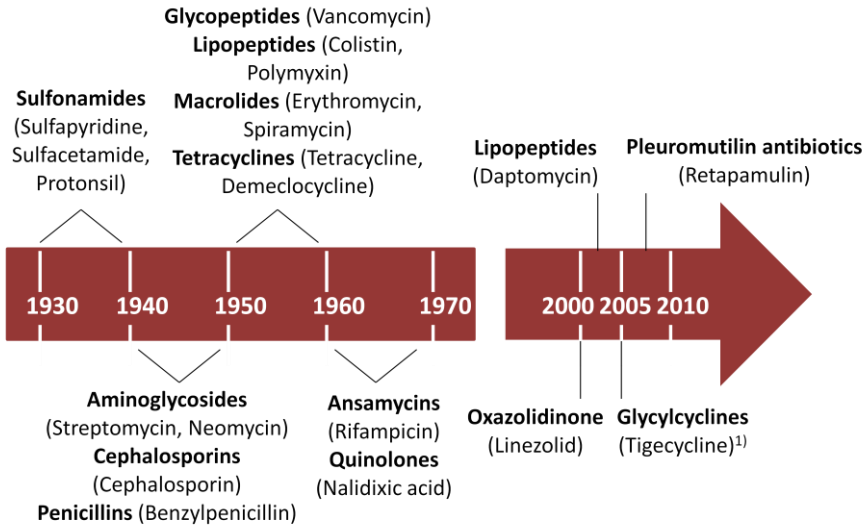

Year dates refers to the market launch of new antibiotic classes. First substances of the respective groups are given in brackets.
1) Tigecycline is an analogue of tetracycline which is able to overcome two mechanism of tetracycline resistance

Figure 2 - Timeline of antibacterial discovery until 2010. Adapted from [4]

Over the last 30 years, antibacterial drug discovery has faced a discovery gap and no new classes of antibacterials were introduced in the market until 2000, when linezolid, belonging to the class of oxazolidinones, was approved.[5], [6]

Currently about 200 conserved proteins in bacteria are essential to their survival, nevertheless, the number of exploited targets is very low. Ribosome, cell wall synthesis, DNA gyrase and DNA topoisomerase are the main targets of the most successful antibacterials **(Fig. 3)**.

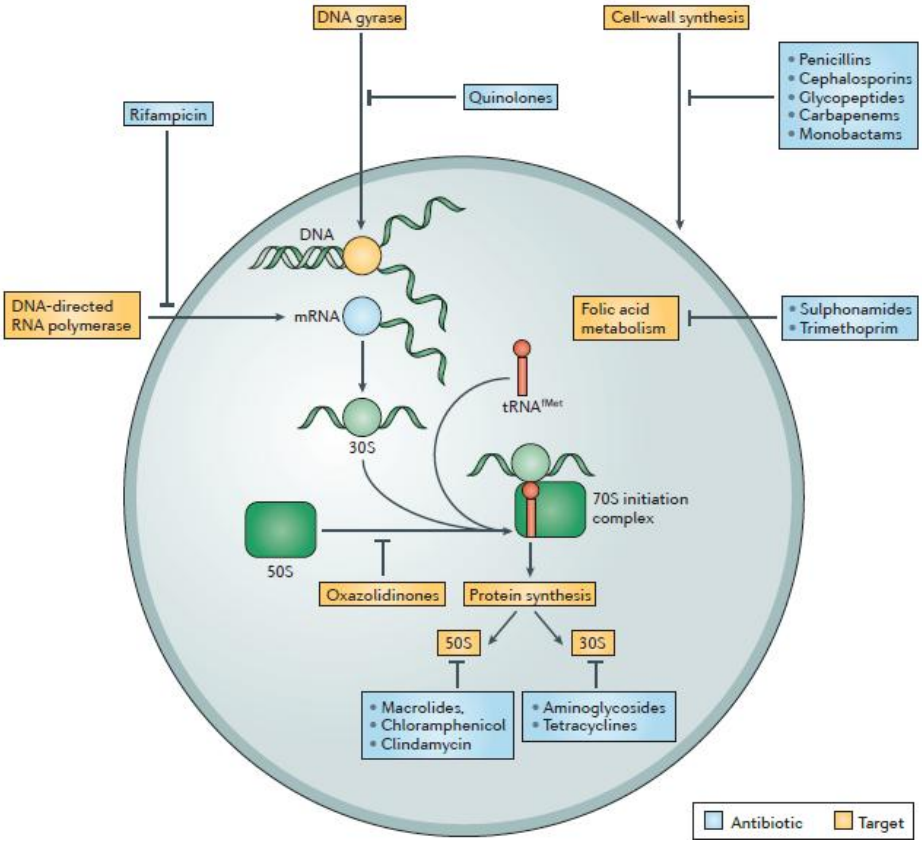

Figure 3 - Targets of the main antibacterial classes curently used. From [6]

1.2. MDR Bacteria

Resistance development in bacteria is a natural phenomenon and the result of billions of years of evolution that occurs even in the absence of human activity. Resistance can be splitted in two groups: Intrinsic resistance or acquired resistance. While intrinsic resistant bacteria comprise all the microorganisms that don't have the target site for the compound, acquired resistance refers to originally susceptible bacteria that acquire a mechanism that allow them to evade the action of the antibacterial. Mechanisms of acquired resistance comprise enzymatic inactivation of the antibacterial,

post-trancriptional or post-translation modification of the antibacterial target, reduced uptake and active efflux of the antibacterial compound **(Fig. 4)**. [7]–[9]

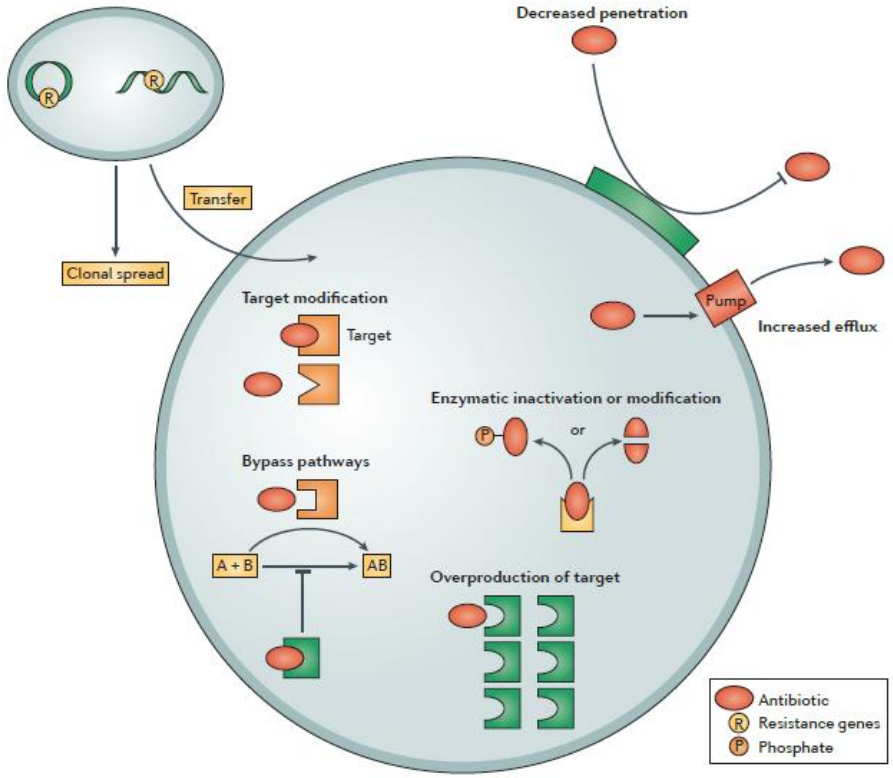

Figure 4 - Mechanisms of antibiotic resistance. From [6]

The major part of antibacterials used in humans are produced by microorganisms in their local environments, this way, all the species that live in the same environment get in contact with these compounds. In the end, environmental selection of resistant organisms occurs and this reservoir of resistance genes can be transferred to human pathogens.

Even though resistance is a natural phenomenon, it can be artificially affected by thoughtless widespread use of antibacterials in human medicine,

animal treatment and horticulture. Genetic manipulation performed in laboratories also increases the evolutionary pressure for the appearance of resistant bacteria. [9] Moreover, the narrow selection of chemical compounds available with a limited range of mechanisms of action contributed greatly to the emergence of resistance. [10]

In the past, antibacterial resistance could be easily managed since the great efforts shed in the identification of several new antibacterials, especially between 1960s and 1980s. [11], [12] However, over the last 30 years a very limited number of antibacterials was introduced in the clinic and resistance has eventually been found in almost all discovered antibiotics. [9], [11], [13], [14] Presently, multidrug resistant (MDR) bacteria cause about 25000 deaths in Europe each year and have an economical burden of about €1.5 billion annually. In USA the scenario is similar with MDR resistant bacteria causing the death of 23000 people among the 2 million infected annually. This way, antibacterial resistance is considered by WHO as one of the three most important public health threats of the 21st century.[9], [15]

1.3. Antibacterial Pipeline

In May 2017, 41 new antibiotics **(Table 1)** that present potential to treat severe bacterial infections, underwent to clinical development in USA. Among the 41 compounds in clinical development only 11 innovative products aim at targeting the most dangerous bacterial pathogens. [16]

Table 1 - Antibacterials pipeline in May 2017. Adapted from [16]

Drug Name	Drug Class	Target	Activity against ESKAPE	Status
Baxdela	Fluoroquinolone	Bacterial type II topoisomerase	Possible	New drug application
Meropenem + Vaborbactam	β-lactam+ β-lactamase inhibitor	PBP; β-lactamase	Yes	New drug application
CRS3123	Diaryldiamine	Methionyl-tRNA synthetase	No	Phase I
ETX2514SUL	β-lactam+ β-lactamase inhibitor	PBP; β-lactamase	Yes	Phase I
GSK-3342830	β-lactam	PBP	Possible	Phase I
KBP-7072	Tetracycline	30S subunit of bacterial ribosome	Possible	Phase I
LCB01-0371	Oxazolidinone	50S subunit of bacterial ribosome	No	Phase I
MCB3837	Oxazolidinone-Quinolone hybrid	50S subunit of bacterial ribosome; Bacterial type	No	Phase I

		II topoisomerase		
MGB-BP-3	Distamycin	DNA minor groove	No	Phase I
Nanubactam	β-lactmase inhibitor	PBP2; β-lactmase	Possible	Phase I
SPR741	Polymyxin	Cell membrane	Possible	Phase I
TD-1607	Glycopeptide-β-lactam hybrid	PG chain elongation; PBP	No	Phase I
TP-271	Tetracyclin	30S subunit of bacterial ribosome	Possible	Phase I
TP-6076	Tetracyclin	30S subunit of bacterial ribosome	Possible	Phase I
WCK 2349	Fluoroquinolone	Bacterial type II topoisomerase	No	Phase I
WCK 771	Fluoroquinolone	Bacterial type II topoisomerase	No	Phase I
Cefepime + Zidebactam	β-lactam + β-lactmase inhibitor	PBP; β-lactmase	Yes	Phase I
Aztreonam + Avibactam	β-lactam + β-lactmase	PBP; β-lactmase	Yes	Phase II

	inhibitor			
Brilacidin	Defensin mimetic	Cell membrane	No	Phase II
CG400549	Benzyl pyridinone	FabI	No	Phase II
Afabicin	Benzofuran naphthyridine	FabI	No	Phase II
Finafloxin	Fluoroquinolone	Bacterial type II topoisomerase	Yes	Phase II
Gepotidacin	Triazaace-naphthlyene	Bacterial type II topoisomerase	No	Phase II
MRX-I	Oxazolidinone	50S subunit of bacterial ribosome	No	Phase II
Nafithromycin	Macrolide	50S subunit of bacterial ribosome	No	Phase II
Nemonoxacin	Quinolone	Bacterial type II topoisomerase	No	Phase II
Murepavadin	Antimicrobial peptide mimetic	LptD	Yes	Phase II
Ramoplanin	Lipodepsi-peptide	Lipid I, II	No	Phase II
Ridinilazole	Bis-benzimidazole	Unknown	No	Phase II

Zoliflodacin	Spiropyrimidene trione	Bacterial type II topoisomerase	No	Phase II
Cadazolid	Oxazolidinone-quinolone hybrid	50S subunit bacterial ribosome	No	Phase III
Cefiderocol	Siderophore-β-lactam	PBP	Yes	Phase III
Eravacycline	Tetracycline	30S subunit bacterial ribosome	Yes	Phase III
Iclaprim	2,4-diamino-pyrimidine	Dihydrofolate reductase	No	Phase III
Imipenem/cilastatin + relebactam	β-lactam + β-lactmase inhibitor	PBP; β-lactmase	Yes	Phase III
Lefamulin	Pleuromutilin	50S subunit bacterial ribosome	No	Phase III
Omadacycline	Tetracycline	30S subunit bacterial ribosome	Yes	Phase III
Plazomicin	Aminoglycoside	30S subunit bacterial ribosome	Yes	Phase III
Solithera	Macrolide	50S sunbunit bacterial ribosome	No	Phase III

Taksta	Fusidane	Elongation factor G	No	Phase III
Zabofloxacin	Fluoroquinolone	Bacterial type II topoisomerase	No	Phase III

Considering the high trial failure rates (generally only one out of five products that enter human testing will be approved for patients), and the statistical data that estimate antimicrobial resistance will be responsible for the death of 10 million people a year by 2050, the need for novel targets and novel approached in this field is particularly high. [16], [17]

1.4. Current treatment for MDR bacteria

Having in mind that the few identified new antibacterials have done little progress in solving the emergence of resistance, nowadays, infections caused by MDR bacteria are treated through the combination of two or more antibacterials. In addition, synergy and drug combination have proved to be a winning strategy in fighting MDR bacteria. For example, the combination of amoxicillin, a potent β-lactam that is inactivated by β-lactamases, and clavulanic acid, a weak antibacterial able to inhibit β-lactamases, has led to Augmentin®, which was the best selling drug in 2001. [14], [18]

1.5. The future of antibacterial therapy: to kill or not to kill bacteria?

In recent years, the paradigm of antibacterial drug discovery has been under discussion: instead of only screen natural sources or develop synthetic compounds to identify bactericidal or bacterioestatic agents, the components of the infectious process, like virulence factors, should be explored as new targets. By targeting virulence, the chemical entity is interfering with the ability of a particular organism to cause disease without

disturbing its survival. Interfering with bacteria's pathogenicity mechanisms enables the clearance of the disarmed pathogen by the host immune system. The down-side of this approach is that it can only be applied with bacterial-specific targets.

Strategies that target the infectious process include vaccines, phage therapy, immunostimulants, adjuvants or probiotics whose activity interferes with adhesion and colonization, toxin production pathways, biofilm formation and quorum sensing. [14], [15], [19] Moreover inhibiting virulence instead of cell division decreases the selective pressure for the evolution of antibiotic resistance because only the pathogens expressing the targeted pathogenicity factor are affected by the therapeutical agent. [20]

Besides, to expand drug targets, small molecules that target non-essential genes can be combined with weak antibiotics. For example, the natural product Cyslabdan produced by actinomycetes, has a potentiator effect of the activity of imipenem against MRSA. Also combination of polyethylenimine with known antibiotics was able to reduce their MIC as much as 56 fold. In addition combination of erythromycin with the Gram negative OM permeabilizer ceragenin broadens erythromycin's activity against Gram negative pathogens. Moreover, fluoroquinolones activity in *P. aeruginosa* and *E. coli* can be potentiated by co-treat bacteria with the efflux pump inhibitor L-Phe-L-Arg-β-naphthalamide (PAβN). [14]

1.6. Metabolism and Cysteine biosynthesis as drug target

Having in mind bacterial physiology, metabolic enzymes are particularly attractive targets. They are highly conserved between different pathogens and enzymatic assays allow HTS identification of new inhibitors. Nevertheless, the identification of a suitable metabolic enzyme depends of the conditions used to grow bacteria. [21]

Some pathogens spend part of their life cycle in extremely hard environmenal conditions, where survival depends of the ability of the pathogen to adapt to the changing settings. Thus, by interfere with the pathogens adaptability mechanisms, virulence and/or persistence and ultimately resistance to the antibacterial agent can be decreased. [22], [23]

In many organisms, swarming motility is associated with higher virulence factors production. In *Salmonella typhimurium*, *Pseudomonas aeruginosa*, *Serratia marcescens*, *Eschirichia coli* and *Bacillus subtilis* swarming cells, there is higher resistance to structurally and functionally different antibacterials. Upregulation of cysteine biosynthetic pathway in swarmers has a role in higher antibacterial resistance. In addition, even though cysteine auxotrophs can grow on swarm media due to the presence of cysteine, the genes that regulate the expression of the enzymes involved in the biosynthesis of cysteine are induced. Analysis of the total thiol content of bacterial cells in swim state showed that ΔcysE and ΔcysB mutants have reduced thiol content. Besides, cysteine is a central building block of glutathione, methionine and cofactors, in both eukaryotes and prokaryotes and it is the main antioxidant in parasitic protozoa.

All in all, therapeutic intervention aiming at targeting the cysteine biosynthetic pathway may afford a new opportunity to treat bacterial infections. The higher sensitivity to antibacterials and oxidative stress of cysteine auxotrophs encourages the exploitation of chemical induced cysteine auxotrophy as a strategy to obtain new antibacterials. Moreover, cysteine biosynthetic enzymes are indispensable during persistence but they can be dispensable during growth or acute infection. This way, interference with cysteine biosynthetic pathway may afford a better therapeutic strategy than antibiotics to fight persistence. [24], [25]

1.7. Sulfur Assimilation Pathway

In bacteria the reductive sulfate assimilation pathway begins with the active transport of sulfate, the most abundant source of sulfur in the environment, inside the cell. After sulfate is incorporated in ATP with formation of adenosine 5'-phosphosulfate (APS). In *S. typhimurium* and *E. coli* APS is then converted into phosphoadenosine-5'-phosphosulfate (PAPS). Combined action of APS Kinase and thioredoxin-dependent PAPS reductase generates sulfite whose reduction by sulfite reductase leads to bisulfide. Bisulfide is then incorporated in an activated form of serine to obtain cysteine in a reaction catalyzed by sulfhydrylase **(Fig. 5)**. [23]

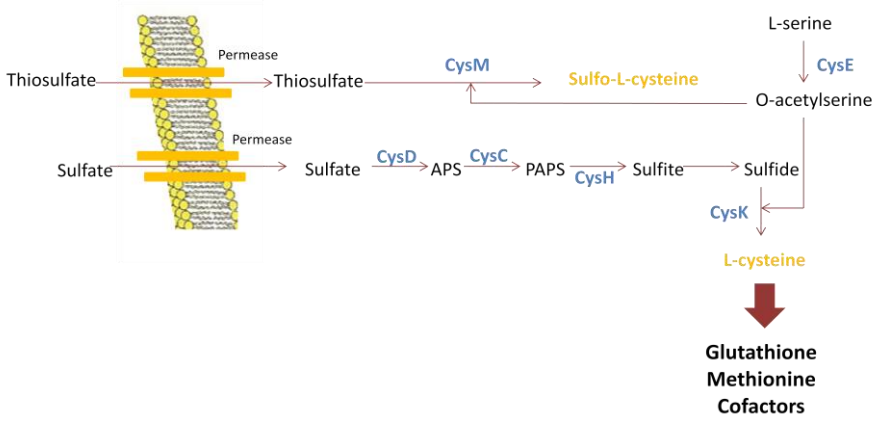

Figure 5 - Sulfur assimilation pathway. Adapted from [23].

For each mole of cysteine produced there is consumption of one mole of GTP, two moles of ATP and three moles of NADPH. [23], [26]

The essential aminoacid cysteine is then the sulfur donor for all sulfur containing biomolecules like glutathione, biotin, Fe-S clusters and methione, among others. [23], [27], [28]

Cysteine biosynthesis machinery is absent in mammals, as they rely on the reverse transsulfuration pathway to synthesize cysteine from methionine **(Fig. 6)**. [23], [29]

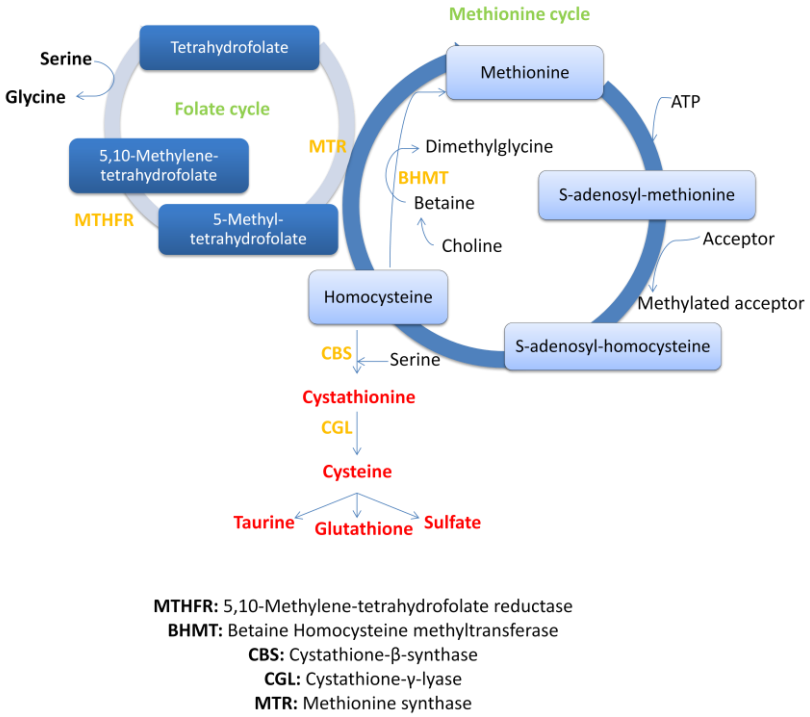

Figure 6 - Transulfuration pathway in mammals. Adapted from [30]

1.7.1. Sulfhydrylases

The enzymes that catalyze the last step of cysteine biosynthesis can be divided in O-acetylserine sulfhydrylases (CysK) and O-phosphoserine sulfhydrylases (CysM), based on the preferred substrate. The active site of CysM is bigger than that from CysK and the first can also use thiosulfate instead of sulfate as substrate.

Both are dimers and pyridoxal 5'-phosphate (PLP) dependent enzymes with a Bi-Bi ping-pong mechanism. OAS binds as the first substrate to the internal aldimine form of the enzyme and acetate is released as the first product. Sulfide then binds to α-aminoacrilate intermediate that is then attacked by sulfide followed by release of cysteine as the final product **(Fig. 7)**. [23], [26], [31]

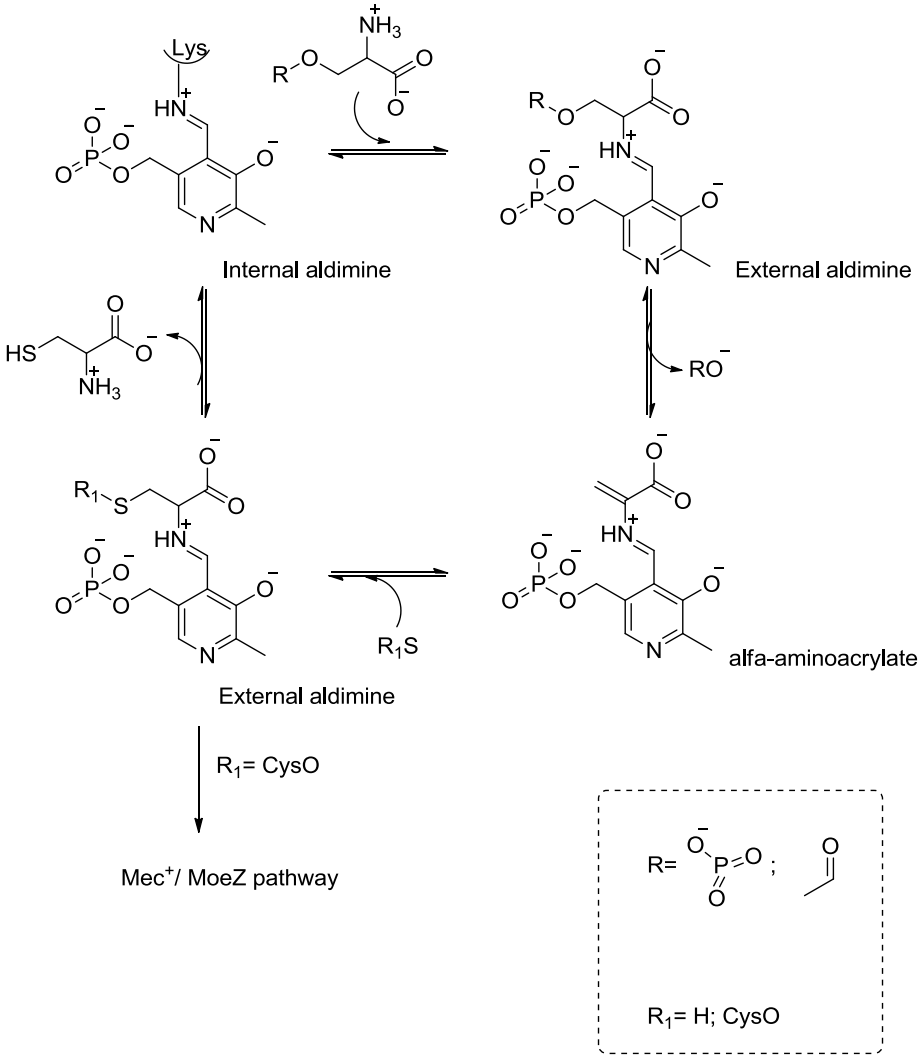

Figure 7 - Catalytic mechanism of cysteine synthase. Nucleophiles and β-substituted serine vary and variations are described in the box. Adapted from [23].

Concerning the tridimensional structure, CysK and CysM are homodimers and each subunit has two domains and the active site with a molecule of PLP. The domains are flexible and the binding of the substrate induces its close-up. The identification of a binding pocket for chlorine whose ionic radius is very similar to sulfide (1.67 Å vs 1.70Å, respectivelly) suggests the accomodation of the OASS physiological inhibitor sulfide in this allosteric pocket. [23], [26], [31]

The product of cysK, OASS-A, is the predominant isozyme and it is the only one able to interact with SAT to form the cysteine synthase complex. [23], [26] OASS-A can also catalyze a reaction between OAS and 1,2,4-triazole with formation of 1,2,4-triazole-1-alanine. Wild type bacteria grown on sulfate synthesize L-cysteine at less than 3% the rate of synthesis of 1,2,4-triazole-1-alanine. This way, 1,2,4-triazole competes with OAS to sulfide, impairing the overall ability of the cell to synthesize L-cysteine. 1,2,4-triazole inhibition of OASS results in a gradual slowing of the growth rate of bacteria. [32]

1.7.2. Serine Acetyltransferase

SAT establishes a connection between serine and cysteine metabolism. [27], [33]

Serine acetyltransferase (SAT) or CysE catalyses the transfer of the acetyl group of Acetyl-CoA to the β-hydroxi group of serine, originating OAS which is unstable and spontaneously converts to N-acetylserine (NAS). The transfer of the acetyl group of Acetyl-CoA to serine whose percursor is the glycolitic intermediate 3-phosphoglycerate by SAT occurs according to the following mechanism **(Fig. 8)**: nucleophilic attack of the β-hydroxyl of serine on the thioester carbonyl of Acetyl CoA **(I)** with the formation of the tetrahedral intermediated, catalyzed by a general base **(II)**. Afterward, the general base acts as a general acid, donating a proton to the sulfur atom of CoA with collapsing of the tetrahedral intermediate and release of OAS and CoA **(III)**.

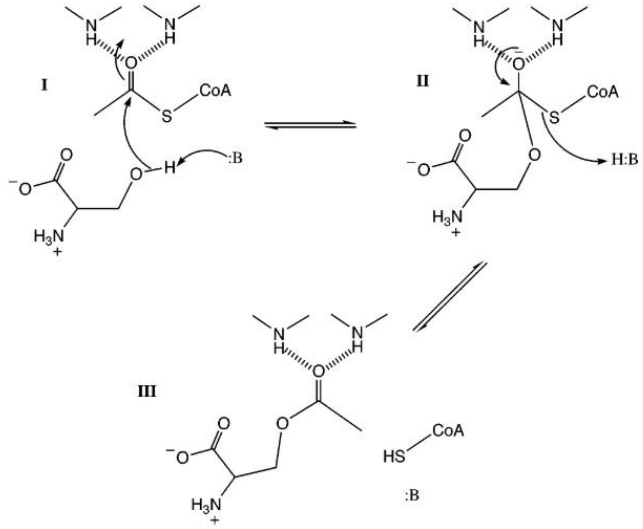

Figure 8 - SAT catalytic mechanism. Adapted from [34]

Kinetically, SAT displays a ping pong mechanism in which OAS inhibits competitively Acetyl CoA and non-competitively serine. Briefly, Acetyl CoA is the first substrate to bind followed by L-serine while OAS is released prior to CoA **(Fig. 9)**. [26], [33]–[35]

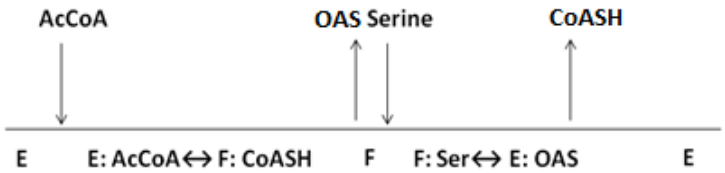

Figure 9 - SAT ping-pong mechanism. Adapted from [35]

In bacteria and higher plants, this is the first and rate-limiting step of L-cysteine biosynthesis.[27], [33]

SAT is a member of the bacterial O-acetyltransferase subfamily of O-acyltransferases, whose predominant folding is a left-handed β-helix recognizable by a hexapeptide repeated signature with the general formula [LIV]-[GAED]-X_2-[STAV]-X. Cross-sections shows a triangular structure formed

by parallel β-strands folding into a helix with three strands per turn. [33], [36]

SAT is a dimer of trimers with a flexible C-terminal essential for function and regulation since it is the part of the protein where it is located the pocket that accommodates cysteine, the inhibitor of the pathway, and also the responsible for binding to OASS with formation of cysteine synthase complex. OAS at concentrations between 0.1 and 1 mM can induce the dissociation of the cysteine synthase complex into a molecule of SAT and two of OASS. The multienzyme complex instead of channeling the intermediate substrate OAS between active sites, it releases OAS in solution and OAS must reassociate with OASS to allow the synthesis of L-cysteine. [37]

Even though SAT synthesis isn't affected by L-cysteine, very low concentrations of L-cysteine are able to inhibit SAT catalytic activity. [23], [29], [31], [37] Serine and cysteine bind to the same pocket but cysteine's binding is tigher and may induce a slight distortion of the Acetyl CoA binding pocket in order to reduce the affinity for the cofactor. [36] L-cysteine is able to inhibit SAT with a noncompetitive feedback mechanism versus Serine and a competitive one against Acetyl CoA with a ki of 1μM. [29], [31], [35]

2. State of the art

Cysteine metabolism has been pointed out as a new drug target in ϒ-proteobacteria (the Gram negative *S. typhimurium*) and actinomycetales (Gram positive *M. tuberculosis*). [23], [38]

S. typhimurium actively migrating swarming cells have increased antibiotic resistance towards several classes of antibiotics with a broad range of cellular targets and complete swarming differentiation is dependent on cysteine.

In *Mycobacterium tuberculosis* (Mtb), cysteine and methionine biosynthesis are two of the several antioxidant mechanisms that are up-regulated during macrophage invasion. [23], [38]–[42] Besides, both essential aminoacids play a role in Mtb pathogenesis since bacterial virulence and persistence, during chronic phase of the infection in mice, are highly attenuated when their biosynthesis is disabled. [43]

2.1. OASS inhibitors

To explore cysteine biosynthesis as a potential new drug target in Gram negative bacteria, a medicinal chemistry campaign was initiated in order to develop the first inhibitors of the O-acetylserine sulfhydrylase (OASS). Analysis of HiOASS-A binding pocket shows that serine acetyltransferase (SAT) penetrates into OASS through its C-terminal and competes with the substrate. Crystallographic data only detects the last four aminoacids of SAT C-terminal which suggests they are the key residues for interaction. In addition, the last residue, isoleucine has been proven essential for binding. Therefore, several pentapeptides with the general structure MNXXI were docked on HiOASS-A. Biochemical evaluation of the most promising 14 pentapeptides was carried out on HiOASS-A and the peptide MNWNI emerged as the most potent binder with a kd of 25 μM. [22]. Nevertheless, as peptides present low in vivo stability and often low bioavailability and

poor pharmacokinetics, the interactions peptide-OASS served as template to develop the first series of non-peptidic inhibitors. This way, the carboxylic acid and lipophilic side chain of isoleucine were kept and linked trough a cyclopropane ring to block both moieties in a predictable favourable configuration. (±)-trans-2-[(E)-prop-1-en-1-yl]cyclopropanecarboxylic acid **(5, Fig.10)** was the most potent inhibitor of the series displaying a kd of 1.5 μM against HiOASS-A. [44]

To overcome the high volatility and susceptibility to decomposition of compound **5** together with the demanding synthesis, further expansion of the series was performed by replacing the vinyl moiety of compound **5** by a phenyl ring **(6, Fig.10)**. Further exploration of positions prone to modification was accessed through docking experiments. A new pocket composed by a small lipophilic area surrounded by mildly polar residues was identifiable which suggested functionalization of the α carbon of the cyclopropane. This way, compound **7 (Fig.10)** bearing an ethyl group on the α carbon of the cyclopropane was prepared as a racemic mixture. [45] Nevertheless as isomers of chiral drugs have often different pharmacology, toxicology, pharmacokinetics, metabolism and potency [46] it was decided to solve the racemic mixture. Biochemical assay of compound **7** on StOASS revealed that introduction of an ethyl group increases the affinity towards the B isoform of the enzyme and while the 1S, 2R enantiomer was inactive the 1R, 2S enantiomer display similar binding affinity to the enzyme than compound **7**. To increase the affinity of the inhibitor for the enzyme and also to explore the available volume of the pocket, a new compound bearing a benzyl group **(8, Fig.10)** at the α carbon was prepared both as a racemic mixture and enantiomeric pure analogues. Compound **8a** (1S, 2S) emerged as the most potent inhibitor of OASS displaying a kd of 28nM towards OASS-A and a kd of 490 nM against OASS-B. Docking experiments showed that the introduction

of substituents at the β position of the cyclopropane would have been detrimental for the activity. [45]

Compound **8a** was then evaluated against *E. coli* in a medium without cysteine, since *E. coli* and *S. typhimurium* CysK/CysM double mutants are cysteine auxotrophs. [47], [48] However, even though its remarkable enzymatic potency, it wasn't able to interfere with bacterial growth.

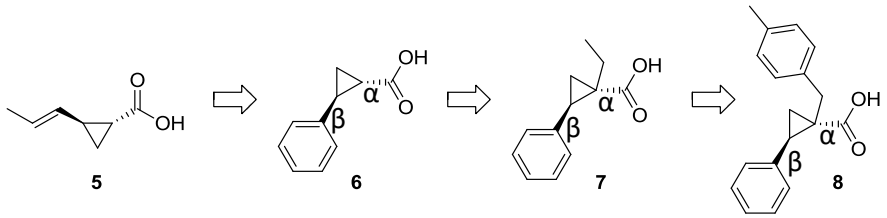

Figure 10 - Chemical structure of inhibitors **5**-**8** of OASS.

2.2. SAT inhibitors

Interference with cysteine biosynthesis by inhibition of SAT, a part of cysteine synthase complex, may also be pharmacologically relevant. Reports of SAT exploitation as drug target are restricted to one example in the protozoan *Entamoeba histolytica.* A virtual screening using the EcSAT enzyme was performed and compound NCI 6535443 **(Fig. 11),** displaying an IC_{50} of 72 μM toward the enzyme, was identified. This compound was also found to interfere with *E. hystolitica* proliferation with an IC_{50} of 0.61 μM, making unlikely the correspondence between *in vitro* and *ex vivo* activity, nevertheless confirming the good overall properties of the molecule. [49]

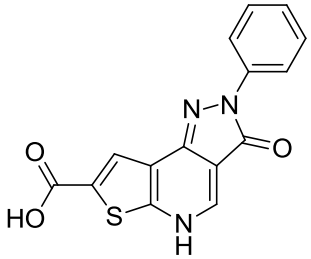

Figure 11 - Chemical Structure of compound NCI 6535443.

This way, shutdown of cysteine biosynthesis through the development of new OASS and SAT inhbitors may afford a new therapeutic strategy against MDR bacteria.

3. Aim of the project

The discrepancy between the high enzymatic inhibitory potency of compound **8a** towards StOASS and its lack of efficacy in the bacterial cell, prompted us to investigate the reason of this unpleasant outcome in order to plan effective chemical intervention.

In addition, since cysteine synthase complex is the result of the association between OASS-A and SAT, another aim of this work was to identify inhibitors of SAT enzyme. Also in this case, *S. typhimurium* SAT was considered, to continuing exploring cysteine biosynthesis shutdown in this bacterial species.

For the first aim, compound **8a** was used as the template for the synthesis of analogues endowed with ameliorated pharmacokinetic characteristics. For the latter, a target based drug design approach was used for the *ex novo* delivery of potential inhibitors.

4. Activity of compound 8a in *E. coli*:

Many Gram negative antibacterial drug discovery programs fail because of the scarce aptitude for numerous small molecules to cross the two cellular membranes together with the lipopolysaccharide-coated outer membrane. [50] In addition, efflux pump proteins that are localized and imbedded in the plasma membrane are capable of recognize and extrude noxious agents that were able to reach the periplasm or cytoplasm. [51]

Thus, it was reasoned that the lack of activity of compound **8a** in *E. coli* could be due to either permeability or efflux. To rule out one of the options, two experimental conditions were set. First, the compound was tested on a mutant with impaired efflux capability. Then, the compound was assayed in bacteria whose external membrane presented higher permeability. Regarding the assay performed with a mutant for the efflux system, the compound wasn't able to interfere with bacterial growth. In order to explore the permeability of the compound and even though there are a plethora of methods to quantify the amount of compound inside bacteria, [52]–[60] at this stage determining if the compound was or not able to cross Gram negative cell wall was the priority. This way, it was decided to assay compound **8a** in the presence and absence of the known permeabilizer agent polymyxin B nonapeptide (PMBN). As PMBN can act as an antibiotic itself since high concentrations lead to complete disruption of the outer membrane with death of the bacteria [61], the next step of the study was to determine the range of concentrations of PMBN that allow it to act as a permeabilizer agent instead of an antibacterial. According to the methodology published by Viljanen and M. Vaara [62], concentrations of PMBN from 0.3 to 10 µg/mL were assayed on *E. coli* and it was observed that at these concentrations PMBN didn't interfere with bacterial growth. After PMBN's ability to sensitize *E. coli* was tested using erythromycin **(Table 2)**.

Table 2 - MIC of erythromycin and compound **8a** in the presence and absence of PMBN.

Cpd	PMBN µg/mL	MIC	Bacteria	Medium
Erythromycin	0	≥ 32	*E coli* top10	Mueller-Hinton
	0.3	4		
	0.5	4		
	1	4		
	3	4		
	5	4		
	10	2		
8a	0	> 256	*E coli* ATCC25922	LB 20%
	1	> 256		
	3	256		

The MIC of erythromycin in *E. coli* top10 is higher than 32 µg/mL but subinhibitory concentrations of PMBN can sensitize *E. coli* to the hydrophobic antibiotic and decrease in about 8 fold erythromycin's MIC.

Compound **8a** is inactive in the absence of PMBN, however in the presence of sub minimal inhibitory concentrations of the permeabilizer agent, it is possible to determine a MIC of 256 µg/mL for compound **8a (Table 1)**. These findings demonstrate that permeability, rather than efflux, seems to be the main issue in commuting the strong binding into bacterial growth inhibition.

4.1. Permeability and Gram Negative bacteria structure

Gram negative outer membrane (OM) was identified through the discovery of Gram staining in 1884. The staining allowed the distinction between Gram negative, that presents an higher lipid content due to the outer membrane,

and Gram positive bacteria. Despite the differences in the OM, overall, Gram positive and Gram negative bacteria have a cell structure that is highly conserved **(Fig. 12)**. [63], [64]

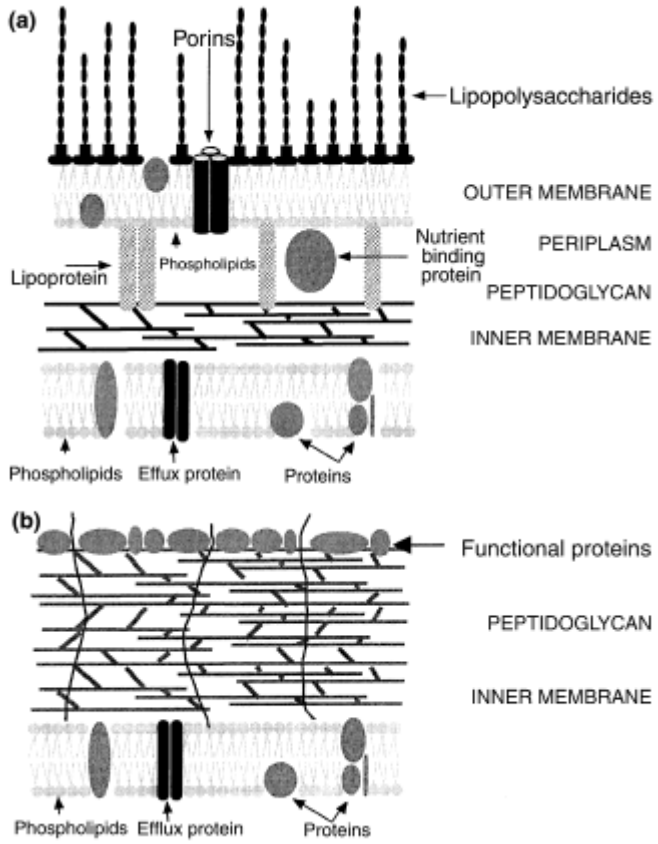

Figure 12 - Representation of the Gram negative **(a)** and Gram positive **(b)** outer membrane. From [64]

As it is displayed in **Fig. 12**, Gram negative cell layer is constituted by an outer membrane (OM), a periplasmic space and a peptidoglycan/ cytoplasmic membrane. Peptidoglycan is similar between Gram positive and Gram negative bacteria and it is a polymer of the disaccharide repeating unit N-acetyl-muramic acid and N-acetyl glucosamine. Different glycan chains are crosslinked through peptides. In Gram negative bacteria generally it is the

carboxyl group of D-alanine and the amino group of meso-diaminopimelic acid that establishes the link between different glycan chains. [64]

In the OM besides the lipopolysaccharide (LPS), there are porins, proteins that are embedded in the membrane. [64] LPS is the main component of the OM and it has a highly ordered crystalline structure with low fluidity due to its composition: lipid A, central core polysaccharide and outer O-polysaccharide side chain **(Fig. 13)**.

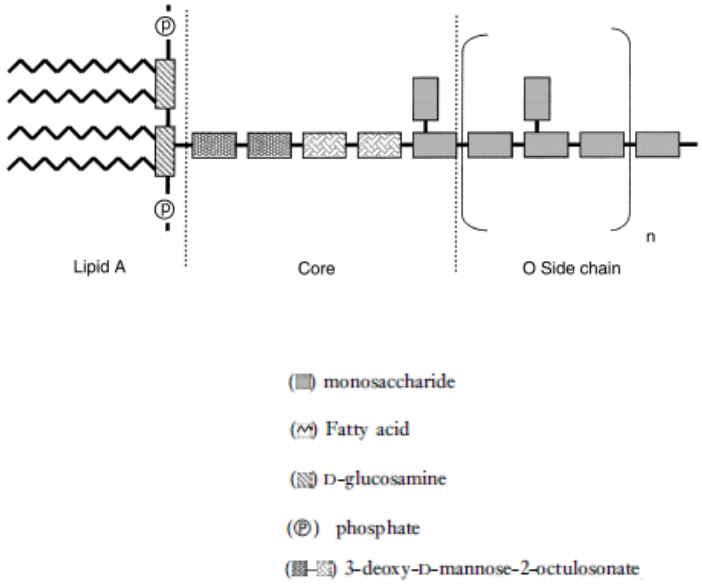

Figure 13 - Structure of LPS.[64]

Lipid A is a hydrophobic structure that generally is conserved across different Gram negative bacteria. It is constituted by a phosphorylated glucosamine disaccharide unit attached to fatty acids. Overall, it presents a negative charge. Linked to lipid A through a 3-deoxy-D-manno-2-octulosonate is a complex polysaccharide designated by core polysaccharide. Repeating units of oligosaccharides constitute the O-side chain of LPS. Adjacent LPS are

linked electrostatically by divalent cations like Calcium and Magnesium. [61], [63]

Gram negative OM is impermeable to macromolecules and only a few hydrophobic substances are able to slowly diffuse across the lipopolysaccharide (LPS)-covered surface since glycerophospholipids, the effective channels for hydrophobic diffusion, are absent. Neutral and anionic detergents also can't cross OM. On the other hand, small hydrophilic compounds use porins, water-filled channels, to cross gram negative OM. Nevertheless, the narrowness of porins remarkably restricts diffusion. Depending on their function, porins can be defined as specific or non-specific, being specific porins the ones that allow the diffusion of particular solutes like ferric ion chelates, maltose, maltodextrins, nucleosides and vitamin B12. [61]

Over the years, porin proteins were found in all Gram negative and even in a few Gram positive bacteria. For example, among the porins produced by *E. coli* are the trimeric proteins OmpC, OmpF and PhoE that show general preferences for charge and size of the solute. While OmpC and OmpF prefer cations, PhoE channel is associated with the passage of negatively charged molecules. In addition, OmpF allows the permeation of larger solutes than OmpC [64], [65]

Influx pathways for antibacterials aren't easy to establish but molecules that contain a strong acidic group, a quaternary ammonium functionality or multiple charged groups should face difficulties in crossing the bilayer regions of the OM. Taking together experimental data and theoretical considerations it is purposed that small agents like β-lactams, tetracyclines, chloramphenicol and fluoroquinolones use porins to penetrate inside bacteria's periplasmic space. On the other hand, large and lipophilic agents such as macrolides, rifamycins, novobiocin and fusidic acid use diffusion to cross the OM. [65]

4.2. OASS inhibition as a new strategy to block cysteine biosynthesis

Mutations of the genes associated with cysteine biosynthesis have already been associated with lower antibiotic resistance. [24], [25] This way and having in mind that the lack of activity in bacteria of compound **8a** is its poor permeability, it was decided to combine compound **8a** with the known antibiotic polymyxin B that act with a detergent-like mechanism of action on bacterial outer membrane. [66] Compound **8a** was able to act synergistically with polymyxin B in *S. typhimurium* ATCC14028 with a fractional inhibitory concentration of 0.25. These results indicate that cysteine biosynthesis shut down through OASS inhibition can be a source of antibacterial enhancers.

5. Expansion of the series - Chemical structure diversification in order to obtain compounds with different pharmacokinetic properties

Assuming permeability as the most likely reason for the poor activity of the hit **8a** *in vitro*, a medicinal chemistry campaign was started in order to obtain derivatives that might be able to accumulate in bacteria.

Physicochemical properties that enable small molecule accumulation in Gram negative bacteria have been predicted based in retrospective analyses of commercial antibiotics. In general, small and polar molecules tend to show higher penetration, and this might be due to the presence of structures such as porins on the surface of the cell. [50], [67], [68] In an attempt to rationalize the properties that allow small molecule penetration in Gram negative bacteria and therefore increase the success of antibacterial discovery programs, researchers have performed the quantification of drug accumulation with a set of compounds exhibiting different properties. The results show that, in order to achieve compound accumulation, important features such as, a non-sterically hindered amine which can take many forms, a non polar functionality, some rigidity and low globularity resulted to be more important than the overall polarity of the molecule. [50]

With all these considerations in mind, four different strategies were considered to increase compound **8a** accumulation in bacteria: **(i)** Redesign the structure of compound **8a** towards higher penetration; **(ii)** Perform a scaffold hopping to identify a new hit that ideally would accumulate better in Gram negative bacteria; **(iii)** Take advantage of the hints provided by a funnel-metadynamic approach combined with STD NMR, that allowed the investigation of the closed conformation of the enzyme, to prepare derivatives with improved pharmacokinetic properties; **(iv)** Additionally, a siderophore was also included in the structure of compound **8a** in order to try to use a trojan horse strategy to deliver compound **8a** inside bacterial cells.

5.1. Redesigning the structure of compound 8a

First, a ligand based drug design strategy was employed to obtain molecules with higher polarity than the parent compound. At this regard, modifications of the molecule at three different parts were proposed **(Fig. 14)**.

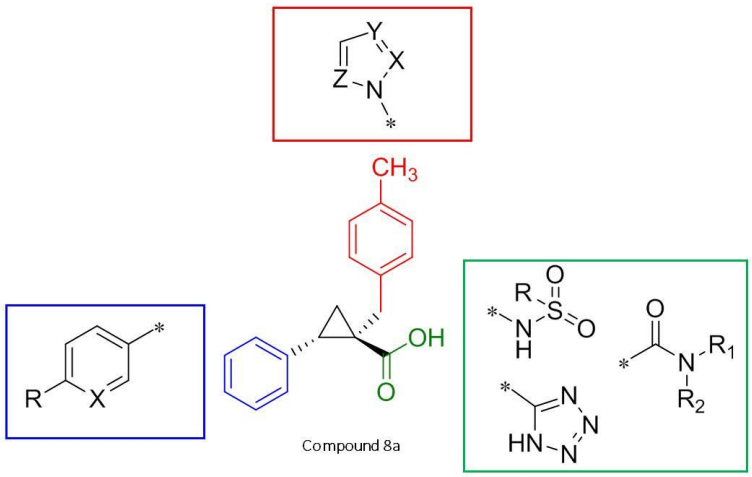

Figure 14 - Modification of the structure of the hit compound **8a**.

Since a higher amphiphilic moment may favour permeability [50], [69], amine groups were introduced at the *para* position of the C2 phenyl ring. Also, the phenyl ring was substituted by a pyridine, in order to improve the overall drug-likeness of the molecule.

To investigate whether the carboxylic acid functionality might be modified, it was replaced with isosteric groups. Among the set of possible substituents, sulfonamides, a tetrazole ring and amides were initially investigated. While the sulfonamide group is a nonplanar isoster of the carboxylic acid, the tetrazole is planar and presents a similar acidity. On a similar line, substituted amides were prepared because it is well known that the nature of the substituents might affect the selectivity of action toward different bacterial strains, either Gram positive or Gram negative [70], [71]. For instance, in the case of sulfonamide drugs, potency and selectivity are modulated by the substituent at the sulfamidic nitrogen [72]. Finally, we investigated the

benzyl group attached at the C1 of the cyclopropane ring, with the aim to evaluate its substitution with heteroaromatic structures like pyridine and five-terms heteroaromatic rings, leading to molecules characterized by a lower lipophilicity **(Table 3)**.

5.1.1. Chemistry

All compounds were prepared as racemic mixtures of the enantiomers in which the phenyl ring and the carboxylic acid group are in the trans configuration, since the rational synthesis of compound **8a** had already shown that configuration as the prefered for enzyme binding [45].

Compounds **16**, **18, 20** and **23** were synthesized using an already reported protocol [45], [73]. The reaction of phosphonoacetate **10** with styrene oxides allowed the stereoselective synthesis of the required stereodefined *trans*-R-phenyl-1-(4-methylbenzyl)cyclopropane-1-carboxylate esters **14**, **15** and **22** [73]. On a similar vein, Horner-Wadsworth-Emmons reaction between phosphonoacetates **10**, **38** or **43-46** and the proper aldehydes provided intermediates **11**, **39** and **47-50,** that were cyclopropanated under Corey-Chaykovsky conditions to give the corresponding esters **12**, **40** and **51-54.** Styrene oxides, when not commercially available, were synthesized from the styrene or the aldehyde derivatives in good overall yields. Nucleophilic substitution of chloride with *i*-propylamine in intermediate **15** gave an ester 1**9** which was hydrolysed to acid **20**, whereas catalytic hydrogenation of nitro group in intermediate **14** and subsequent hydrolysis of ester **17** provided acid **18 (Scheme 1)**.

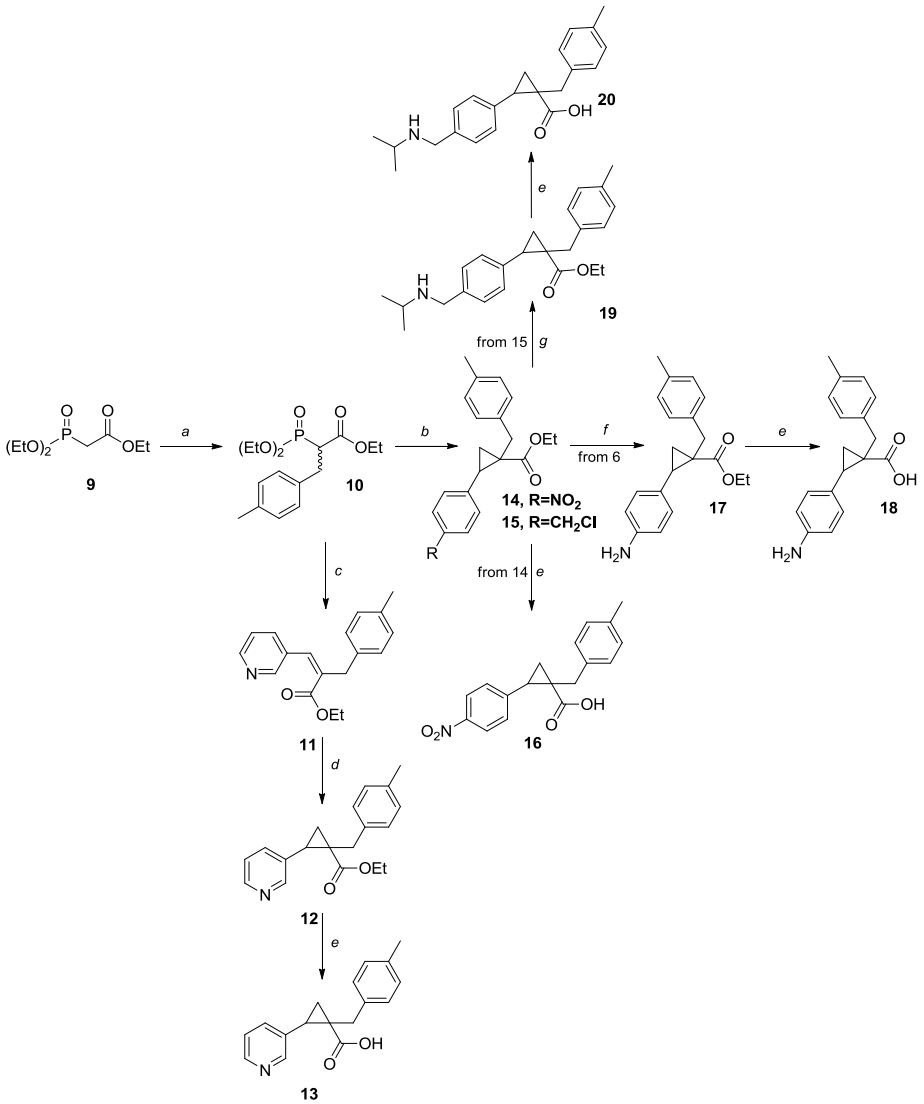

Scheme 1 - Synthetic routes to compounds **13**, **16**, **18** and **20**.

Reagents and Conditions: a) NaH, DME, 4-MeBnBr, RT-60°C; 63%; b) *n*-Buli, DME, (R)-phenyloxirane, RT- 90°C; 11% - 20% c) *t*-BuOK, THF, 0°C- RT; 86%; d) $(CH_3)_3SOI$, NaH, DMSO; 0°C- RT; 54%; e) LiOH, THF/MeOH/H_2O, 100°C; 50-60%; f) TES, Pd/C, MeOH, RT; 100%; g) $NH_2CH(CH_3)_2$, RT; 55%;

Hydrolysis of ester **22** gave raise to key intermediate acid **23**, that was used as key intermediate for the synthesis of amides **24-30** using standard amide bond forming conditions. Carboxylic acid **23** was also subjected to Curtius rearrangement in the presence of diphenylphosphoryl azide, triethylamine, and using *tert*-butanol as a solvent. The resulting Boc-amine **31** was deprotected under acidic conditions and transformed to sulfonamides **32** and **33**.

Tetrazole analogue **37** was prepared in two steps from diethyl (1-cyano-2-(p-tolyl)ethyl)phosphonate **35**. The reaction of phosphonoacetate **35** with styrene oxide provided nitrile **36** which was subjected to the tetrazole forming reaction with sodium azide. **(Scheme 2)**

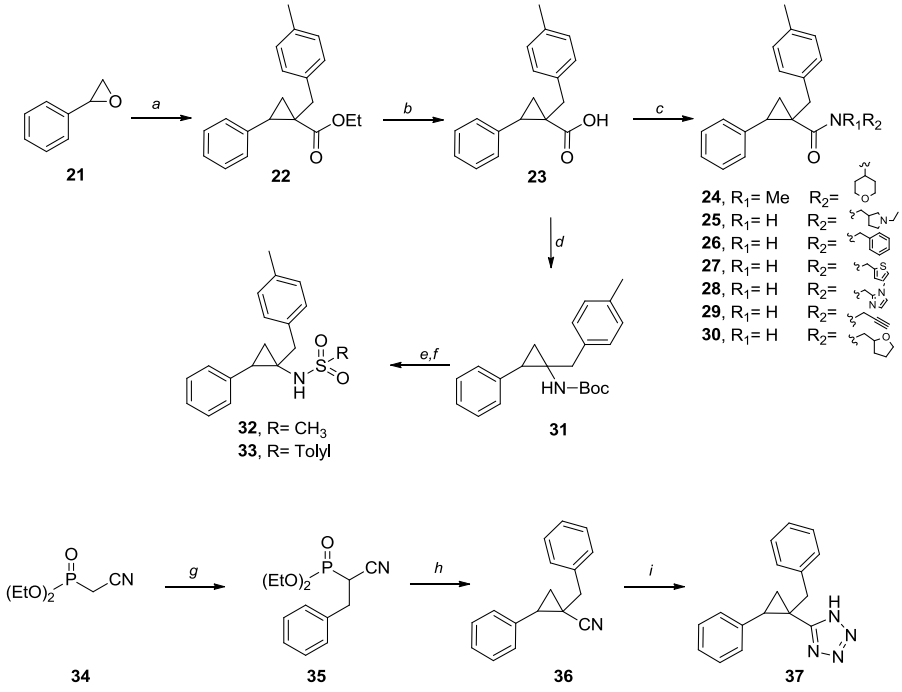

Scheme 2 - Synthetic routes to compounds **24-30**, **32**, **33**, **36** and **37**.

Reagents and Conditions: a) *n*-Buli, DME, ethyl 2-(diethoxyphosphoryl)-3-(p-tolyl)propanoate (**2**), RT-90°C; 63%; b) LiOH, THF/MeOH/H_2O, 100°C; 87%; c) HOBt, DIPEA, EDC.HCl, DMF, R_1R_2NH; 34-60%; d) TEA, DPPA, *t*-BuOH, RT, 50%; e) TFA, DCM, RT;100%; f) TEA, RSO_2Cl; -15°C; 50-61%. g) NaH, DME, BnBr, RT-60°C, 90%; h) *n*-Buli, DME, Phoxirane, RT-90°C, 25%; i) NaN_3, TEA, DMF, 130°C, 46%.

Pyridylmethyl substituted carboxylic acid **41** was prepared starting form triethyl phosphonoacetate (**9**). This was transformed to ethyl 2-(diethoxyphosphoryl)-3-(pyridin-4-yl)propanoate (**38**) by alkylation with 4-(bromomethyl)pyridine in the presence of sodium hydride. The reaction of intermediate **38** with benzaldehyde provided substrate **39** for Corey-Chaykovsky cyclopropanation that gave ester **40**. The condensation of triethyl phosphonoacetate (**9**) with paraformaldehyde gave unsaturated phosphonoacetate **42** which was subjected to Michael addition with a set of heterocycles, affording compounds **43-46**. Horner–Wadsworth–Emmons reaction of these intermediates gave the corresponding acrylates **47-50**, that were subjected to cyclopropanation using Corey-Chaykovsky conditions, as described above.

All of the title carboxylic acids herein reported were obtained after hydrolysis of the corresponding ethyl ester **(Scheme 3)**.

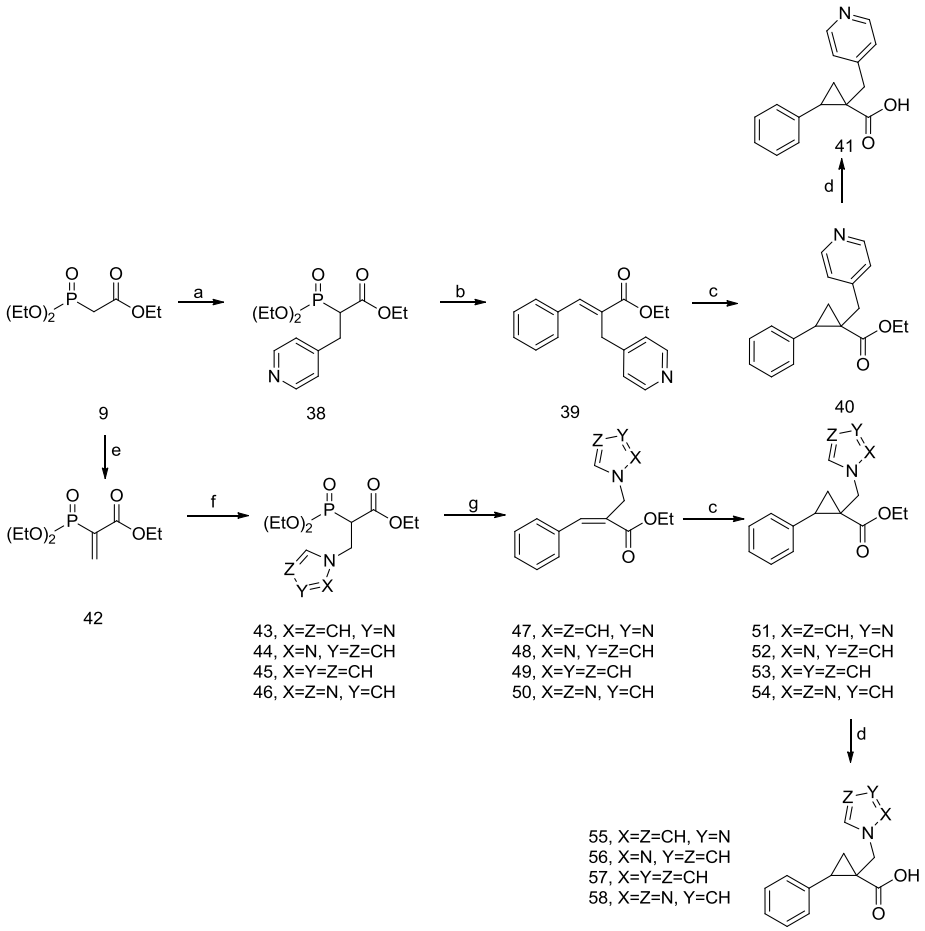

Scheme 3 - Synthetic routes to compounds **41**, **55-58**.

Reagents and Conditions: a) NaH, DMF/THF, 4-bromomethylpyridine, RT; 20%; b) K_2CO_3, THF, benzaldehyde, RT – 60°C; 40% c) NaH, $(CH_3)_3SOI$, DMSO, RT; 33-64%; d) LiOH, THF/MeOH/H_2O, 100°C; 25-89%; e) MeOH, piperidine, paraformaldehyde, *p*TSA, toluene, 100%; f) heterocycle, $CHCl_3$, Et_3N, RT; g) *t*-BuOK, THF, benzaldehyde, RT; 11-38%.

5.1.2. Biochemical Binding Studies

The new set of molecules with different polarity and ionization compared to the parent compound was then biochemically evaluated on both isoforms of the recombinant OASS enzyme from *Salmonella* to determine their potency **(Table 3)**. For most compounds the potency was assessed by fluorimetric titration, exploiting the increase in the fluorescence emission of the cofactor upon binding to the active site. Compounds without the carboxylic acid moiety were unable to elicit the fluorescence changes and for this reason their potency was measured by activity assays.

Table 3 – Inhibitory potency of compounds **13**, **16**, **18**, **20**, **24-30**, **32, 33, 36, 37, 41, 55-58**.

Cpd	OASS-A		OASS-B		ClogD[1] (pH 7.4)	tPSA[2]
	K_d (µM)	IC_{50} (µM)	K_d (µM)	IC_{50} (µM)		
13	0.4 ± 0.1		6.1 ± 0.5		0.48	49.66
16	61 ± 6		145 ± 2		1.34	89.11
18	1.4 ± 0.3		5.7 ± 0.7		1.16	63.32
20	155 ± 5		7.1 ± 2.2		2.48	49.33
24	¥	17 ± 2	¥	137 ± 10	4.23	29.54
25	¥	>100	¥	>100	3.66	32.34
26	¥	>100	¥	>100	5.77	29.10
27	¥	>100	¥	>100	5.68	29.10
28	¥	>100	¥	>100	3.93	44.70
29	¥	>100	¥	>100	4.27	29.10
30	¥	>100	¥	>100	4.46	38.33
32	0.37 ± 0.13	PI (20 %)**	0.16 ± 0.04	PI (40 %)**	3.10	46.17
33	4.30 ±2.10	PI (15 %)**	0.38 ±0.16	PI (40 %)**	5.73	46.17
36	¥	> 250	¥	ND	4.68	23.79
37	90 ± 14		ND		2.64	49.11
41	24 ± 2		275 ± 42		-0.05	49.66
55	7.6 ± 0.5		397 ± 42		0.33	52.90
56	1.5 ± 0.2		96 ± 7		-0.91	52.90
57	0.5 ± 0.1		22 ± 2		0.30	40.54
58	18 ± 5		250 ± 14		-1.74	65.26
8a	0.03 ± 0.01		0.5 ±0.1		1.94	37.3

*ND = not determined due to solubility issues

**values in brackets are the percent inhibition measured at 20 μM inhibitor (a concentration which is saturating, based on the dissociation constants)

[1] ClogD was calculated with ChemAxon software at pH 7.4

[2] tPSA was calculated with ChemDraw

Regarding the C2 phenyl ring **(Scheme 1)**, small electron donor groups (EDGs) such as the amino moiety (compound **18**, $K_{dOASS\text{-}A}$ = 1.4 μM), when not substituted, allowed to maintain good binding properties, whereas bulkier groups such as the nitro and a substituted alkylamine (compound **16**, $K_{dOASS\text{-}A}$ = 61 μM; compound **20**, $K_{dOASS\text{-}A}$ = 155 μM) weakened the interaction of the molecule with the active pocket, thus decreasing the affinity. It is possible to conclude that expansion of the series towards the *para* position of the phenyl ring, unless carried out with small groups, is detrimental for the activity of the compounds. To increase the polarity of the molecule, substitution of the C2 phenyl ring with a pyridine showed to be a more fruitful strategy, with high affinity toward both the isoforms (compound **13**, $K_{dOASS\text{-}A}$ = 0.4 μM, $K_{dOASS\text{-}B}$ = 6.1 μM). Even though the carboxylic acid group is essential for the binding to OASS [44], [45], [74], its scarce diffusion across biological membranes is a well-known issue [75], [76]. Therefore, in order to preserve the key interactions with the target, we carried out the replacement of the carboxylic acid by several isosters **(Scheme 2)**. Substitution with a sulfonamide led to molecules unable to elicit significant changes in the fluorescence emission of the cofactor, potentially indicating that the compounds did not bind to the active site of the enzyme. This

prompted us to further investigate the mechanism of inhibition of these molecules, since the residual activity at saturating concentrations is significant (about 40-50 %, **Fig. 15**).

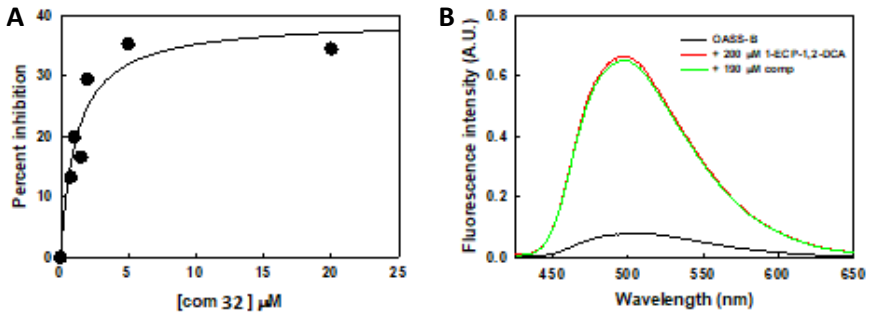

Figure 15 - Interaction of compound 32 with OASS-B.

Panel A. Dependence of the percent inhibition of OASS-B catalytic activity on compound 32 concentration. Activity assays were carried out in the presence of 0.6 mM bisulfide and 1 mM OAS at 25 °C. Line through data points is the fitting to a hyperbolic function, drawn to guide the eye. **Panel B.** Competitive binding assay. Fluorescence emission spectra upon excitation at 412 nm were collected in the absence and presence of 200 μM 1-ethylcyclopropane-1,2-dicarboxylic acid (1-ECP-1,2-DCA)[77]. The increase in the fluorescence emission indicates the formation of a specific complex with OASS-B. Addition of 190 μM compound 32 does not change the emission spectrum. Spectra were collected in 100 mM Hepes buffer, 1% DMSO, pH 7, 20 °C.

The molecules are poorly soluble in the buffer used for activity assays, compound **32** having a solubility limit of about 250 μM and compound **33** of about 50 μM. This hampers the accurate determination of the inhibition mechanism due to limitations to the range of inhibitor concentration that can be explored. However, since partial inhibition is a typical feature of allosteric inhibitors, we used a method developed by our group [77] to assess if compound **32** is able to displace a low affinity active site binder, 1-

ethylcyclopropane-1,2-dicarboxylic acid, that forms a highly fluorescent complex with OASS. Compound **32** is unable to displace the compound up to an equimolar concentration of about 200 μM. This is a strong indication that compound **32** is not able to compete for binding to the active site with 1-ethylcyclopropane-1,2-dicarboxylic acid. Therefore, either the dissociation constant of compound **32** for OASS-B is much higher than 170 μM (the Kd of 1-ethylcyclopropane-1,2-dicarboxylic acid for OASS-B) or compound **32** does not bind to the active site of the enzyme **(Fig. 15**, panel B). Unfortunately, replacement of the carboxylic acid by a tetrazole resulted in the decrease of the binding affinity (compound **37**, $K_{dOASS\text{-}A}$ = 90 μM). Additional derivatization of the carboxylic acid group to deliver a small series of amides (compounds **24**-**30**) was attempted as well in order to gain further insights into the anchoring groups that can be tolerated by StOASS. Either unsubstituted or substituted amides, regardless of the moiety attached to the nitrogen atom, had in general a detrimental effect on the binding constant. Rather surprisingly, the good activity of the tertiary amide **24** (compound **24**, $IC_{50\ OASS\text{-}A}$ = 17.2 μM) represents an exception to the SAR information collected. Indeed, from the bulk of experimental data so far described, it can be speculated that carboxylic acid replacement is tolerable as long as at that position the presence of a sharable hydrogen is granted. By contrast, the lack of a hydrogen for H-bond formation in compound **24** makes difficult its collocation within the SAR. With the help of computational methods, further efforts on the study of the mechanism of binding for this molecule will help in the explanation of this odd result.

Finally, the benzylic moiety at the C1 position showed to be the most suitable for chemical intervention **(Scheme 3)**. Its substitution with smaller size heterocycles, endowed with ameliorated drug-like characteristics, in all cases allowed to maintain good binding properties in the low micromolar or submicromolar range (compounds **41**, **55**-**58**, **table 3**). To some extent, a

correlation between polarity of the heterocycle and binding to the target enzyme seems to be present. In fact, higher polarity of compound somehow correlates with the decrease in binding affinity, with the pyrrole derivative (compound **49**, $K_{dOASS\text{-}A}$ = 0.5 μM) being the most active of the series, and the triazole (compound **50**, $K_{dOASS\text{-}A}$ = 18 μM) exhibiting the highest K_d.

5.1.3. Antibacterial Activity

Even though in terms of enzyme binding alterations are tolerable, after we evaluated if any of the carried out modifications was able to produce a molecule that is accumulated by bacteria in sufficient amounts to generate chemical induced cysteine auxotrophy. Thus, minimal inhibitory concentration (MIC) in a medium without cysteine, using the Gram negative model organism, *E. coli* ATCC25922 [78], was performed for the most potent enzyme binders: compounds **13**, **18**, **24**, **32**, **41**, **55-58**.

Unfortunately, and even though the different polarity and ionization at pH 7.4, none of the synthesized compounds was able to interfere significantly with bacterial growth, which shows that the chemical modifications, although suitable to grant enzyme inhibition, did not allow to achieve sufficient inhibitor accumulation in bacteria.

One of the main hurdles in the development of small molecules inhibitors of OASS is the consistent lower affinity that compounds display towards the B-isoform with respect to the A-isoform. Also the molecules here reported showed dissociation constants in the high-macromolar range for the B-isoform and this could be too high to completely saturate the enzyme *in vivo*.

5.2. Scaffold Hopping

In addition to the chemical modification of the structure of the previous identified hit, compound **8a**, using medicinal chemistry to try to increase small molecule accumulation [50], [67], [79], another strategy used to inhibit the desired target was to perform a scaffold hopping in order to escape the chemically challenging cyclopropane ring and to identify molecules that may cross Gram negative cell wall.

Compound **8a** was docked on the chain A of *Salmonella typhimurium*'s crystal structure (pdb code 1OAS) using LeadIt software. Protein preparation was performed using Yazara and LeadIT tools and the aminoacid residues Asn70 and Gln143 were flipped while Thr73 was rotated in a 90º angle. Moreover, the pharmacophore Gln143 and Thr73 was applied. Ligand preparation was performed on Chemaxon software, Marvin. After, using the ReCore tool of LeadIt software and keeping both the tolyl and the carboxylic acid moieties, scaffold hopping of compound **8a** using ZINC database was performed. Several molecules were obtained as possible hits **(Fig. 16)**.

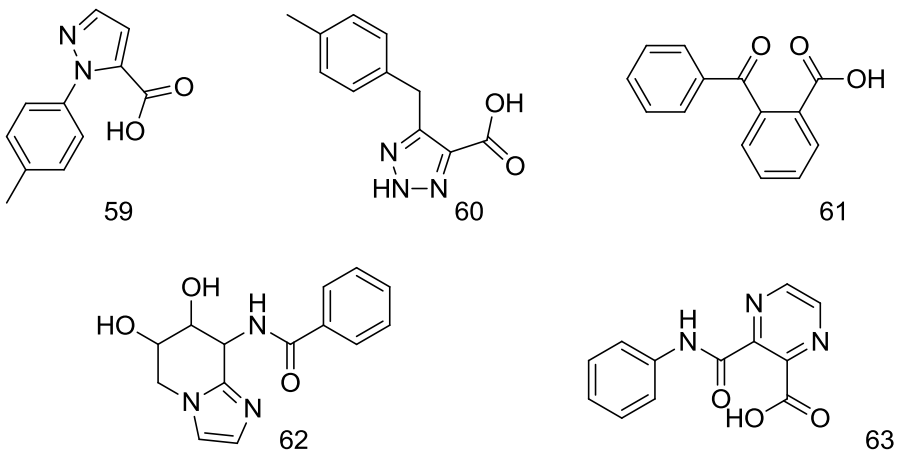

Figure 16 - Putative hits obtained after scaffold hopping of the previously identified compound **8a**.

Pyrazole **59** was selected for biochemical evaluation on the pure OASS enzyme since the key interactions with OASS backbone **(Fig. 17)** were very similar to the ones established by the previous identified hit (**8a**).

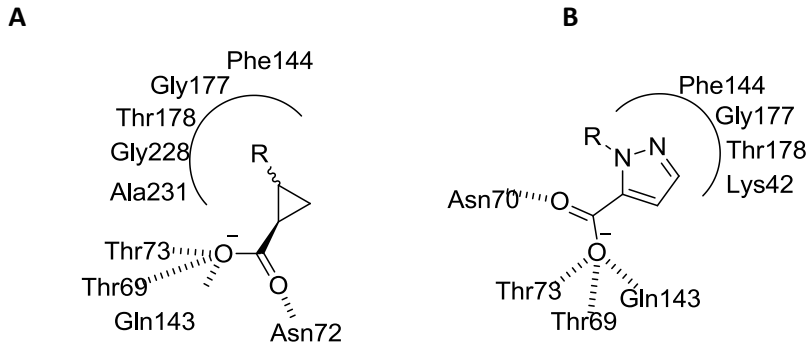

Figure 17 - List of interactions OASS - cyclopropane scaffold (A) and OASS - compound **59** (B).

After visual inspection, it was possible to envisage also a structural similarity of **59** when superimposed with some of our previously reported derivatives bearing a cyclopropane scaffold **(Fig. 18)**.

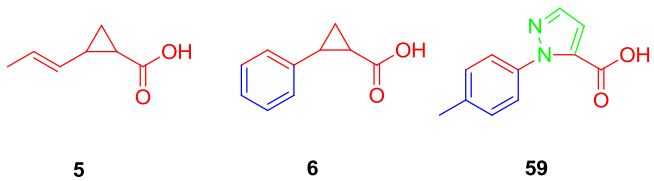

Figure 18 - Visual comparison of the structures of compounds 5, 6 and 59.

Moreover, compared to compound **6** and to the most active derivative compound **8a**, molecule **59** has a higher total polar surface area (TPSA) and comparable ClogP, anticipating improved drug-like properties. The synthetic feasibility of compound **59** is another advantage, since substituents can be easily added to the pyrazole core.

Since compound **59** wasn't commercial available it was decided to prepare as well a small library of analogues in order to perform preliminary structure-

activity relationships. Issues like the most favourable attachment point for the phenyl ring (N-1 or N-2), whether the aromatic ring could be adorned with small electron-withdrawing groups (EWG) or electron-donating groups (EDG), whether the aromatic ring could be substituted with a cycloaliphatic structure and, finally, if the small fragment-like pyrazolecarboxylic acid alone was active were investigated.

5.2.1. Chemistry

Pyrazole derivatives were synthesized according to a protocol already reported for the preparation of heterocyclic compounds [80]. This procedure was deemed of interest because of its lack of regiospecificity, that allowed us to obtain in one pot both the regioisomers, which could be easily isolated with flash chromatography. Ethyl (*E*)-4-(dimethylamino)-2-oxobut-3-enoate **65** was prepared from commercially available ethyl pyruvate **64**, that reacted with dimethylformamide diethyl acetal in dichloromethane at room temperature **(Scheme 4)**. Reacting **65** with the properly substituted hydrazine hydrochloride in methanol afforded both the 1-arylpyrazole-3-carboxylic acid ethyl esters **66a-h** and the 1-arylpyrazole-5-carboxylic acid ethyl ester isomers **67d-h**, which were therefore hydrolyzed to obtain the desired title compounds **59a-h** and **68d-h.**

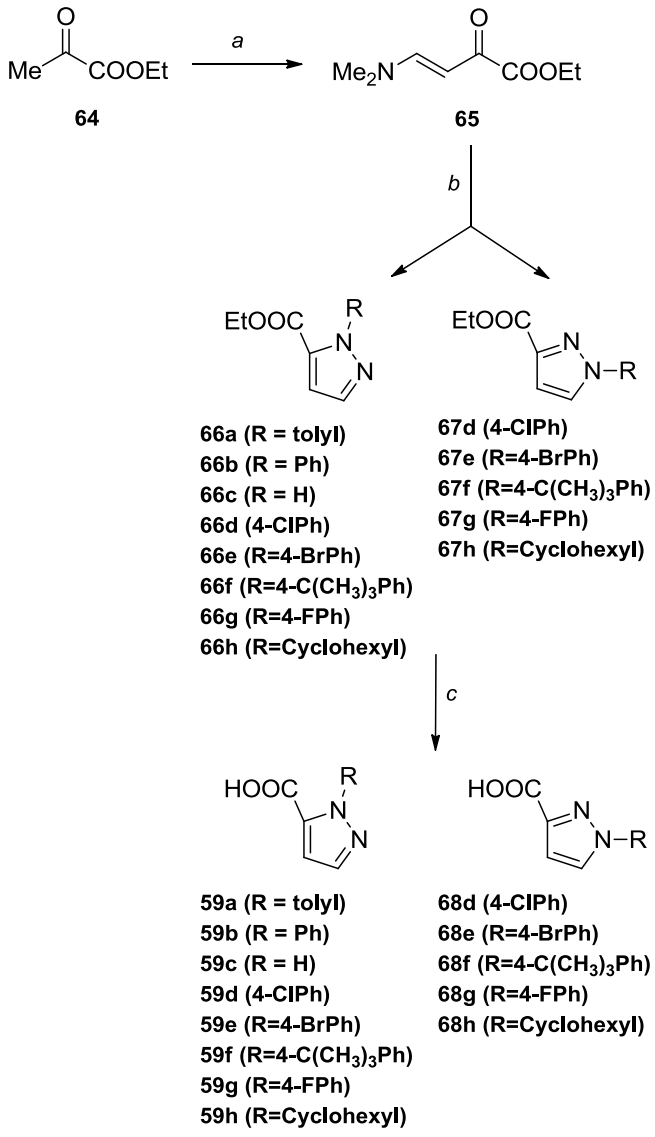

Scheme 4 - Syntehtic methodology used to synthesize compounds **59** and **68**.

Reagents and Conditions: a) $Me_2NCH(OEt)_2$, CH_2Cl_2, rt; b) R-NH_2NH_2.HCl, MeOH, 20-60 °C; c) NaOH, EtOH, 80 °C.

Enaminone **65** exists in solution in $CDCl_3$ as a single isomer, the *trans*-orientated nuclei since the magnitude of the coupling constant (J=12.5 Hz).

As anticipated, cyclocondensation of compound **65** with the properly substituted hydrazine hydrochloride afforded both the pyrazole carboxylates **66** and the regioisomers **67 (Fig. 19)**.

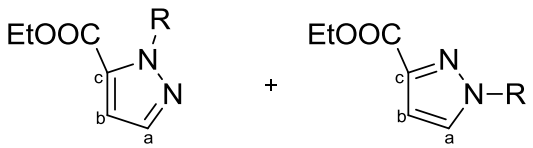

66 **67**

Figure 19 - Pyrazole carboxylates **66** (1,5 - isomer) and **67** (1,3 - isomer).

Pyrazole carboxylate **66**, which corresponds to the 1,5-isomer, is the product obtained in higher yield. The presence and the identification of the two regioisomers **(Fig. 20)** was investigated by NMR analysis since the proton at C_a in compound **67** is de-shielded compared with that in compound **66**. Moreover, the 1,3 and 1,5 isomers also present characteristic ^{13}C spectra where the C_a and C_c present different chemical shields, being C_a more shielded and C_c located upfield in the case of regioisomer **67** versus regioisomer **66 (Fig. 20)**. In order to refine this conformational analysis, HMQC-NMR experiments were also performed (**Fig. 20**).

(A)

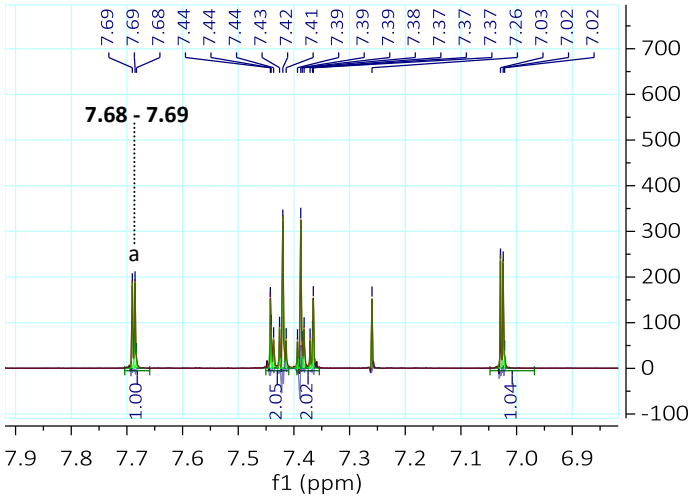
7.69
7.69
7.68
7.44
7.44
7.44
7.43
7.42
7.41
7.39
7.39
7.39
7.38
7.37
7.37
7.37
7.26
7.03
7.02
7.02
7.68 - 7.69
a
1.00
2.05
2.02
1.04
700
600
500
400
300
200
100
0
-100
7.9
7.8
7.7
7.6
7.5
7.4
7.3
7.2
7.1
7.0
6.9
f1 (ppm)

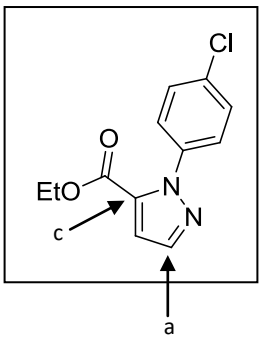
Cl
O
EtO
N
N
c
a

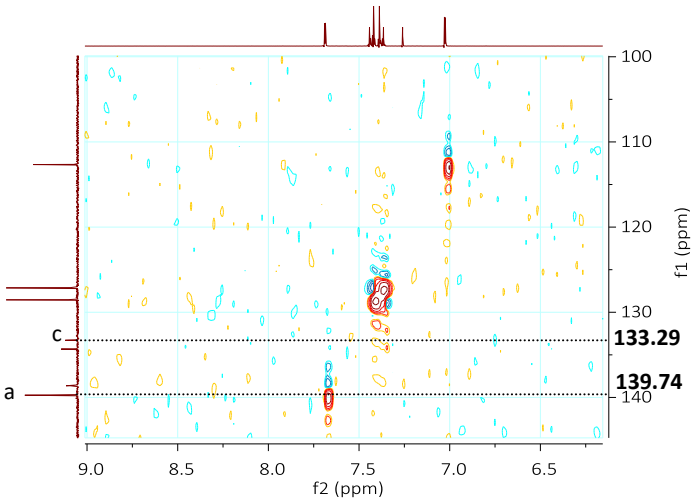
100
110
120
130
140
f1 (ppm)
c
a
133.29
139.74
9.0
8.5
8.0
7.5
7.0
6.5
f2 (ppm)

(B)

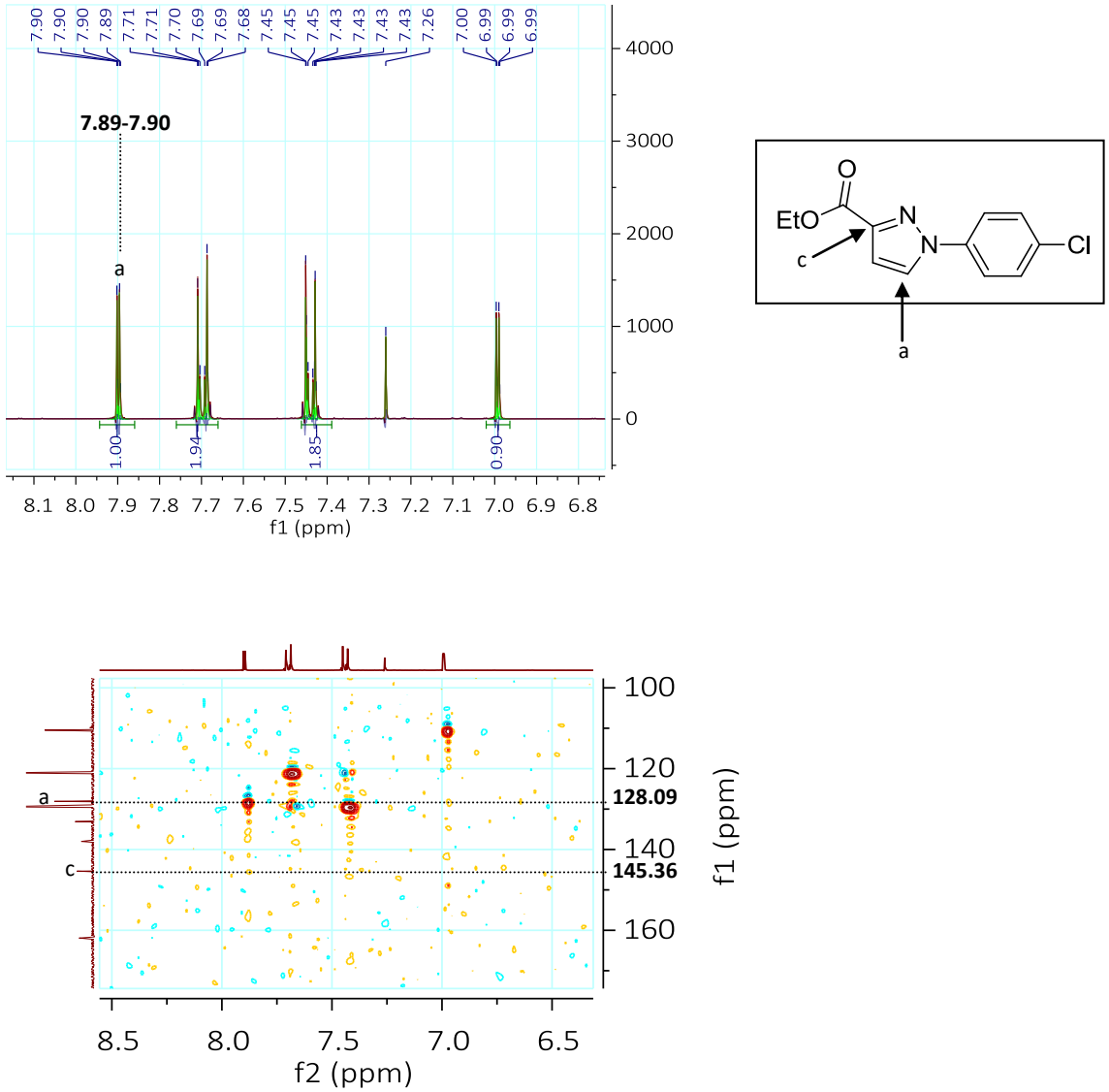

Figure 20 - ^{1}H and HMQC NMR spectra of regioisomers **66d** (A) and **67d** (B).

Curiously, cyclocondensation of enaminone **65** with *p*-tolylhydrazine hydrochloride afforded only the 1,5 isomer. Hydrolysis of the carboxylic group in the presence of sodium hydroxide afforded the desired final

compounds. Afterwards compounds **59** and also **68**, when available, were evaluated on the recombinant enzyme from *S. typhimurium* **(Table 4)**.

5.2.2. Biochemical Binding Studies

Table 4 – Biochemical evaluation of pyrazole **59** and **68** on the recombinant OASS from *Salmonella typhimurium*.

Cpd	R	% inhibition OASS-A		% inhibition OASS-B	
		1 µM	1000 µM	1 µM	1000 µM
59a	H	9.46±7	94.02±0.6	5.65±1.06	82.02±0.0
59b	tolyl	0	45.41±3.3	5.53±0.01	65.17±1.6
59c	4-ClPh	1.21±1.4	59.95±2.2	9.06±6.05	56.37±0.2
59d	4-BrPh	0	83.95±0.2	0	58.40±2
59e	4-C$(CH_3)_3$Ph	0	46.81±0.4	1.08±3.01	52.23±4.9
59f	4-FPh	0	74.07±11	0	53.37±0.7
59g	CyH	0.68±1.4	57.07±1.3	0	29.70±0.8
59h	Ph	0	66.45±0.5	11.45±3.51	64.94±0.8
68c	4-ClPh	18.00±19.6	62.78±0.6	0	59.86±1.5
68d	4-BrPh	0	61.69±0.5	0	35.46±1.8
68e	4-C$(CH_3)_3$Ph	0	81.39±0.1	10.69±5.60	81.68±0.6
68f	4-FPh	0.13±0.3	72.87±0.4	0	35.79±3.1
68g	CyH	1.08±1.9	78.71±0.6	0	42.91±2.6

In the cases of small EWGs attached at the phenyl ring, no differences in the potency were noticed for compounds **59d** vs **68d** and **59g** vs **68g (Table 4)**. A bulkier substituent such as the bromine remarkably favours the 1,5-isomer compared to the 1,3-isomer **(59e** vs **68e**, **Table 4)**, giving a >80% inhibition on OASS-A at 1 mM. An opposite pattern is noticed when bulky EDGs such as

the *tert*-Butyl are introduced at the phenyl ring, as in this case the 1,3-isomer that displayed a two-fold higher affinity to the target enzyme than the corresponding 1,5-isomer **(59f** vs **68f**, **Table 4)**. A smaller EDG such as the methyl does not affect the activity **(59f** vs **59a**, **Table 4)**. Interestingly, substitution of the aromatic ring with a cyclohexane is still tolerated, with a percentage of inhibition similar to that of the derivatives bearing an aromatic substituent (see compounds **59h** and **59b**).

Despite the range of activity allowed only a rough SAR, these results somehow confirmed the presence of a lipophilic pocket in the proximity of the enzyme active site where the pyrazole substituent can locate, as previously described [81]. Interestingly, the 1H-pyrazole-5-carboxylic acid **(59c)** was found to be the most potent fragment-like hit of the series, with more than 90% inhibition at 1 mM and an experimental K_d of 122 µM to OASS-A and a K_d of 272 µM towards OASS-B.

Having in mind compound **59b** good docking pose **(Fig. 21)** it is hypothesized that the low inhibitory potency of the set might be related with the proximity between the nitrogen atom of the pyrazole and the positively ionized nitrogen atom of the aminoacid residue lysine of pyridoxal 5'-phosphate (PLP), the enzyme's cofactor **(Fig. 21)**. Probably that proximity is the responsible for the poor accommodation of compounds **59** in the enzyme pocket and the associated low potency. To further explore this hypothesis and considering compound **59c** low ClogP, high TPSA and the reduced size, which may be beneficial for Gram negative penetration, [50], [79] other five member heterocycles substituted with a carboxylic acid in different positions were tested on the recombinant enzyme from *S. typhimurium* **(Table 5)**.

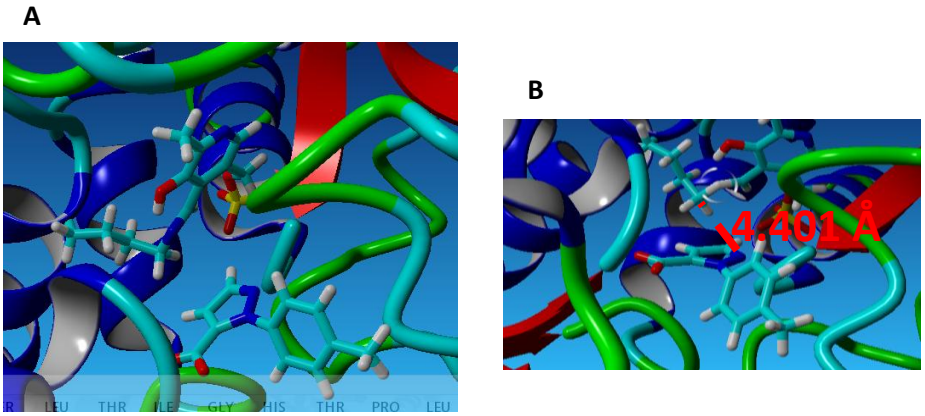

Figure 21 -**(A)** Docking pose of compound **59b** in the crystal structure of StOASS with PDB code 1OAS; **(B)** Distance between the nitrogen atom of pyrazole and lysine's nitrogen in Å.

Table 5 - Dissociation constant and ligand efficiency of compounds **69-71** determinated in StOASS.

Cpd	Structure	MW (g/mol)	Kd OASS-A (µM)	Kd OASS-B (µM)	LE (OASS-A)* Kcal/ mol/ HA	LE (OASS-B)* Kcal/ mol/ HA
69	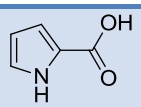	111.1	59.0±11.0	339.2±66.2	0.72	0.60
70	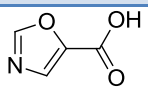	113.07	120.2±11.9	320.7±13.0	0.67	0.60
71	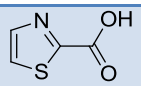	129.14	51.5±5.6	316.7±23.4	0.74	0.60

* LE= (1.37/HA). pIC_{50} where HA refers to heavy atoms

Compounds **69** and **71** display higher potency against StOASS than compound **70 (Table 5)**. Thus, it is possible to conclude that 2-substituted five membered heterocycles are preferred ligands to StOASS than 5-substituted heterocycles probably due to proximity of the ligand to PLP lysine's aminoacid residue. The high ligand efficiency (LE) of compounds **69** and **71** together with the molecular weight and overall analyses of the structure of the fragments in terms of rotatable bonds and acceptors or donor of hydrogen bonds[82]–[84] **(Table 5)**, presents these fragments as suitable candidates to start a fragment based drug discovery (FBDD) program aiming at identifying new inhibitors of StOASS.

5.3. Funnel-metadynamic STD NMR approach

The 3D crystal structure of StOASS is known but there isn't a crystal structure of the enzyme in complex with a small molecule inhibitor which hampers the prediction of the binding mode of inhibitors, that this way can only be done by docking experiments.

STD NMR can identify the moieties of the ligand that are relevant for the binding to the target, nevertheless no structural details about the complex ligand-target can be identified. [85]

Molecular dynamics of the ligand within the protein pockets can be simulated for a sufficient amount of time, in order to define the number of contacts that each proton atom is establishing with the protein environment. Ligand protons can be ranked through the highest number of contacts with protein environment which can be compared with the experimental STD. If the simulation time is prolonged to infinitum, the ligand-protein complex will be able to explore every configurational microstate and the most stable state will be populated for a longer time which, in turn, will drive the computed STD profile. However, an unbiased molecular dynamics simulation should cover the timeframe of the spin saturation transfer effect, which is in the range of milliseconds to seconds time. This limitation can be overcome by using enhanced sampling techniques which can be used to describe at atomic scale the behaviour of complex systems [86]. Thus, funnel metadynamics was employed in order to reconstruct the STD profile of a previously identified StOASS **(Fig. 22)**. [45]

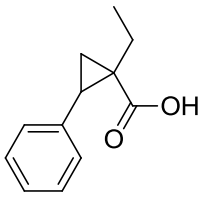

UPAR 315

Figure 22 - Chemical structure of the previous reported StOASS subject to funnel metadynamics.

Binding conformations of the inhibitor were compared to experimental STD and rescored accordingly, which allowed the study of the complex target-ligand from a dynamic point of view. Besides rationalization of the SAR of the previously reported inhibitors, the dynamic analysis of the complex target-ligand resulted in the identification of a new druggable sub-pocket. In order to better explore the new identifiable pocket a small library of derivatives was prepared.

5.3.1. Chemistry

Styrene oxide **73** was obtained from the commercially available 3-bromostyrene **72** by oxidation with *m*-chloroperbenzoic acid, according to a previously established protocol **(scheme 5).** [45] Alkylation of triethyl phosphonoacetate **9** with bromoethane in the presence of sodium hydride afforded ethyl 2-(diethoxyphosphoryl)-3-(p-tolyl)propanoate **74** in good yield. Wittig-Horner reaction between precursors **73** and **74**, in anhydrous dimethoxyethane at 90 °C and in the presence of *n*-buthyllithium as base, allowed us to obtain the required key intermediate trans ethyl 2-(3-bromophenyl)-1-ethylcyclopropanecarboxylate **75**. Suzuki-Miyaura cross-coupling reaction between the proper boronic acid and compound **75** gave derivatives **76a-d**, that were treated with LiOH at 100°C under microwave irradiation to afford the final compounds **77a-d** in good overall yields.

Since previously performed work with the cyclopropane scaffold had already proved that the (-) enantiomer has more affinity to StOASS than the (+) [45], it was decided to separate the two enantiomers of the most potent hit of the series, compound **77a**, in order to access the difference in potency between the two optically active compounds.

Techniques like chiral resolution of the racemate, asymetric synthesis through the employment of chiral catalysts or by using chiral starting materials or even direct methodologies where a chiral selector either as a part of the chiral stationary or the chiral mobile phases, can be employed in order to separate the optically active molecules. [87], [88]

Industrial scale production often uses chiral resolution instead of asymetric synthesis once that at the early stages of drug development, the set-up and optimization of the asymetric syntheses requires expensive chemicals and considerable experimentation. In addition, direct methodologies also involve identification of proper selectors for a specific pair of enantiomers which takes considerable amounts of time, material and labor. [87], [89] Therefore, chiral resolution of the racemic mixture was employed in order to isolate both optically active compounds. To do so, the racemate **77a** was reacted in dichloromethane at room temperature with the chiral precursor (R)-(−)-2-Phenylglycinol, according to a standard amide synthesis procedure **(scheme 6)**. After separation of the two diastereoisomers by flash column chromatography, hydrolysis in acidic conditions of diastereoisomers **78a** and **79a** afforded the desired enantiomers **80a** and **81a**.

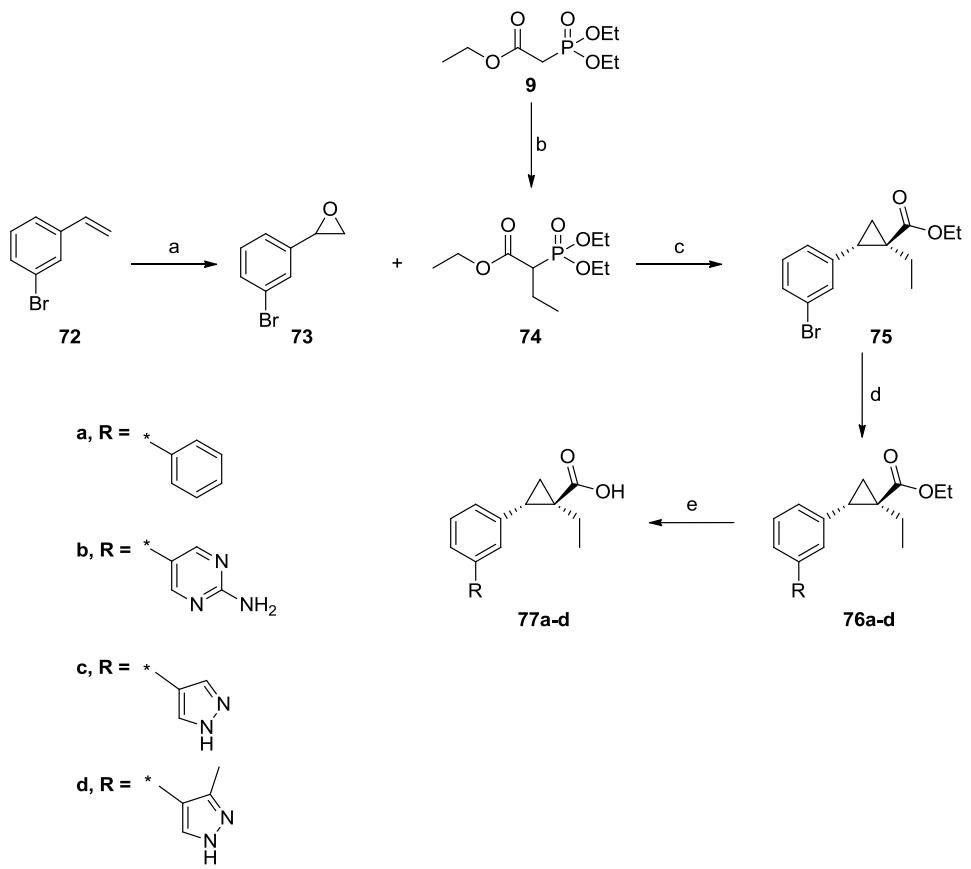

Scheme 5 - Synthetic methodology employed to obtain compounds **77a-d**.

Reagents and conditions: a) m-CPBA, $CHCl_3$, 0°C 3h, rt 18h, 98%; b) ethyl bromide, NaH, DME dry, 0°C -> rt 2h, 60°C 3h, 80%; c) n-buthyllithium, DME dry, rt -> 90°C, 18h, 71%; d) **Method A:** tetrakis(triphenylphosphine)palladium, phenylboronic acid, K_2CO_3 2M, toluene/MeOH/H_2O, 18h, 110°C, 81-96%; **Method B:** Bis(diphenylphosphino)ferrocene]dichloropalladium(II), R-boronic acid pinacol ester, DME/H_2O, Cs_2CO_3, µW, 30min, 140°C, 40-42%; e) LiOH, THF/MeOH/H_2O, MW 10 min, 100°C, 21-83%.

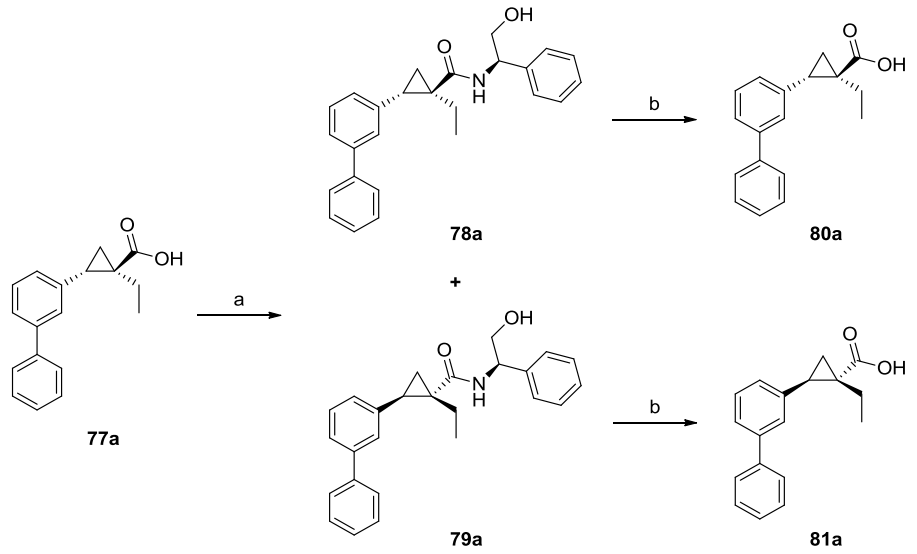

Scheme 6 - Synthetic methodology employed to obtain compounds **80a** and **81a**.

Reagents and conditions: a) (R)-(-)-2-Phenylglycinol, TBTU, EDC*HCl, TEA, DCM, 0°C 1h,r.t. 6h, 60%; b) H_2SO_4 3N, dioxane, r.t., 18h, 42-56%.

5.3.2. Biochemistry

The synthesized compounds were then biochemically evaluated on the recombinant OASS-A from *S. typhimurium* **(Table 6)**.

Table 6 - Determination of the dissociation constant for the synthesized compounds and the reference compounds UPAR 315, 393 and 421.

Cmpd	Structure	Absolute configuration	R	Kd StOASS-A (µM)
UPAR 315	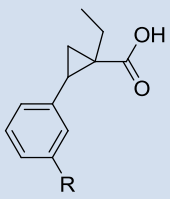	Racemic	H	15.1±1.0
UPAR 421		-	H	12.1±0.5
UPAR 393		+	H	1200±300
77a		Racemic	Phenyl	13.7±0.5
77b		Racemic	2-amino-(5)-pyrimidyl	38.3±5.1
77c		Racemic	1H-(4)-pyrazyl	18.9±1.0
77d		Racemic	1H-3-methyl-(4)-pyrazyl	16.7±0.9
80a		-	Phenyl	9.2±1.1
81a		+	Phenyl	10.2±0.9

Interestingly, compounds 7**7a, c** and **d** show comparable activities against StOASS-A, while **77b** shows a reduced ability to bind StOASS-A. Resolution of the racemic mixture of compound **77a**, leading to the isolation of compounds **80a** and **81a**, showed similar affinity of both enantiomers to StOASS-A. Those results were surprising since previously performed work, clearly

demonstrated that StOASS-A ligand requires a defined stereochemistry in order to be properly accommodated in the active site, being usually one of the enantiomers more active than the other **(UPAR 393 vs. UPAR 421, Table 6)**. This way, it is hypothesized that the modifications planned at position 3' of the phenyl ring allowed to overcome such stereo-chemical requirements, since both enantiomers display equal affinity towards OASS **(80a and 81a, Table 6)**. Thus, it can be speculated that the introduction of bulkier substituents at the 3' position can lead to energetically favourable contacts with the protein active site, overcoming the stereo-chemical requirements of the pocket.

Since the chiral resolution of the racemate or an enantioselective synthesis are no longer required, a significant enhancement in the preparation of analogues can be reached to expand the series and refine the SAR.

In terms of activity in bacteria, MIC determination in the minimal medium LB20%, for compounds **77b** and **77c** was attempted. Nevertheless, compounds **77b** and **77c** weren't able to interfere with bacterial growth.

5.4. Trojan horse Strategy:

Iron is one of the most common elements in the Earth crust, but iron (III) low solubility at physiological pH and in aerobic conditions compromises its availability to living organisms. Even though iron (III) concentration in the environment is around 10^{-9} M, in human biological fluids its concentration is about 10^{-18} M, being the major part sequestered into host proteins like transferrin, lactoferrin and ferritin. [90], [91]

Microorganisms survive to the low iron availability in the host because they obtain iron extracellularly from proteins like transferrin or precipitated ferric oxides and also intracellularly from hemoglobin. Iron acquisition can be done by cognate receptors using siderophores or by receptor mediated iron acquisition of the hosts proteins **(Fig. 23)**. [90]–[92]

Since Gram negative outer membrane doesn't have an ion gradient or ATP to allow transport, the coupling of the proton motive force of the cytoplasmic membrane to the outer membrane occurs via TonB, ExbB and ExbD proteins. [91]

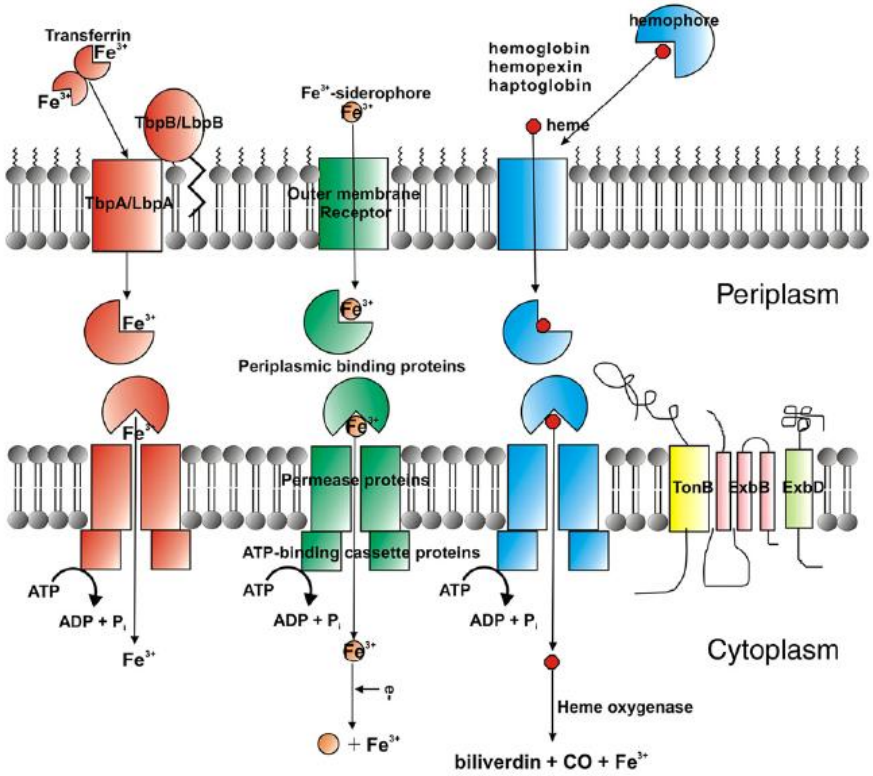

Figure 23 - Iron uptake systems in Gram negative bacteria. Iron uptake systems require an outer membrane receptor, a PBP and an inner membrane ABC transporter. From [91]

Up to now more than 500 compounds had been identified as siderophores, low molecular weight iron chelating compounds. In terms of overall structure siderophores are very different, nevertheless, the functional groups that coordinate iron are hydroxamates **(82, 84, Fig. 24)**, catecholates **(83, 84, Fig. 24)** and α-hydroxycarboxylates **(85, Fig. 24)**. [91], [93]

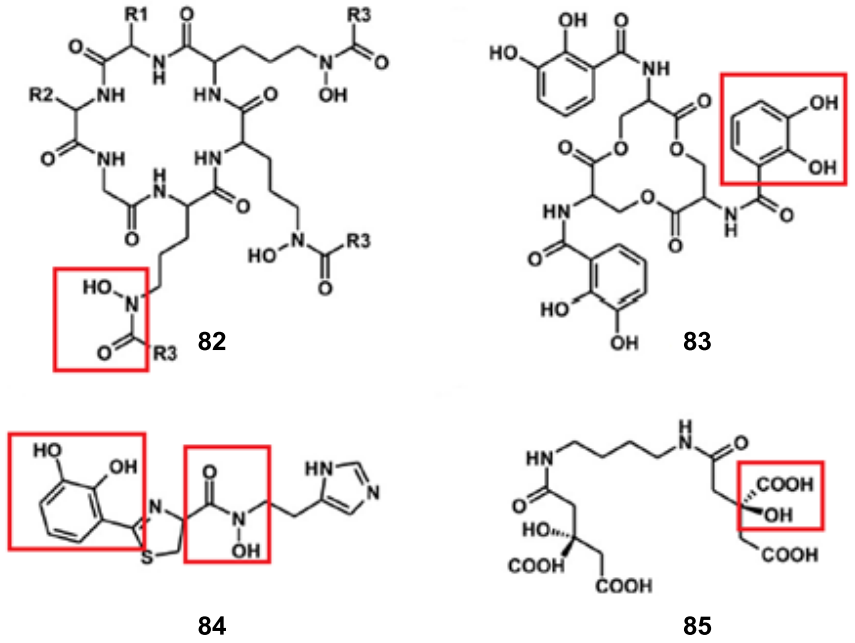

Figure 24 - Examples of siderophores with highlight of the groups responsible for coordinate iron. Adapted from [91]

Depending on the siderophore, the binding constant for iron (III) is different. In addition, the binding constant of a particular siderophore for iron depends on the pH as only deprotected donor atoms of oxygen or nitrogen are effective methal chelators. This way, the choice of a siderophore depends of the physicochemical properties of the body niche we are interested in. [93]

Sideropore biosynthesis is regulated by intracellular iron concentration, low levels of iron induce the expression of genes associated with siderophore production. [93] Siderophores are then excreted, scavenge ferric ions and the complex is transported inside the cell. [94]

This way, in order to promote the uptake of our hit compound **8a**, it was decided to incorporate the bidentate moiety catechol in the structure of our previously identified hit. Having in mind the SAR requirements exploited in

chapter 5.1 of this thesis, the benzylic moiety at the C1 position of the cyclopropane was the selected position to introduce the catechol moiety.

5.4.1. Chemistry

The catechol derivative **92** was synthesized using the same synthetic strategy used to obtain compounds **13**, **41** and **55-58** (Chapter 5.1). Briefly phosphonoacetate **9** was alkylated with 5-(bromomethyl)benzo[d][1,3]dioxole in the presence of sodium hydride and using DME as solvent. After Horner–Wadsworth–Emmons reaction using benzaldehyde afforded compound **89** that was cyclopropanated using Corey-Chaykovsky conditions. Hydrolysis of the ester afforded the carboxylic acid and cleavage of the ether bond of the dioxole using boron tribromide allowed the isolation of the final compound **92 (Scheme 7)**.

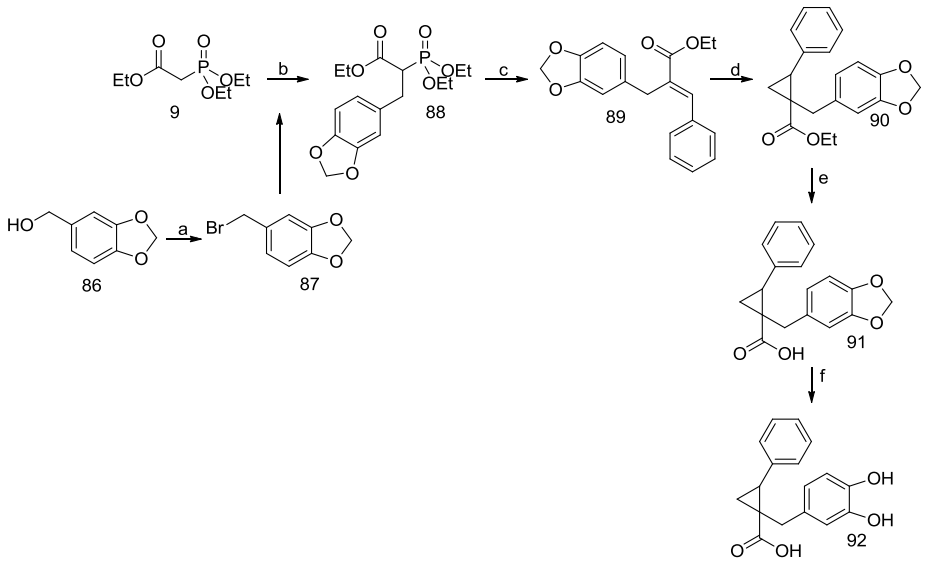

Scheme 7 - Synthetic methodology employed to synthesize the catechol derivative **92**.

Reagents and Conditions: a) PBr_3, DCM, 0°C-rt; 76% b) NaH, DME, 0°C-60°C; 84% c) t-BuOK, Benzaldehyde, THF, 0°C-rt; 47% d) NaH, DMSO, 0°C-rt; 21% e) LiOH, THF/MeOH/H_2O, 100°C, µW; 41% f) BBr3, DCM, 0°C-rt; 10%.

Considering the yields of each reaction, the rate limiting step of the synthetic methodology is the deprotection of the catechol group, so other synthetic strategies were employed to overcome this synthetic challenge. For example instead of protecting the catechol group with an ether, protection of the catechol with a more labile acetal was performed. Nevertheless, protection of the catechol with an acetal didn't allow the isolation of the final compound **92** because Ethyl 2-((2,2-dimethylbenzo[d][1,3]dioxol-5-yl)methyl)-3-phenylacrylate **(98)** couldn't be cyclopropanated under Wittig-Horner or Corey-Chaykovsky conditions **(Scheme 8)**.

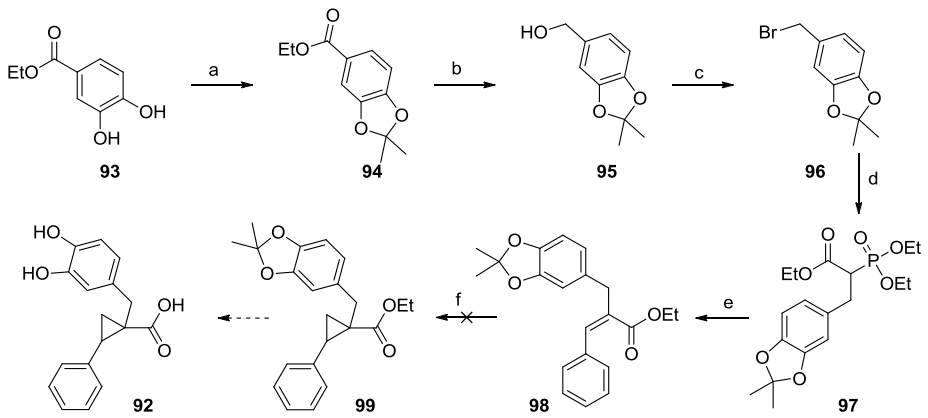

Scheme 8 - Synthetic methodology used to obtain compound **92** after protecting the cathecol group with an acetal.

Reagents and conditions: a) Acetone, C_6H_6, PBr_3; 76%; b) THF, $LiAlH_4$, THF; 73%; c) PBr_3, Et_2O, Pyridine; 100%; d) NaH, DME, Triethyl posphonoacetate; e) THF, *t*-BuOK, Benzaldehyde; 38%;

In order to try to decrease the number of synthetic steps of the procedure and also simplify purification, cyclopropanation under Wittig-Horner conditions was also attempted using ethyl 2-(diethoxyphosphoryl)-3-(3,4-dimethoxyphenyl)propanoate **(100)** to avoid possible lithiation of the benzodioxole ring. The reaction was successful but even though after deprotection of the methoxy groups it was possible to identify the peaks of the product by ^{1}H NMR and COSY, it wasn't possible to purify the reaction mixture **(Scheme 9)**.

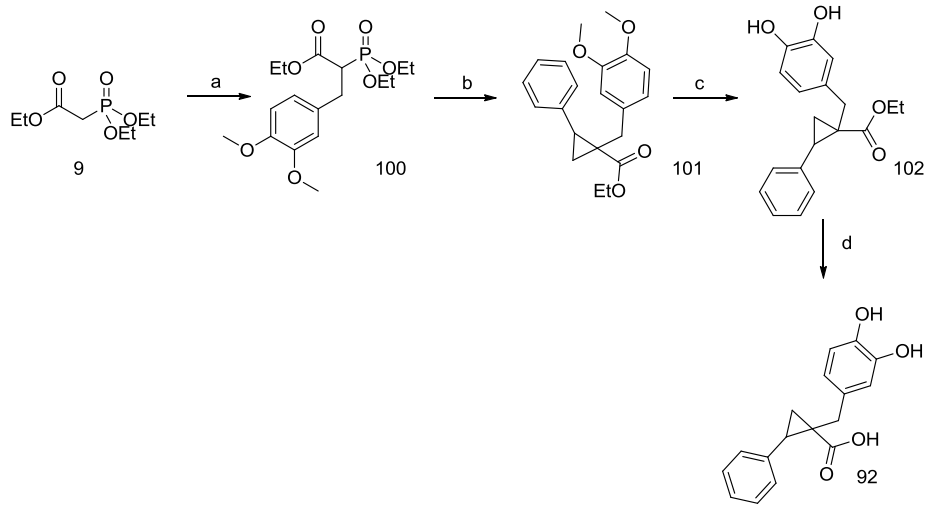

Scheme 9 - Synthetic scheme employed to obtain compound **92** through Wittig-Horner reaction.

Reagents and Conditions: a) NaH, DME, 1-bromomethyl-3,4-dimethoxybenzene, 0°C-60°C; 31% b) n-BuLi, DME, phenyloxirane, rt-90°C; 46% c) PBr_3, DCM, 0°C-rt; 43% d) LiOH, THF/MeOH/H_2O, 100°C, μW; 44%

5.4.2. Biochemical Assays

Both compounds **91** and **92** were biochemically evaluated on StOASS **(Table 7)**.

Table 7 - Kd of compounds 91 and 92 against StOASS.

Cpd	Kd StOASS-A (µM)	Kd StOASS-B (µM)
91	0.2	1.4
92	ND*	ND*

*ND (Not determined) the Kd values are as yet not available

The introduction of the protected catechol moiety at the C1 benzylic moiety of the cyclopropane scaffold induced an about 10 fold decrease in the binding affinity towards StOASS-A (compound **91** vs compound **8a**). At the moment biochemical and antibacterial evaluation of compound **92** is still ongoing.

6. Serine Acetyltransferase

6.1. Virtual Screening of in house library

Even though OASS is the enzyme that catalyze the last step of cysteine biosynthesis, in bacteria and higher plants, SAT is the rate limiting step of the biochemical pathway. Therefore, exploitation of cysteine biosynthesis shut down through SAT inhibition might represent an attractive strategy.

To identify the first inhibitors of StSAT enzyme, a virtual screening of our in house library using the available crystal structures of EcSAT (pdb code: 1T3D) and HiSAT (pdb code: 1SSM), since SAT is highly conserved among bacteria [36] was performed.

A total of seven compounds **(Fig. 25)** were then selected to be evaluated on the recombinant enzyme from *S. typhimurium* **(Table 8)**.

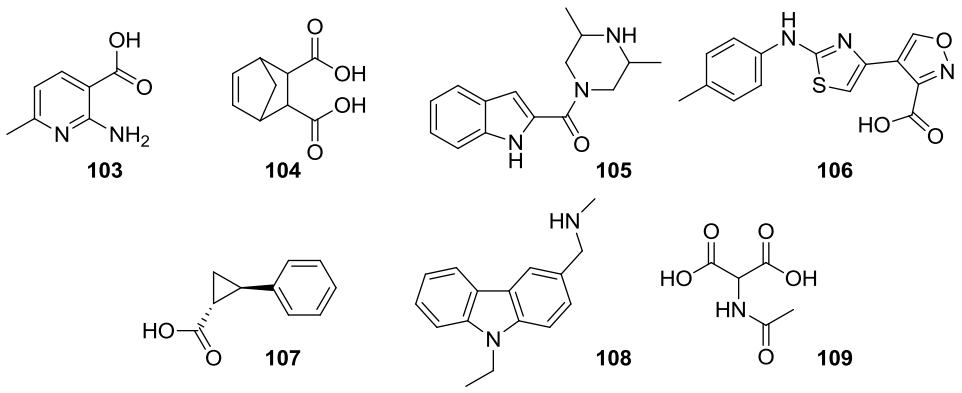

Figure 25 - Chemical structure of the seven compounds selected by virtual screening of the in house library.

6.1.1. Biochemical evaluation of the selected hits

Table 8 - Evaluation of compounds **103-109** on the recombinant SAT from *S. typhimurium*.

Cpd	% inhibition@1mM	IC_{50} (µM)	Ki (µM)	Mechanism
103	19.40±0.91	ND*	ND*	ND*
104	34.95±5.59	ND*	ND*	ND*
105	31.40±5.12	ND*	ND*	ND*
106	98.64±0.01	110±0.02	52±0.01	Competitive vs AcCoA
107	41.98±4.68	>2	ND*	ND*
108	23.61±0.04	ND*	ND*	ND*
109	18.67±5.59	ND*	ND*	ND*

*ND = Not determined

The inhibitory potency of compounds **103-109** was first assayed at a fixed concentration of 1mM. Then, only compounds **106** and **107** were selected for IC_{50} determination as they were found to inhibit the activity of the enzyme in a percentage higher than 40%, at 1mM concentration. Compound **106** emerged as the most potent hit of the set displaying an IC_{50} of 110 µM. Further biochemical studies characterized it as a competitive inhibitor of the enzyme towards Acetyl CoA binding pocket. Computational studies predict that the compound is accommodated in both L-serine and Acetyl CoA pockets: its L-shape allow partially filling of the Acetyl CoA cavity at the tail level, while the carboxylic acid functionality can mimic the natural substrate, L-serine, carboxylic acid group **(Fig. 26)**. This binding mode is compatible with a competitive displacement of Acetyl CoA. However, other regions of Acetyl CoA pocket can't be firmly excluded.

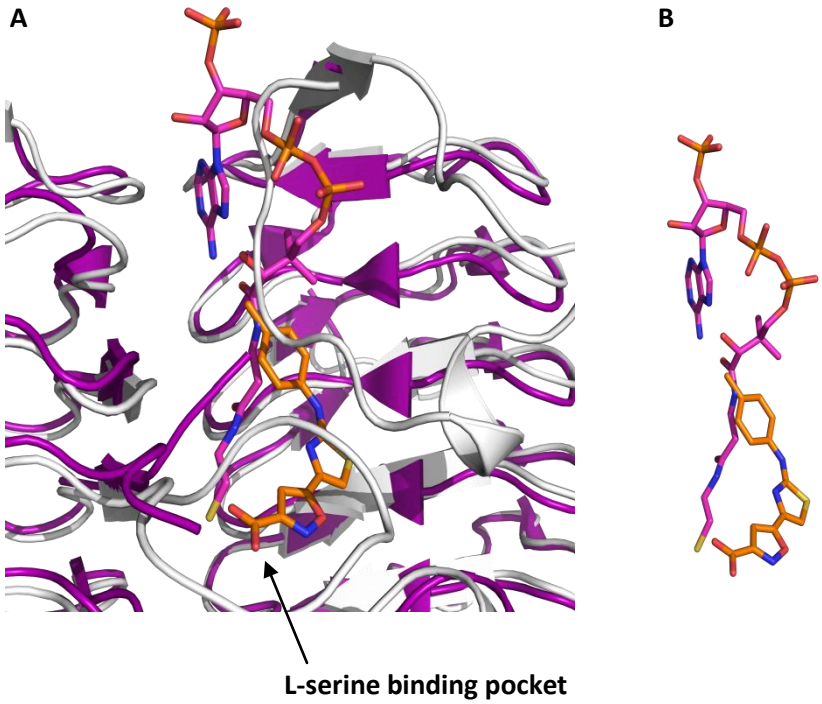

Figure 26 - **(A)** Docking pose of compound **106** in AcCoA pocket in EcSAT (alignment of structures with pdb code 1T3D and pdb code 1SSM). **(B)** Overlay of the docking pose of compound **106** and Acetyl CoA structure.

Since compound **106** was part of a set of antitubercular agents [95], several analogues were available in house. This way, in order to define preliminar SAR, the IC_{50} determination of 13 analogues was performed **(Table 9)**.

Table 9 - IC_{50} of the 13 analogues of the previous identified hit compound **106**.

UPAR	Structure	IC_{50} (µM)
325	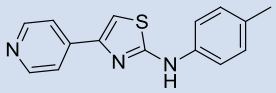	>400
456	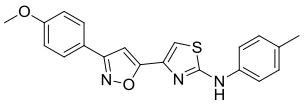	12 ± 2
330	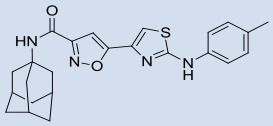	9 ± 3
451	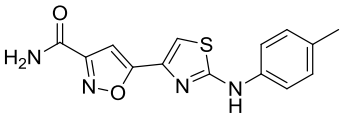	26 ± 4
465	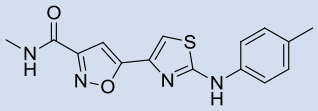	60
452	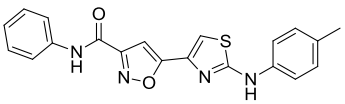	16 ± 3
326	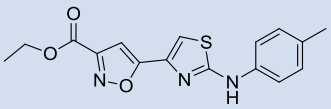	10
327	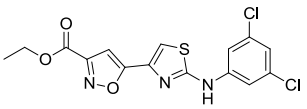	18 ± 4
460	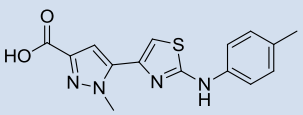	184 ± 13
463	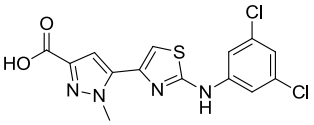	21 ± 5

750	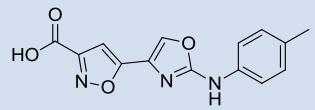	2.6 ± 0.3
751	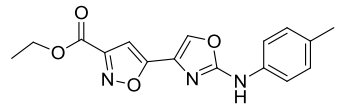	7.3 ± 1.8
329	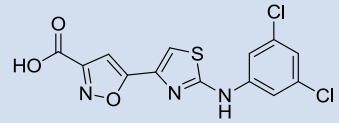	11 ± 1

Structure simplification (UPAR 325) and replacement of the isoxazole ring for a methyl pyrazole (UPAR 763) led to a decrease in the potency of the compound. Nevertheless, if substitution of the isoxazole ring for a methyl pyrazole is performed together with the introduction of electron withdrawing groups in the phenyl ring (UPAR 463), the activity of the compound is improved.

Replacement of the carboxylic acid moiety by either aliphatic or aromatic amides allows the obtention of more potent derivatives (UPAR 330, 451 and 452). However, small aliphatic and non-hindered amides are less potent enzyme binders (UPAR 465). Among the acid series, introduction of electron withdrawing groups in the phenyl ring seems to produce more potent analogues (UPAR 329 vs 106). On the other hand, regardless of the effect of the substituent in the phenyl ring, ester moiety can replace the carboxylic acid group (UPAR 326, UPAR 327).

Replacement of the thiazole moiety by an oxazole led to the obtention of the most potent derivatives of the series (UPAR 750, UPAR 751).

This way and once the effect of the substitution of the carboxylic acid, by an acid, ester or amide have already been assayed it was decided to synthesize a small library of derivatives in order to better explore the effect of introducing different substituents on the phenyl ring. The synthesis was

performed according to a synthetic protocol developed in our lab **(Scheme 10)**.

6.1.2. Chemistry

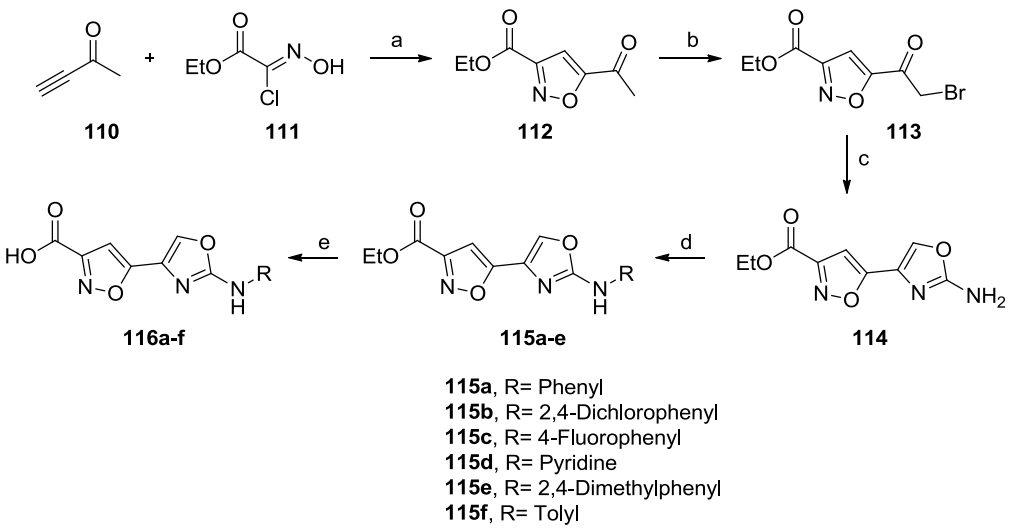

Scheme 10 - Synthetic scheme employed to obtain compounds **116a-f**.

Reagents and Conditions: a) Et_3N, THF, rt; b) NBS, *p*-TSA, MeCN, reflux; c) urea, DMF, reflux; d) XphosPdG2, NaOtBu, suitable bromobenzene derivative,Toluene/t-BuOH, 100°C, μW; e) LiOH, THF/H_2O, rt.

6.1.3. Biochemical evaluation of the hits

Both esters and acid derivatives were assayed on the recombinant enzyme from *S.typhimurium* once that the carboxylic acid functionality might be associated with poor permeability of the derivatives **(Table 10)**.

Table 10 - IC_{50} of compounds **115a-d** and **116a-e** on StSAT.

Cpd	Structure	R1	R2	StSAT IC_{50} (µM)
115a	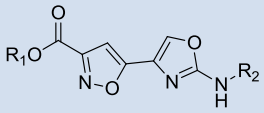	Et	Phenyl	2.68
115b		Et	2,4-Dichlorophenyl	2.52
115c		Et	4-Fluorphenyl	3.04
115d		Et	Pyridine	3.95
116a		H	Phenyl	1.55
116b		H	2,4-Dichlorophenyl	8.03
116c		H	4-Fluorphenyl	2.51
116d		H	Pyridine	12.02*
116e		H	2,4-Dimethylphenyl	4.24

* Compound partially soluble at 10 mM concentration in DMSO

Biochemical evaluation of the compounds on StSAT showed that both the carboxylic acid group and ester moiety are equally tolerable by the enzyme **(compounds 116a-e vs compounds 115a-d)**. In addition, introduction of electron withdrawing groups **(compounds 115b, 115c, 116b, 116c)** or electron donating groups **(compound 116e)** in the phenyl ring doesn't interfere with the potency of derivatives but the best results are obtained when no substituents are present in the phenyl ring **(compound 116a)**. Moreover, the pyridine ring instead of the phenyl is also tolerable in terms of SAR.

Overall, the SAR of these derivatives is very flat, either amides, ester and carboxylic acid groups are tolerated at the R1 position of the structure and a

similar behaviour is displayed by the different substituents at position R2. Having in mind that the first hit **(compound 106)** is a competitive inhibitor of Acetyl CoA predicting by the computational studies to be accomodated in both pockets of Acetyl CoA and L-serine, it is possible that the structure we are currently exploring is only occupying a part of the pocket and the substitutions we are performing are all tolerable due to the empty space in the cavity.

6.1.4. Stability of the isoxazole-oxazole nucleus:

Changes in the appearance of the DMSO solution overtime at room temperature raised some questions about the chemical stability of the compounds. Therefore, in order to evaluate it, ^{1}H NMR analysis at different time points of the DMSO solution was performed. Since the time required to observe changes in the colour of the solution was dependent of the substituent at position R_2 of series **116**, to establish the effect of the substituent in the overall stability of the compound, analogue **116a** (R_2 = phenyl) which contains the non-substituted phenyl group, analogue **116b** (R_2 = 2,4-dichlorophenyl) substituted with an electron withdrawing group and analogue **116e** (R_2 = 2,4-dimethylphenyl) substituted with an electron donating group were selected to perform the chemical stability studies **(Table 11)**.

Table 11 - Chemical stability of compounds 116a, 116b and 116e in DMSO evaluated by ^{1}H NMR.

Cpd	R2	Stability in DMSO (h)
116a	Phenyl	< 20h
116b	2,4 - Dichlorophenyl	< 2h30
116e	2,4 - Dimethylphenyl	> 7 days

As it can be observed in **Table 11**, the stability of the compounds increases in the following order 116b < 116a < 116e. Thus, it is possible to conclude that electron withdrawing groups like the simple phenyl or the phenyl replaced with two chlorines produce less stable molecules. On the other hand, the phenyl replaced with electron donating groups contribute to the overall stability of the molecule.

It is hypothesized that the mild oxidative properties of DMSO are able to interfere with the oxazole scaffold which leads to the opening of the ring and then full degradation of the compound in study. [96]

6.1.5. Antibacterial Activity

Having in mind series **116** stability issues in DMSO, MIC in a medium without cysteine, using the Gram negative model organism *E. coli*, was performed only for compound UPAR 329 **(Table 11)**. [78]

Table 12 - MIC of compound **UPAR 329** in the presence and absence of the permeabilizer agent PBMN.

Cpd	Structure	MIC (µg/mL)	MIC (µg/mL) with 3 µg/mL PMBN
UPAR 329	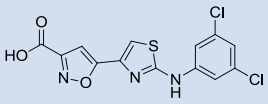	> 64	32

As it can be observed in **Table 12** compound UPAR 329 suffers from poor intrinsically permeability, displaying interference with bacterial growth only in the presence of the permeabilizer agent PMBN. That might be due to the presence of the carboxylic acid group once generally this functionalization is associated with poor penetration. [50]

6.2. Virtual Screening of the commercial library

Since after identifying this enzymatic inhibitor of StSAT, permeability seems to be once again the reason for the lack of activity of the compound in bacterial cells, other virtual screening (VS), now using the commercial available focused anti-infective, antifungals and antiviral/antibacterial libraries from Chemdiv using SAT crystal structures of *E. coli* and *H. influenzae* was performed. Focused libraries were chosen because analysis of the size and hydrophobicity of 147 antibacterials, in the market or under clinical trials, suggested that broad spectrum antibacterials are considerable more polar than other drugs. [79], [97], [98]

6.2.1. Compound selection after Virtual Screening

Visual inspection of the 1,409 identified hits by VS allowed the selection of a set of 1,391 compounds to perform further analysis. Being permeability one of the main attrition points in converting an enzyme inhibitor into a compound with whole cell activity in bacteria [97] and since permeability rules aren't defined yet [50], [79], [98], it was decided to calculate PSA and ClogD for all compounds. 37 molecules with PSA below 200 and ClogD lower than 2 were filtered from the set of 1,391 compounds because analysis of commercial antibacterials with activity towards Gram negative pathogens display an average ClogD of -2.8 and polar surface area of 165 Å. [98]

Principal components were calculated for the remaining 1,354 compounds using Chemgps software [99], [100] in order to evaluate scaffold similarity and then purchase the most diverse scaffolds possible. Several principal components were calculated but 3D representation **(Figure 27)** was performed using PC1 (shape, size and polarizability), PC2 (aromaticity and conjugation) and PC3 (lipophilicity, polarity and H-bond capacity)**.** Those were the selected molecular descriptors because having in mind that

hydrophilic antibiotics cross the outer membrane through porin diffusion and lipophilic molecules reach the cytoplasm by diffusion across the peptidoglycan [69], shape, size, aromaticity/ lipophilicity and polarity might be the main properties leading bacterial permeation.

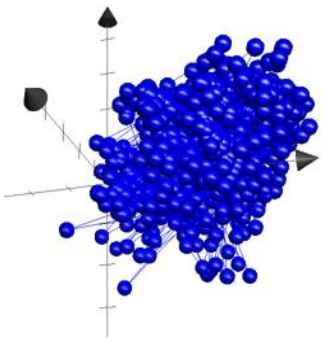

Figure 27 - Graphical representation of the principal components of the 1,354 compounds. PC1 is represented in the x axis, PC2 is in y axis and PC3 is represented in z axis.

Analysis of **Fig. 27** allowed the selection of further 37 compounds and in the end 73 compounds were purchased to be biochemically evaluated on StSAT.

6.2.2. Determination of StSAT inhibition

SAT catalyzes the transfer of the acetyl group of Acetyl CoA to serine, with release of CoASH. Generally SAT activity is determined by measuring the decrease in OD_{232} due to hydrolysis of the thioester bond of Acetyl CoA [101], [102], nevertheless this methodology isn't very suitable for screening of libraries of compounds since most organic molecules display high absorbance at 232 nm. In addition, this wavelength would require plates compatible with UV radiation which would increase the cost of the overall methodology.

Since the transfer of the acetyl group of Acetyl CoA to serine occurs with release of CoASH, a thiol, we decided to use an indirect assay to determine SAT activity. Ellman's reagent (DTNB or 5,5'-dithiobis-(2-nitrobenzoic acid)) has a highly oxidizing disulfide bond that is stoichiometrically reduced by free

thiols originating a mixed disulfide and a molecule of 5-thio-2-nitrobenzoic acid (TNB). DTNB displays weak absorption at 412 nm but the yellow product TNB can be detected spectrophotometrically at 412 nm at pH higher than 7. [103]

SAT activity was then measured at pH 7.4 by determine the absorbance of the mixture at 412 nm (visible region of the electromagnetic spectrum) through the measurement of the amount of TNB since by each molecule of CoASH released due to SAT catalyzes, it was produced one molecule of TNB **(Scheme 11)**.

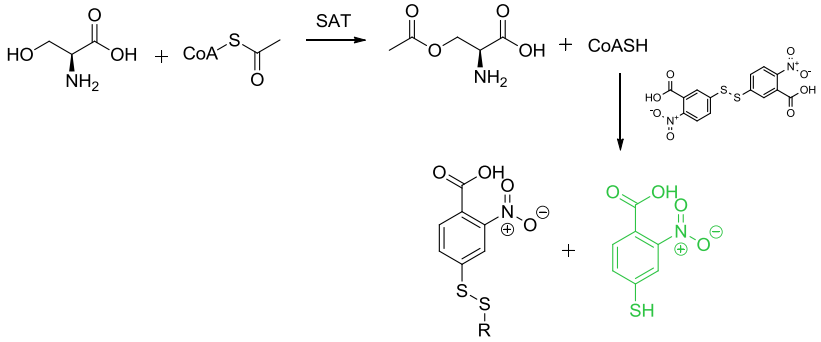

Scheme 11 - Scheme representing the methodology used to determine SAT activity through indirect assay.

Employing the above described methodology and starting the reaction with the addition of substrate instead of the addition of enzyme to avoid dispensing foaming enzyme amounts in the mixture, the inhibitory percentage of the 73 commercial acquired compounds was determined at 100 µM **(Fig. 28)**.

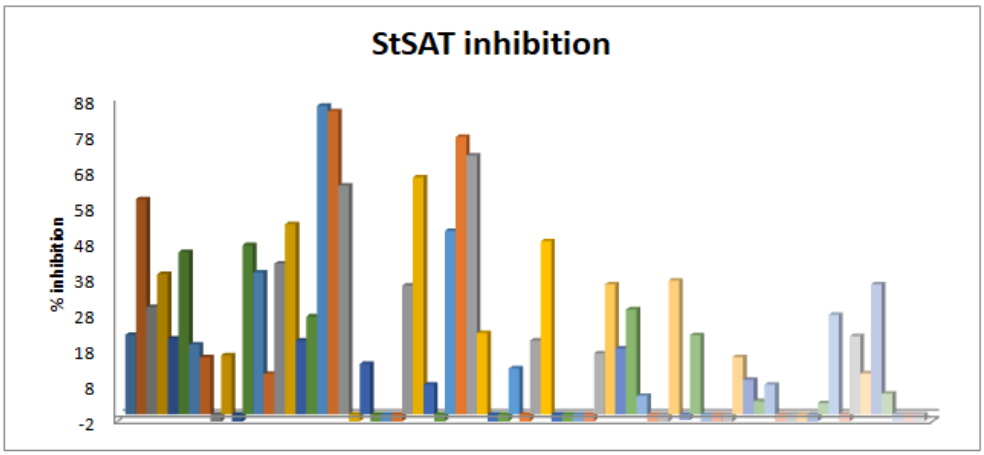

Figure 28 - Determination of the inhibitory potential of the 73 purchased compounds against StSAT at time 180s using as positive control compond UPAR 329.

Obtained Z', SW and S/B allowed us to conclude that the assay can be used for screening procedures. [104], [105]

Determination of the % percentage of inhibition for each compound was done at different kinetic time points, 27s intervals, since the total amount of compounds allowed such measurements. Nevertheless, time 180s was selected to perform endpoint kinetic measurement since it was the time point associated with higher robustness of the parameters Z', SW and S/B.

Compounds displaying a percentage of inhibition higher or equal to 40% were reassayed at 100 µM and after this second screening, dose-response curves were performed for all the compounds displaying a percentage of inhibition higher than 50% at 100 µM concentration, in order to calculate IC_{50} **(Table 13)**.

Table 13 - Inhibition and IC_{50} values against StSAT of the Hits derived from Virtual Screening.

Cpd	Chemdiv code	Structure	% inhibition@ 100µM	IC_{50} (µM)
117	D319-0482	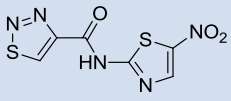	68	48.6±8
118	D319-0733	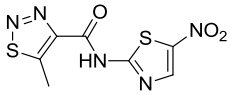	72	47.8±5
119	D392-0319	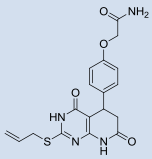	57	84.1±5
120	D511-0020	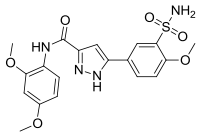	52	False positive
121	D511-0060	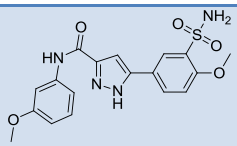	75	13.6±2
122	D511-0063	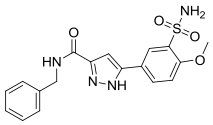	79	52.8±2

All the assayed compounds displayed micromolar IC_{50} values towards StSAT being compound **121** the most potent identified inhibitor with an IC_{50} of 14 µM **(Table 13)**.

6.2.3. Antibacterial Activity

To verify if any of the identified enzyme inhibitors had the potential to be active in bacterial cells, minimal inhibitory concentration determination in the Gram negative model oraganism *E. coli* ATCC25922 was done **(Table 14)**. MIC was performed in both minimal and complete media [78] to exclude off target effects because SAT inhibition in a complete medium that also contains cysteine shouldn't have any effect on bacterial growth.

Table 14 - MIC of the hits derived from the virtual screening

Cpd	Chemdiv code	MIC LB 20% (µg/mL)	MIC MHB (µg/mL)
117	D319-0482	64	>128
118	D319-0733	>128	>128
119	D392-0319	>128	>128
120	D511-0020	>128	>128
121	D511-0060	>128	>128
122	D511-0063	>128	>128

Compound **117** was the only one able to interfere with bacterial growth in LB20% **(Table 14)**. The mechanism by which compound **117** inhibits bacterial growth seems to be SAT inhibition since that in MHB no MIC was determined at concentrations up to 128 µg/mL .

6.2.4. Exploitation of the binding modes of compound 117

In **Fig. 29** the binding modes of the feedback inhibitor cysteine and **117** are depicted. Cysteine is bound inside SAT active site through a network of H-bonds with Asp92, Asp157, His158, Arg192, and His193 **(Fig. 29a**, **dashed black lines)**. Interestingly **117** establishes (*i*) similar interaction with Asp92,

Asp157, Arg192, and His193; (*ii*) a hydrophobic interaction with His158; (*iii*) further H-bond interaction with Gln133 and Gln258 **(Fig. 29b)**. The comparison of the binding modes of both cysteine and **117** reveals how compound **117** is able to mimic the interaction observed for cysteine **(Fig. 29c, d)**.

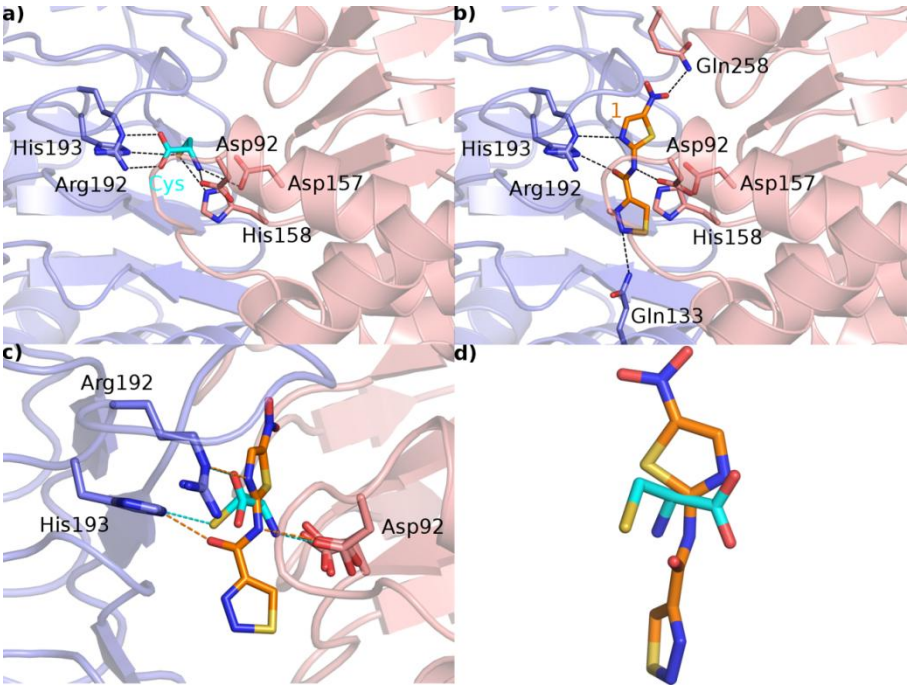

Figure 29 - a) X-ray crystal structure of SAT in complex with cysteine (PDB code: 1T3D). The two monomeric chains of SAT are depicted as blue and pink transparent cartoon, amino acid side chains are depicted as sticks and color coded depending on the chain they belong to, the feedback inhibitor cysteine is depicted in cyan sticks, while relevant H-bonds are depicted as dashed black lines; b) Binding mode of 117 (orange sticks) into SAT active site, the color code is the same reported in a); c) Superposition of the SAT-cysteine and SAT-1 complexes, highlighted with dashed lines h-bonds conserved in both complexes (cyan dash lines for cysteine, while the orange ones for 117); d) Superposition of 117 (orange sticks) and cysteine (orange sticks).

6.2.5. Chemistry

Compound D319-0482 was resynthesized in order to confirm the previously obtained results with the commercial sample. In addition, having in mind the positioning of this compound in the pocket **(Fig. 29c)** a few derivatives were prepared in order to establish preliminary SAR.

Compounds were synthesized employing peptide coupling agents **(Scheme 12)**. Briefly, the carboxylic acid functionality was activated with 1,1'-Carbonyldiimidazole (CDI) during 1h and then 4-nitrothiazol-2-amine was added to the reaction mixture. Heterocycles functionalized with the carboxylic acid group were acquired commercially with the exception of 1,2,3-thiadiazole-4-carboxylic acid that was synthesized according to **scheme 13**.

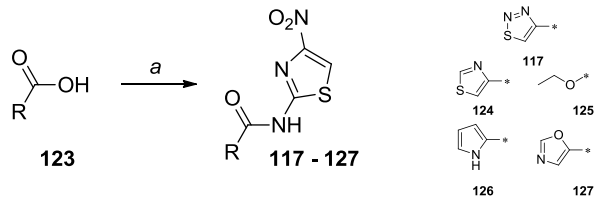

Scheme 12 - Synthetic methodology employed to obtain compounds **117-127**.

Reagents and conditions: a) CDI, DMF, $C_3H_3N_3O_2S$; 6%-15%.

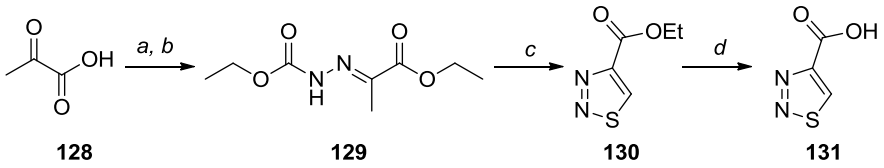

Scheme 13 - Synthetic methodology employed to synthesize 1,2,3-thiadiazole-4-carboxylic acid.

Reagents and conditions: a) EtOH, $SOCl_2$; 100%; b) EtOH; $C_3H_8N_2O_2$ 61%; c) DCM, $SOCl_2$; 39%; d) NaOH 2N, MeOH; 38%.

6.2.6. Biochemical Binding Assays

IC_{50} determination was performed for the resynthesized compound and the prepared analogues **(Table 15)**, employing the same methodology.

Table 15 - IC_{50} of the resynthesized compound and the prepared analogues.

Compound	IC_{50} (µM)	Notes
117	44	Commercial Batch
117	39	Synthesized Batch
124	> 50	-
125	25	-
126	> 50	-
127	> 50	-

The results obtained with the resynthesized compound matched the ones obtained with the commercial sample. The only modification tolerable by SAR was structure simplification **(compound 125)** being all the other derivatives less potent than the parent compound.

7. Experimental

All the reagents were purchased from Sigma-Aldrich, Alfa-Aesar, and Fluorchem at reagent purity and, unless otherwise noted, were used without any further purification. Dry solvents used in the reactions were obtained by distillation of technical grade materials over appropriate dehydrating agents. MCRs were performed using CEM Microwave Synthesizer-Discover model. Reactions were monitored by thin layer chromatography on silica gel-coated aluminum foils (silica gel on Al foils, SUPELCO Analytical, Sigma-Aldrich) at 254 and 365 nm. Where indicated, intermediates and final products were purified by silica gel flash chromatography (silica gel, 0.040−0.063 mm), using appropriate solvent mixtures. ^{1}H NMR and ^{13}C NMR spectra were recorded on a BRUKER AVANCE spectrometer at 400 and 100 MHz, respectively, with TMS as internal standard. ^{1}H NMR spectra are reported in this order: multiplicity and number of protons. Standard abbreviation indicating the multiplicity were used as follows: s = singlet, d = doublet, dd = doublet of doublets, t = triplet, q = quadruplet, m = multiplet, and br = broad signal. HPLC/MS experiments were performed with an Agilent 1100 series HPLC apparatus, equipped with a Waters Symmetry C18, 3.5 µm, 4.6 mm × 75 mm column and an MS: Applied Biosystem/ MDS SCIEX instrument, with API 150EX ion source. HRMS experiments were performed with an LTQ ORBITRAP XL THERMO apparatus. Analytical, preparative HPLC and Electron Spray Ionization condition (ESI) mass spectra were performed on an Agilent uHPLC (1290 Infinity) and an Agilent Prep-HPLC (1260 Infinity) both equipped with a Diode Array Detector and a Quadrupole MS Dosing mixture gradients of Formic acid/water/acetonitrile as system solvent. All compounds were tested as 95% purity or higher (by HPLC/MS).

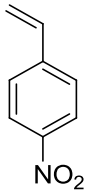

***1-nitro-4-vynilbenzene*.** To a suspension of 4-nitrobenzaldehyde (1g, 6.6mmol) and K_2CO_3 (2.5g, 7.9mmol) in anhydrous THF (19.2mL) stirring at room temperature and under nitrogen was added $[PPh_3CH_3]Br$ (2.8g, 7.9mmol) and the reaction was then subjected to reflux for 6h. After the solvent was evaporated and the residue was dissolved with ethyl acetate and water. The aqueous layer was extracted with ethyl acetate (3 x 100 mL) and the organic layers were combined, dried over anhydrous sodium sulfate and concentrated under reduce pressure. 1-nitro-4-vynilbenzene was obtained as a yellow oil (76% yield) after purification by column chromatography (5:95 Ethyl acetate/ Petroleum Ether). ^{1}H NMR (400 MHz, $CDCl_3$) δ 8.19 (d, *J* = 8.7 Hz, 2H), 7.54 (d, *J* = 8.7 Hz, 2H), 6.78 (dd, *J* = 17.6, 10.9 Hz, 1H), 5.93 (d, *J* = 17.6 Hz, 1H), 5.50 (d, *J* = 10.9 Hz, 1H).

General procedure for the syntheses of styrene oxides: To a solution of the proper styrene (1 eq) in dichloromethane (7 mL/ mmol) stirring on ice was added *m*CPBA (3.1 eq). The reaction mixture was allowed to warm until room temperature and 5h later the unreacted *m*CPBA was neutralized with a saturated solution of $NaHCO_3$. After were performed extractions with dichloromethane and the organic layers were combined, dried over anhydrous Na_2SO_4, concentrated under reduced pressure and purified by flash column chromatography on silica gel.

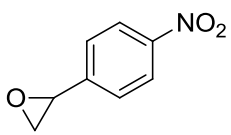

***2-(4-nitrophenyl)oxirane*.** The product was purified by column chromatography (5:95 Ethyl Acetate/ Petroleum Ether) to afford a light yellow solid (76% yield). ^{1}H NMR (400 MHz, $CDCl_3$) δ 8.22 (d, *J* = 8.7 Hz, 2H), 7.45 (d, *J* = 8.7 Hz, 2H), 3.96 (dd, *J* = 3.9, 2.6 Hz, 1H), 3.23 (dd, *J* = 5.4, 4.2 Hz, 1H), 2.78 (dd, *J* = 5.5, 2.4 Hz, 1H).

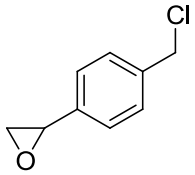

2-(4-(chloromethyl)phenyl)oxirane. After purification by flash column chromatography on silica gel (2:98 Ethyl Acetate/Petroleum Ether), the product was obtained as a colourless oil in 60% yield. ^{1}H NMR (400 MHz, $CDCl_3$) δ 7.35 (d, *J* = 38.4 Hz, 4H), 4.61 (s, 2H), 3.89 (s, 1H), 3.17 (s, 1H), 2.80 (s, 1H).

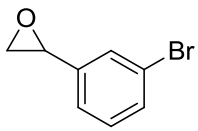

2-(3-bromophenyl)oxirane (73). The product was obtained as a colourless oil in quantitative yield. ^{1}H NMR (400 MHz, $CDCl_3$) δ 7.42 (d, *J* = 4.3 Hz, 2H), 7.21 (d, *J* = 4.8 Hz, 2H), 3.89 – 3.72 (m, 1H), 3.21 – 3.08 (m, 1H), 2.76 (dd, *J* = 5.5, 2.5 Hz, 1H).

General Procedure for the alkylation of triethyl phosphonoacetate (10, 38, 74, 88, 97 and 100): Ethyl 2-(diethoxyphosphoryl)acetate (1 eq) was added dropwise to a cooled suspension of NaH (1.1 eq) in dry DME (2 mL/ mmol). After stirring at room temperature for 2 h, the proper bromide (1.1 eq) was added, and the mixture was stirred at 60 °C for additional 2 h. After quenching with water, the mixture was extracted with ethyl acetate (3 × 50

mL), and the combined organic layers were washed with brine, dried over Na_2SO_4 and concentrated under reduced pressure. The crude material was purified through flash chromatography.

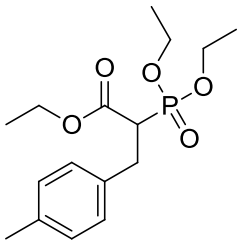

Ethyl 2-(diethoxyphosphoryl)-3-(*p*-tolyl)propanoate (10). Purification using Ethyl Acetate/ Petroleum Ether (3:7) afforded the title compound as colourless oil in 75% yield. ^{1}H-NMR (300 Mhz-$CDCl_3$): δ= 7.2-7.0 (m, 4H), 4.2-4.1 (m, 6H), 3.3-3.1 (m, 3H), 2.3 (s, 3 H), 1.4-1.1 (m, 9H).

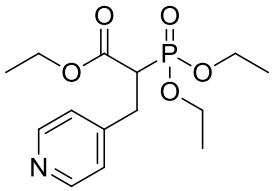

Ethyl 2-(diethoxyphosphoryl)-3-(pyridin-4-yl)propanoate (38). Following a similar procedure used to obtained compound **10**, but using (Bromomethyl)pyridine hydrobromide in place of 1-(bromomethyl)-4-methylbenzene, and THF/DMF (1:1) as the solvent, compound **38** was obtained. Purification with Acetone/ Ethyl Acetate (15:85→20:80) afforded the desired compound as a yellow oil in 20% yield. ^{1}H NMR (300 MHz, $CDCl_3$) δ 8.50 (d, *J* = 5.7 Hz, 2H), 7.14 (d, *J* = 6.0 Hz, 2H), 4.36 – 3.94 (m, 6H), 3.42 – 3.06 (m, 3H), 1.35 (t, *J* = 7.1 Hz, 6H), 1.16 (t, *J* = 7.1 Hz, 3H).

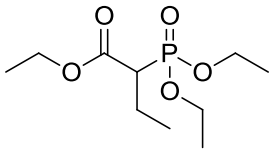

Ethyl 2-(diethoxyphosphoryl)butanoate (74). The product was obtained as a colourless oil in 80% yield after purification by flash column chromatography on silica gel using a gradient of Ethyl Acetate in Petroleum Ether. ^{1}H NMR (300 MHz, $CDCl_3$) δ 4.29 – 4.06 (m, 6H), 2.84 (ddd, *J* = 22.3, 10.6, 4.4 Hz, 1H), 2.10 – 1.82 (m, 2H), 1.38 – 1.24 (m, 9H), 0.98 (td, *J* = 7.3, 0.9 Hz, 3H).

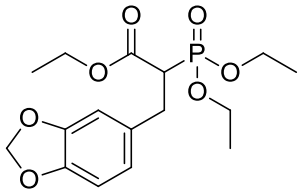

Ethyl 3-(benzo[d][1,3]dioxol-5-yl)-2-(diethoxyphosphoryl)propanoate (88). Purification by flash column chromatography on silica gel using a gradient of Ethyl Acetate in Petroleum Ether afforded the product as slightly yellow oil in 84% yield. ^{1}H NMR (400 MHz, $CDCl_3$) δ 6.84 – 6.58 (m, 3H), 5.91 (s, *J* = 5.8 Hz, 2H), 4.27 – 4.07 (m, 6H), 3.23 – 3.05 (m, 3H), 1.35 (t, *J* = 7.1 Hz, 4H), 1.28 (ddd, *J* = 7.1, 5.9, 2.3 Hz, 2H), 1.18 (t, *J* = 7.1 Hz, 3H).

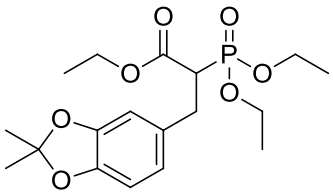

Ethyl 2-(diethoxyphosphoryl)-3-(2,2-dimethylbenzo[d][1,3]dioxol-5-yl)propanoate (97). Purification by flash column chromatography using Ethyl

Acetate/ Petroleum Ether (3:7→ 1:1) afforded the product as a brown oil in 40% yield. ^{1}H NMR (300 MHz, $CDCl_3$) δ 6.65 – 6.51 (m, 3H), 4.28 – 4.03 (m, 6H), 3.27 – 2.97 (m, 3H), 1.64 (s, 6H), 1.39 – 1.29 (m, 6H), 1.17 (t, *J* = 7.1 Hz, 3H).

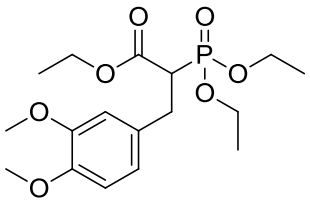

Ethyl 2-(diethoxyphosphoryl)-3-(3,4-dimethoxyphenyl)propanoate (100). Purification by flash column chromatography on silica gel using Dichloromethane/ Diethyl Ether (1:9) afforded the product as a colourless oil in 31% yield. ^{1}H NMR (300 MHz, MeOD) δ 6.90 – 6.72 (m, 3H), 4.28 – 3.99 (m, 6H), 3.80 (d, *J* = 5.2 Hz, 6H), 3.45 – 3.35 (m, 1H), 3.21 – 3.02 (m, 2H), 1.41 – 1.30 (m, 6H), 1.15 (t, *J* = 7.1 Hz, 3H).

General procedure for the Wittig-Horner reaction (14, 15, 22, 75 and 101): *n*-BuLi (2 eq) was added dropwise to a solution of compound **10** (2 eq) in dry DME (2.5 mL/mmol), stirring under nitrogen at room temperature. After 30 min, the proper styrene oxide (1 eq) was added in one portion. The reaction was stirred at 90 °C for about 18 h and then quenched with the addition of saturated NH_4Cl aq. Solution (8 mL). The product was extracted with ethyl acetate (3 × 20 mL) and the combined organic layers were separated, washed with brine, dried over anhydrous Na_2SO_4, and concentrated under reduced pressure to yield a residue that is purified by flash chromatography on silica gel. Yields, purification methods and other analytical data are reported below.

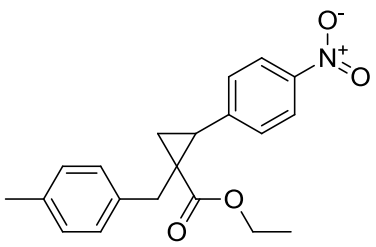

Ethyl 1-(4-methylbenzyl)-2-(4-nitrophenyl)cyclopropane-1-carboxylate (14). The product was obtained as a yellow oil in 9% yield after purification by flash column chromatography using Ethyl Acetate/ Petroleum Ether (1:99) as eluent. ^{1}H NMR (300 MHz, $CDCl_3$) δ 8.18 (d, *J* = 8.8 Hz, 2H), 7.39 (d, *J* = 8.4 Hz, 2H), 7.00 (q, *J* = 8.1 Hz, 4H), 4.15 (tt, *J* = 7.1, 3.5 Hz, 2H), 3.12 (d, *J* = 15.6 Hz, 1H), 2.99 – 2.82 (m, 1H), 2.29 (s, 3H), 2.08 – 1.88 (m, 2H), 1.47 (dd, *J* = 7.2, 5.3 Hz, 1H), 1.21 (t, *J* = 7.1 Hz, 3H).

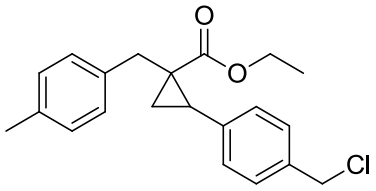

Ethyl 2-(4-(chloromethyl)phenyl)-1-(4-methylbenzyl)cyclopropane-1-carboxylate (15). Purification by flash column chromatography on silica gel using Ethyl Acetate/ Petroleum Ether (1:99→3:97) afforded the product as a colourless oil in 30% yield. ^{1}H NMR (400 MHz, $CDCl_3$) δ 7.39 (d, *J* = 7.5 Hz, 2H), 7.27 (d, *J* = 7.9 Hz, 2H), 7.06 (s, 4H), 4.62 (s, 2H), 4.25 – 4.09 (m, 2H), 3.20 (d, *J* = 15.4 Hz, 1H), 2.86 (t, *J* = 7.9 Hz, 1H), 2.32 (s, 3H), 1.98 (d, *J* = 15.6 Hz, 2H), 1.49 – 1.38 (m, 1H), 1.24 (t, *J* = 7.1 Hz, 3H).

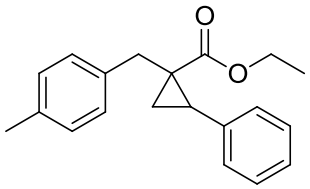

Ethyl 1-(4-methylbenzyl)-2-phenylcyclopropane-1-carboxylate (22). Flash chromatography on silica gel using Ethyl Acetate/ Petroleum Ether (1:99) afforded the product as yellow oil in 65% yield. ^{1}H NMR (300 MHz, $CDCl_3$) δ 7.30 (dddd, *J* = 13.4, 11.6, 7.5, 3.7 Hz, 5H), 7.03 (s, *J* = 7.9 Hz, 4H), 4.21 – 4.08 (m, 2H), 3.22 – 3.06 (m, 1H), 2.86 – 2.77 (m, 1H), 2.29 (s, 3H), 1.91 – 1.83 (m, 2H), 1.40 (dd, *J* = 7.2, 5.0 Hz, 1H), 1.21 (t, *J* = 7.1 Hz, 3H).

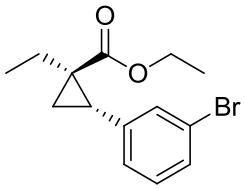

***Trans*-ethyl-2-(3-bromophenyl)-1-ethylcyclopropane-1-carboxylate (75).** Purification by flash column chromatography on silica gel using Ethyl Acetate/ Petroleum Ether (1:99) afforded the product as a colourless oil in 73% yield. ^{1}H NMR (300 MHz, $CDCl_3$) δ 7.47 – 7.28 (m, 2H), 7.20 – 7.06 (m, 2H), 4.38 – 4.05 (m, 2H), 2.89 – 2.64 (m, 1H), 1.71 – 1.59 (m, 2H), 1.29 (td, *J* = 7.1, 2.7 Hz, 3H), 1.12 (dd, *J* = 7.1, 4.7 Hz, 1H), 0.96 – 0.78 (m, 4H).

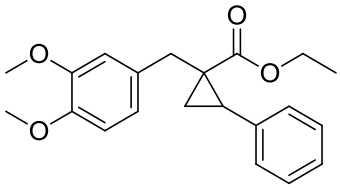

Ethyl 1-(3,4-dimethoxybenzyl)-2-phenylcyclopropanecarboxylate (101). Purification by flash column chromatography on silica gel using Ethyl Acetate/ Petroleum Ether (1:99→5:95) afforded the product as a yellow oil in 46% yield. ^{1}H NMR (300 MHz, $CDCl_3$) δ 7.40 – 7.19 (m, 5H), 6.81 – 6.57 (m, 3H), 4.21 – 4.06 (m, 2H), 3.83 (s, 3H), 3.80 (s, 3H), 3.13 (d, *J* = 15.6 Hz, 1H), 2.86 (dd, *J* = 8.9, 7.5 Hz, 1H), 2.04 (d, *J* = 3.6 Hz, 1H), 1.86 (ddd, *J* = 9.1, 4.9, 1.2 Hz, 1H), 1.39 (dd, *J* = 7.2, 4.9 Hz, 1H), 1.21 (dd, *J* = 8.0, 6.3 Hz, 3H).

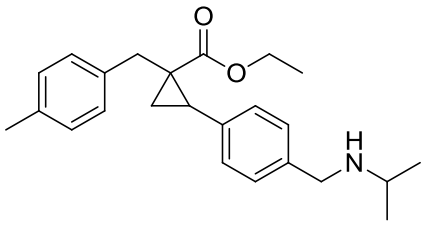

Ethyl 2-(4-((isopropylamino)methyl)phenyl)-1-(4-methylbenzyl)cyclopropane-1-carboxylate (19). Isopropylamine (26 µL, 0.292 mmol) was added dropwise to compound **15** (50 mg, 0.15 mmol) in neat at 0 °C, and the mixture was allowed to stir at room temperature for 24 h. The reaction was quenched with the addition of 4M NaOH aq. solution, extracted with dichloromethane (3 × 5 mL), and the combined organic layers were separated, washed with brine, dried over anhydrous Na_2SO_4, and concentrated under reduced pressure. The residue obtained was purified by flash chromatography on silica gel using Methanol/ Dichloromethane (2:98) to obtain the title compound as a colourless oil in 60% yield. ^{1}H NMR (300 MHz, $CDCl_3$) δ 7.36 – 7.19 (m, 4H), 7.05 (s, 4H), 4.27 – 4.06 (m, 2H), 3.81 (s, 2H), 3.19 (d, *J* = 15.6 Hz, 1H), 2.87 (ddd, *J* = 16.3, 13.4, 7.1 Hz, 2H), 2.31 (s, 3H), 1.93 – 1.79 (m, 2H), 1.40 (dd, *J* = 7.2, 5.0 Hz, 1H), 1.22 (t, *J* = 7.1 Hz, 3H), 1.14 (d, *J* = 6.3 Hz, 6H).

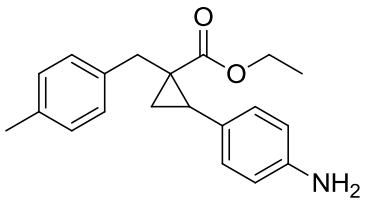

Ethyl 2-(4-aminophenyl)-1-(4-methylbenzyl)cyclopropane-1-carboxylate (17). Pd/C (18 mg) and triethylsilane (73 µL, 0.46 mmol) were added portion-wise to a solution of compound **14** (44 mg, 0.13 mmol) in dry methanol (6 mL), and the reaction mixture was stirred at room temperature under argon until complete consumption of the starting material. After filtration through

a plug of celite, the organic layers were washed with brine, dried over anhydrous sodium sulfate, and concentrated under reduced pressure to afford the target compound as a yellow oil in quantitative yield. ^{1}H NMR (400 MHz, MeOD) δ 7.05 – 6.97 (m, 6H), 6.72 (d, *J* = 8.5 Hz, 2H), 4.75 (s, 2H), 4.10 (dq, *J* = 11.0, 3.5 Hz, 2H), 3.06 (d, *J* = 15.5 Hz, 1H), 2.68 (dd, *J* = 9.2, 7.3 Hz, 1H), 2.27 (s, 3H), 1.98 (d, *J* = 15.5 Hz, 1H), 1.74 (ddd, *J* = 9.2, 4.9, 1.3 Hz, 1H), 1.38 (dd, *J* = 7.2, 4.9 Hz, 1H), 1.19 (t, *J* = 7.1 Hz, 3H).

General procedure for the synthesis amides (24–30): To a solution of 1-(4-methylbenzyl)-2-phenylcyclopropanecarboxylic acid (1 eq) in dry DMF (20 mL/ mmol), *N*-ethyldiisopropylamine (5 eq), 1-hydroxybenzotriazole hydrate (1.5 eq) and N-(3-Dimethylaminopropyl)-N'-ethylcarbodiimide hydrochloride (2 eq) were added in one portion. The reaction mixture was stirred at room temperature for 30 min and then the proper amine (2 eq) was added. Afterwards, reaction mixture was heated at 50 °C overnight. Volatiles were evaporated and the residue was solubilized in acetonitrile (1 mL), filtered and purified by HPLC. Yields and other analytical data are reported below.

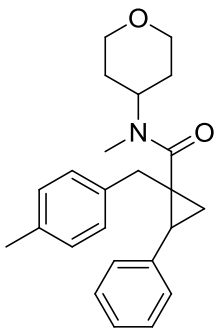

N-methyl-1-(4-methylbenzyl)-2-phenyl-N-(tetrahydro-2H-pyran-4-yl)cyclopropane-1-carboxamide (24). Colourless oil in 45% yield.^{1}H NMR (400 MHz, $CDCl_3$) δ 7.41 – 7.32 (m, 2H), 7.31 – 7.25 (m, 3H), 7.02 – 6.94 (m, 2H), 6.87 (s, 2H), 4.50 (s, 1H), 3.99 (d, *J* = 8.8 Hz, 2H), 3.44 (t, *J* = 12.3 Hz, 2H), 2.77 (s, 4H), 2.51 – 2.43 (m, 1H), 2.38 (d, *J* = 14.3 Hz, 1H), 2.26 (s, 3H), 1.77 –

1.58 (m, 3H), 1.36 (dd, *J* = 6.6, 5.9 Hz, 1H), 0.83 (dd, *J* = 6.5, 3.3 Hz, 2H).^{13}C NMR (101 MHz, $CDCl_3$) δ 179.66, 147.71, 136.63, 135.75, 131.71, 128.58, 128.53, 128.21, 126.41, 67.15, 59.84, 36.93, 29.54, 27.82, 25.45, 22.51, 20.85, 13.97. HRMS (ESI): calculated for $C_{24}H_{30}O_2N$ [M+H] 364.22711 found 364.22717.

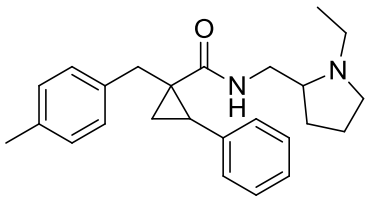

N-((1-ethylpyrrolidin-2-yl)methyl)-1-(4-methylbenzyl)-2-phenylcyclopropane-1-carboxamide (25). White oil in 34% yield. ^{1}H NMR (400 MHz, $CDCl_3$) δ 8.55 (s, 1H), 7.35 – 7.20 (m, 4H), 7.16 – 6.95 (m, 5H), 3.54 – 3.35 (m, 3H), 3.21 – 3.07 (m, 1H), 2.70 – 2.52 (m, 3H), 2.31 – 2.17 (m, 4H), 2.10 – 1.44 (m, 6H), 1.44 – 1.30 (m, 1H), 1.23 – 1.11 (m, 2H), 1.07 – 0.91 (m, 2H). ^{13}C NMR (101 MHz, $CDCl_3$) δ 168.80, 136.98, 136.15, 135.12, 129.08, 128.72, 128.66, 128.10, 126.54, 53.27, 52.85, 40.74, 33.80, 33.25, 31.17, 30.41, 28.12, 23.01, 20.73, 17.15, 10.46. HRMS (ESI): calculated for $C_{25}H_{32}ON_2$ [M+H] 377.25874 found 377.25821.

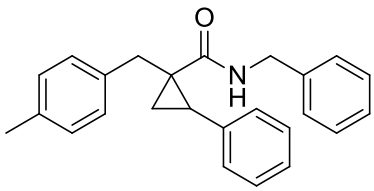

N-benzyl-1-(4-methylbenzyl)-2-phenylcyclopropane-1-carboxamide (26). Pearl powder in 55% yield. ^{1}H NMR (400 MHz, $CDCl_3$) δ 7.42 – 7.17 (m, 8H), 7.05 (dd, *J* = 18.9, 8.1 Hz, 4H), 6.92 – 6.77 (m, 2H), 5.84 (s, 1H), 4.43 (dd, *J* = 15.0, 5.8 Hz, 1H), 4.28 (dd, *J* = 15.0, 4.9 Hz, 1H), 3.04 – 2.90 (m, 1H), 2.83 (d, *J* = 17.5 Hz, 1H), 2.38 – 2.20 (m, 4H), 1.99 (dd, *J* = 8.6, 4.1 Hz, 1H), 1.44 (dd, *J* =

7.0, 4.7 Hz, 1H). ^{13}C NMR (101 MHz, $CDCl_3$) δ 173.81, 138.49, 137.76, 136.62, 135.92, 129.87, 129.60, 128.82, 128.70, 128.38, 127.61, 127.52, 127.14, 44.33, 34.65, 31.04, 30.80, 21.40, 18.90. HRMS (ESI): calculated for $C_{25}H_{28}ON$ [M+H] 356.20089 found 356.20071.

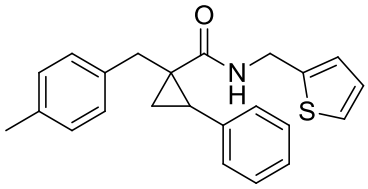

1-(4-methylbenzyl)-2-phenyl-N-(thiophen-2-ylmethyl)cyclopropane-1-carboxamide (27). Pearl powder in 56% yield. ^{1}H NMR (400 MHz, $CDCl_3$) δ 7.37 – 7.21 (m, 5H), 7.15 (d, *J* = 5.1 Hz, 1H), 7.03 (q, *J* = 8.2 Hz, 4H), 6.92 – 6.81 (m, 1H), 6.65 (d, *J* = 3.1 Hz, 1H), 5.89 (s, 1H), 4.52 (d, *J* = 4.4 Hz, 2H), 2.94 (t, *J* = 8.1 Hz, 1H), 2.83 (d, *J* = 17.3 Hz, 1H), 2.32 – 2.23 (m, 4H), 1.96 (dd, *J* = 9.1, 4.7 Hz, 1H), 1.47 – 1.36 (m, 1H). ^{13}C NMR (101 MHz, $CDCl_3$) δ 173.81, 141.41, 137.71, 136.65, 135.79, 129.89, 129.67, 128.76, 128.42, 127.22, 127.13, 125.83, 125.24, 39.29, 34.50, 31.33, 30.82, 21.43, 18.86. HRMS (ESI): calculated for $C_{23}H_{24}ONS$ [M+H] 362.15731 found 362.15735.

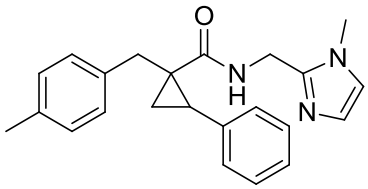

N-((1-methyl-1H-imidazol-2-yl)methyl)-1-(4-methylbenzyl)-2-phenylcyclopropane-1-carboxamide (28). Yellow oil in 52% yield.^{1}H NMR (400 MHz, $CDCl_3$) δ 8.33 (s, 1H), 7.28 (tdd, *J* = 7.7, 4.9, 3.7 Hz, 5H), 7.03 – 6.88 (m, 5H), 6.77 (d, *J* = 1.4 Hz, 1H), 4.47 (dd, *J* = 5.7, 1.9 Hz, 2H), 3.55 (d, *J* = 16.5 Hz, 3H), 2.96 (d, *J* = 16.8 Hz, 1H), 2.79 – 2.67 (m, 1H), 2.26 (s, *J* = 8.6 Hz, 3H), 2.18 (d, *J* = 16.8 Hz, 1H), 1.94 (ddd, *J* = 9.1, 5.0, 1.3 Hz, 1H), 1.38 (dd, *J* = 7.0,

5.0 Hz, 1H). ^{13}C NMR (101 MHz, $CDCl_3$) δ 173.80, 167.08, 144.91, 137.11, 135.84, 129.33, 129.10, 128.40, 128.16, 126.89, 125.37, 121.32, 34.72, 34.10, 33.23, 31.23, 30.84, 21.07, 17.49. HRMS (ESI): calculated for $C_{23}H_{26}N_3O$ [M+H] 360.20704 found 360.20645.

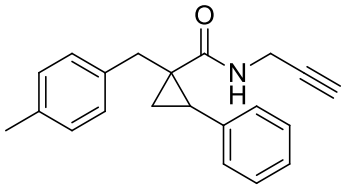

1-(4-methylbenzyl)-2-phenyl-N-(prop-2-yn-1-yl)cyclopropane-1-carboxamide (29). Pearl powder in 57% yield. ^{1}H NMR (400 MHz, $CDCl_3$) δ 7.34 – 7.28 (m, 2H), 7.26 – 7.20 (m, 2H), 7.13 – 6.97 (m, 5H), 5.73 (s, 1H), 3.93 (tddd, *J* = 32.3, 27.2, 5.3, 2.5 Hz, 2H), 3.02 – 2.78 (m, 2H), 2.30 (d, *J* = 3.3 Hz, 4H), 2.13 (t, *J* = 2.5 Hz, 1H), 1.93 (ddd, *J* = 9.1, 4.7, 1.3 Hz, 1H), 1.41 (dd, *J* = 7.1, 4.8 Hz, 1H). ^{13}C NMR (101 MHz, $CDCl_3$) δ 173.62, 137.25, 136.42, 135.34, 129.60, 129.37, 128.90, 128.46, 128.10, 126.96, 79.61, 71.47, 33.98, 31.19, 29.81, 21.12, 18.62. HRMS (ESI): calculated for $C_{21}H_{22}ON$ [M+H] 304.16959 found 304.16946.

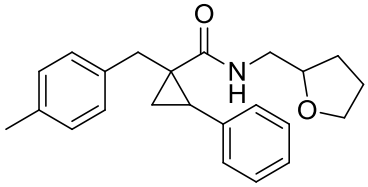

1-(4-methylbenzyl)-2-phenyl-N-((tetrahydrofuran-2-yl)methyl)cyclopropane-1-carboxamide (30). White oil in 51% yield. ^{1}H NMR (400 MHz, $CDCl_3$) δ 7.40 – 7.17 (m, 5H), 7.16 – 6.96 (m, 4H), 5.93 (s, 1H), 3.69 – 3.50 (m, 2H), 3.45 – 3.30 (m, 2H), 3.21 (d, *J* = 13.6 Hz, 1H), 2.93 – 2.79 (m, 2H), 2.36 – 2.19 (m, 4H), 2.01 (dd, *J* = 8.2, 4.7 Hz, 1H), 1.87 (dd, *J* = 9.0, 4.6 Hz, 1H), 1.80 – 1.65 (m, 2H), 1.39 (ddd, *J* = 10.4, 7.6, 4.0 Hz, 2H). ^{13}C NMR

(101 MHz, $CDCl_3$) δ 173.41, 128.99, 128.94, 128.89, 127.99, 127.80, 127.66, 126.44, 67.71, 42.85, 42.16, 33.82, 30.36, 27.96, 27.44, 25.49, 25.36, 20.70, 18.08. HRMS (ESI): calculated for $C_{23}H_{28}O_2N$ [M+H] 350.21146 found 350.21121.

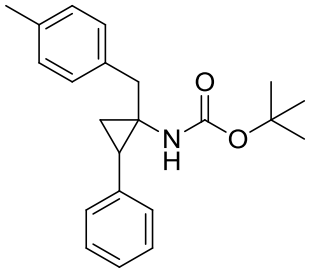

Tert-butyl (1-(4-methylbenzyl)-2-phenylcyclopropyl)carbamate (31). Dry triethylamine (300 µL, 2.2 mmol) and diphenylphosphoryl azide (365 µL, 1.7 mmol) were added to a solution of compound **23** (409 mg, 1.5 mmol) in dry *t*-BuOH (5 mL). After stirring overnight at 90 °C under nitrogen atmosphere, the reaction mixture was then concentrated under vacuum and gently poured into a 10% Na_2CO_3 aq. solution. The mixture was extracted with Et_2O (3 × 40 mL) and the organic layers separated, washed with brine, dried over anhydrous Na_2SO_4 and concentrated under reduced pressure, to give a black pitch that was purified by flash chromatography on silica gel using ethyl acetate/ petroleum ether (1:99→3:97). The title compound was obtained as a yellowish oil in 50% yield. ^{1}H NMR (400 MHz, $CDCl_3$) δ 7.35 (t, *J* = 36.4 Hz, 5H), 7.06 (d, *J* = 6.6 Hz, 2H), 6.91 (d, *J* = 6.9 Hz, 2H), 4.82 (s, 1H), 2.97 (d, *J* = 13.4 Hz, 1H), 2.60 – 2.43 (m, 1H), 2.32 (s, 3H), 2.12 – 1.93 (m, 2H), 1.49 (s, *J* = 53.5 Hz, 9H), 1.14 (d, *J* = 6.0 Hz, 1H).

General procedure for the preparation of sulfonamides (32 and 33): Trifluoroacetic acid (55 eq) was added dropwise to a solution of tert-butyl (1-(4-methylbenzyl)-2-phenylcyclopropyl)carbamate (1 eq) in dichloromethane (18 mL/mmol) kept at 0 °C, and the reaction mixture was stirred at the same

temperature for 1 h. After removal of the solvent in vacuum, the residue was dissolved in dry dichloromethane (7 mL/mmol) and cooled to -15 °C under nitrogen atmosphere. Dry triethylamine (3 eq) and the proper sulfonyl chloride (1 eq) were then added, and, after stirring at -15 °C for 1 h, additional triethylamine (3 eq) and sulfonyl chloride (0.1 eq) were added dropwise. After 90 min, the reaction was quenched with the addition of water (2 mL), and the organic layers were separated, washed with brine, dried over anhydrous Na_2SO_4, filtrated and concentrated under reduced pressure to obtain a residue that was purified by flash column chromatography on silica gel using Ethyl Acetate/ Petroleum Ether (9:91). Yields, purification methods and other analytical data are reported below.

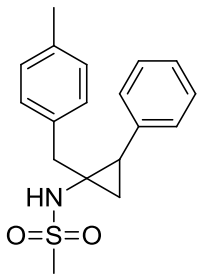

N-(1-(4-methylbenzyl)-2-phenylcyclopropyl)methanesulfonamide (32). The product was obtained as a pearl powder in 61% yield. ^{1}H NMR (400 MHz, $CDCl_3$) δ 7.49 – 7.32 (m, 4H), 7.31 (dd, *J* = 18.9, 11.8 Hz, 1H), 7.09 (dd, *J* = 21.7, 7.7 Hz, 4H), 4.76 (s, 1H), 3.02 (d, *J* = 15.2 Hz, 4H), 2.85 (t, *J* = 8.3 Hz, 1H), 2.33 (s, 3H), 2.13 (d, *J* = 14.8 Hz, 1H), 1.43 – 1.33 (m, 2H). ^{13}C NMR (101 MHz, $CDCl_3$) δ 136.78, 136.38, 134.54, 129.42, 129.33, 129.22, 128.45, 126.93, 44.01, 41.94, 38.98, 29.83, 21.02, 18.14. HRMS (ESI): calculated for $C_{18}H_{21}O_2NS$ [M+H] 316.13658 found 316.13721.

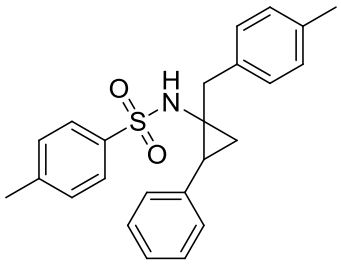

4-methyl-N-(1-(4-methylbenzyl)-2-phenylcyclopropyl)benzenesulfonamide (33). The product was obtained as a white powder in 50% yield. ^{1}H NMR (400 MHz, $CDCl_3$) δ 7.81 (d, *J* = 8.3 Hz, 2H), 7.43 – 7.23 (m, 7H), 7.06 (d, *J* = 7.9 Hz, 2H), 6.87 (d, *J* = 7.9 Hz, 2H), 4.94 (s, 1H), 2.88 (d, *J* = 14.6 Hz, 1H), 2.64 (dt, *J* = 15.5, 7.8 Hz, 1H), 2.45 (s, 3H), 2.33 (s, 3H), 1.93 (s, 1H), 1.35 – 1.19 (m, 2H). ^{13}C NMR (101 MHz, $CDCl_3$) δ 143.44, 139.66, 137.06, 136.17, 134.57, 129.70, 129.31, 129.25, 129.16, 128.37, 127.17, 126.74, 41.88, 38.24, 28.86, 21.54, 21.02, 17.88. HRMS (ESI): calculated for $C_{25}H_{25}O_2NS$ [M+H] 392.16788 found 414.15045 [M+Na].

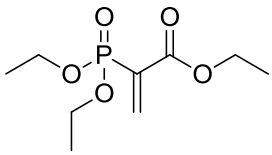

Ethyl 2-(diethoxyphosphoryl)acrylate (42). Triethyl phosphonoacetate (2.23 mmol, 440 µL) was added to a suspension of paraformaldehyde (4.46 mmol, 138 mg) in piperidine (0.02 mmol, 22 µL) and methanol (5.4 mL) at 80 °C, and the reaction mixture was stirred at the same temperature for about 36 h until consumption of the starting material. The solvent was then evaporated under reduced pressure, and the residue obtained was taken up in toluene (1 mL/ mmol), treated with *p*-toluenesulfonic acid monohydrate (0.22 mmol, 38 mg), and refluxed in a Dean-stark apparatus for 16 h. After removal of the solvent, the desired compound was obtained as a yellow-brownish oil in quantitative yield and used in the next reaction step without further

purification. ^{1}H NMR (400 MHz, $CDCl_3$) δ 6.98 (dd, *J* = 42.0, 1.7 Hz, 1H), 6.74 (dd, *J* = 20.4, 1.7 Hz, 1H), 4.41 – 4.03 (m, 6H), 1.32 (tdd, *J* = 13.6, 7.9, 5.6 Hz, 9H).

General procedure for the synthesis of phosphonoacetates (43–46): The desired heterocycle (1.1 eq) was added to a solution of ethyl 2-(diethoxyphosphoryl)acrylate (1 eq) in triethylamine (1 eq). The solution gradually turned pale yellow and after 15min at room temperature the starting material was completely consumed and the volatiles were evaporated to dryness. The crude material obtained was purified by flash column chromatography on silica gel using a gradient of Ethyl Acetate in Petroleum Ether to afford the desired compounds. Yields, purification methods and other analytical data are reported below.

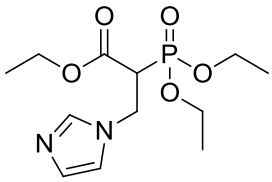

Ethyl 2-(diethoxyphosphoryl)-3-(1H-imidazol-1-yl)propanoate (43). Compound 43 was synthesized without triehtylamine and using dichloromethane (5 mL/ mmol) as solvent. Light yellow oil in quantitative yield. ^{1}H NMR (400 MHz, $CDCl_3$) δ 7.51 (d, *J* = 8.0 Hz, 1H), 7.01 (d, *J* = 12.1 Hz, 1H), 6.91 (s, 1H), 4.59 (ddd, *J* = 14.4, 10.8, 5.8 Hz, 1H), 4.40 (ddd, *J* = 14.3, 7.4, 3.5 Hz, 1H), 4.28 – 4.08 (m, 6H), 3.43 – 3.26 (m, 1H), 1.47 – 1.28 (m, 6H), 1.29 – 1.13 (m, 3H).

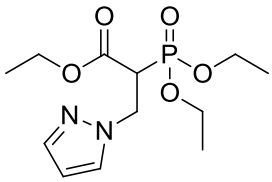

Ethyl 2-(diethoxyphosphoryl)-3-(1H-pyrazol-1-yl)propanoate (44). Light yellow oil in 35% yield. ^{1}H NMR (300 MHz, $CDCl_3$) δ 7.50 (d, *J* = 1.5 Hz, 1H), 7.41 (d, *J* = 1.9 Hz, 1H), 6.18 (t, *J* = 2.1 Hz, 1H), 4.70 (ddd, *J* = 13.8, 10.5, 7.1 Hz, 1H), 4.57 (ddd, *J* = 13.8, 6.7, 4.1 Hz, 1H), 4.26 – 4.05 (m, 6H), 3.75 (ddd, *J* = 23.2, 10.5, 4.1 Hz, 1H), 1.35 (tdd, *J* = 7.0, 2.0, 0.4 Hz, 6H), 1.20 (t, *J* = 7.1 Hz, 3H).

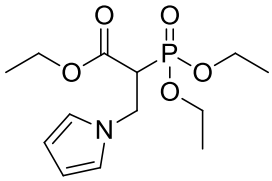

Ethyl 2-(diethoxyphosphoryl)-3-(1H-pyrrol-1-yl)propanoate (45). Light yellow oil in 30% yield. ^{1}H NMR (300 MHz, MeOD) δ 6.65 (t, *J* = 2.1 Hz, 2H), 6.01 (t, *J* = 2.1 Hz, 2H), 4.47 (ddd, *J* = 14.1, 10.5, 7.4 Hz, 1H), 4.32 (ddd, *J* = 14.1, 6.8, 4.2 Hz, 1H), 4.22 – 4.05 (m, 6H), 3.56 (ddd, *J* = 22.9, 10.5, 4.2 Hz, 1H), 1.43 – 1.26 (m, 6H), 1.19 (dd, *J* = 9.4, 4.9 Hz, 3H).

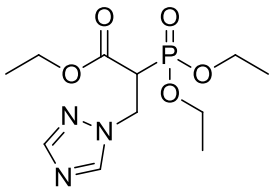

Ethyl 2-(diethoxyphosphoryl)-3-(1H-1,2,4-triazol-1-yl)propanoate (46). Light yellow oil in 86% yield. ^{1}H NMR (400 MHz, MeOD) δ 8.47 (s, 1H), 7.98 (s, 1H), 4.86 – 4.77 (m, 1H), 4.61 (dd, *J* = 14.1, 7.4 Hz, 1H), 4.29 – 4.09 (m, 7H), 1.35 (dt, *J* = 7.0, 6.4 Hz, 6H), 1.21 (t, *J* = 7.1 Hz, 3H).

General procedure for Wittig reaction (11, 39, 47-50, 89 and 98): *t*-BuOK (1M in THF, 1.2 eq) was added dropwise to a solution of the properly functionalized propanoate (1.1 eq) in dry THF (0.9 mL/ mmol) stirring at 0 °C under nitrogen atmosphere. After reacting for 30 min, the proper aldehyde

(1 eq) was added to the mixture, and the reaction was allowed to warm to room temperature. After complete consumption of the starting material according to TLC, volatiles were evaporated. The residue was taken up with Ethyl Acetate (15 mL), that was washed with water (3 × 10 mL), brine, dried over anhydrous Na_2SO_4 and concentrated under reduced pressure to yield a residue that was purified by flash column chromatography. Yields, purification methods and other analytical data are reported below.

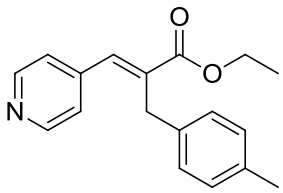

Ethyl (E)-2-(4-methylbenzyl)-3-(pyridin-4-yl)acrylate (11). Flash column chromatography eluting with Ethyl Acetate/ Petroleum Ether (1:9→3:7) afforded the desired product as a yellowish oil in 42% yield. **E:** ^{1}H NMR (300 MHz, CDCl3) δ 8.52 (d, *J* = 5.8 Hz, 2H), 8.02 (s, 1H), 7.49 – 7.31 (m, 5H), 7.15 (s, 2H), 4.24 (q, *J* = 7.1 Hz, 2H), 3.95 (s, 2H), 1.26 (dd, *J* = 12.0, 4.9 Hz, 3H).

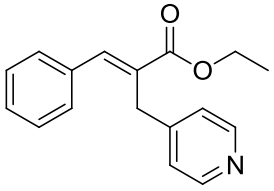

Ethyl (E)-3-phenyl-2-(pyridin-4-ylmethyl)acrylate (39). Purification by flash column chromatography on silica gel using Ethyl Acetate/ Petroleum Ether (2:8) allowed the isolation of the desired product in 40% yield as an orange oil. E and Z isomers were obtained. **E:** ^{1}H NMR (300 MHz, $CDCl_3$) δ 8.52 (d, *J* =

5.8 Hz, 2H), 8.02 (s, 1H), 7.49 – 7.31 (m, 5H), 7.15 (s, 2H), 4.24 (q, *J* = 7.1 Hz, 2H), 3.95 (s, 2H), 1.26 (dd, *J* = 12.0, 4.9 Hz, 3H).

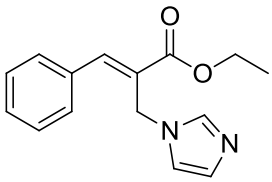

Ethyl (E)-2-((1H-imidazol-1-yl)methyl)-3-phenylacrylate (47). Purification using Methanol/ Dichloromethane (5:95) allowed the isolation of the product as a brown oil; 48% yield. **E:** ^{1}H NMR (300 MHz, $CDCl_3$) δ 8.03 (s, 1H), 7.40 (ddd, *J* = 32.4, 20.1, 7.5 Hz, 6H), 7.02 (s, 1H), 6.86 (s, 1H), 4.97 (s, 2H), 4.26 (q, *J* = 7.1 Hz, 2H), 1.30 (t, *J* = 7.1 Hz, 3H).

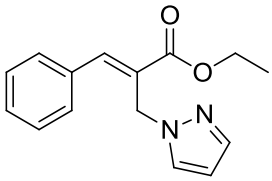

Ethyl (E)-2-((1H-pyrazol-1-yl)methyl)-3-phenylacrylate (48). Purification using Ethyl Acetate/ Petroleum Ether (5:95→2:8) allowed the isolation of the product as a colourless oil in 31% yield. **E:** ^{1}H NMR (300 MHz, $CDCl_3$) δ 8.03 (s, 1H), 7.67 (dd, *J* = 7.7, 1.3 Hz, 2H), 7.54 (dd, *J* = 8.7, 2.0 Hz, 2H), 7.47 – 7.36 (m, 3H), 6.32 – 6.20 (m, 1H), 5.18 (s, 2H), 4.25 (q, *J* = 7.1 Hz, 2H), 1.30 (t, *J* = 7.1 Hz, 3H).

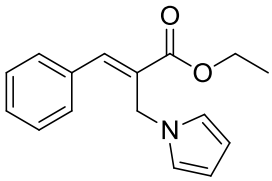

Ethyl (E)-2-((1H-pyrrol-1-yl)methyl)-3-phenylacrylate (49). Purification using Ethyl Acetate/ Petroleum Ether (1:99) allowed the isolation of the product as

a colourless oil in 69% yield. It wasn't possible to separate E/Z isomers and they were used as a mixture in the next step. ^{1}H NMR (300 MHz, $CDCl_3$) δ 7.98 (s, 1H), 7.38 (dd, *J* = 7.5, 2.2 Hz, 5H), δ 7.32 – 7.18 (m, 5H), 6.72 (t, *J* = 2.1 Hz, 2H), 6.65 (t, *J* = 2.1 Hz, 2H), 6.57 (s, 1H), 6.12 (t, *J* = 2.2 Hz, 4H), 4.94 (s, 2H), 4.84 (d, *J* = 1.5 Hz, 2H), 4.25 (q, *J* = 7.1 Hz, 2H), 4.09 (q, *J* = 7.1 Hz, 2H), 1.29 (t, *J* = 7.1 Hz, 3H),1.06 (t, *J* = 7.1 Hz, 3H).

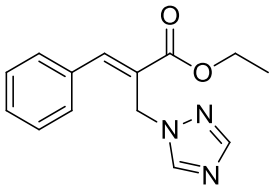

Ethyl (E)-2-((1H-1,2,4-triazol-1-yl)methyl)-3-phenylacrylate (50). Purification using Ethyl Acetate/ Petroleum Ether (2:8→1:1) allowed the isolation of the product as a white powder in 44% yield. **E:** ^{1}H NMR (300 MHz, $CDCl_3$) δ 8.23 (s, 1H), 8.06 (s, 1H), 7.97 (s, 1H), 7.77 – 7.62 (m, 2H), 7.57 – 7.34 (m, 3H), 5.20 (s, 2H), 4.26 (q, *J* = 7.1 Hz, 2H), 1.31 (t, *J* = 7.1 Hz, 3H).

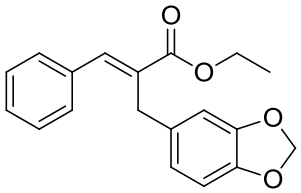

Ethyl 2-(benzo[d][1,3]dioxol-5-ylmethyl)-3-phenylacrylate (89). Purification by flash column chromatography using Ethyl Acetate/ Petroleum Ether (2:98→ 10:90) afforded the product as a colourless oil in 47% yield but it wasn't possible to isolate Z and E isomers. ^{1}H NMR (300 MHz, $CDCl_3$) δ 7.89 (s, 1H), 7.49 – 7.11 (m, 8H), 6.80 – 6.58 (m, 5H), 5.92 (d, *J* = 3.5 Hz, 3H), 4.22 (q, *J* = 7.1 Hz, 2H), 4.05 (d, *J* = 7.1 Hz, 1H), 3.86 (s, 2H), 3.66 (s, 1H), 1.36 – 1.21 (m, 5H), 1.02 (t, *J* = 7.1 Hz, 1H).

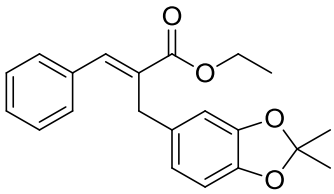

Ethyl 2-((2,2-dimethylbenzo[d][1,3]dioxol-5-yl)methyl)-3-phenylacrylate (98). Purification by flash column chromatography using Ethyl Acetate/ *n*-Hexane (1:99) afforded the mixture of cis and trans isomers as a colourless oil in 38% yield. ^{1}H NMR (300 MHz, $CDCl_3$) δ 7.87 (s, 1H), 7.45 – 7.20 (m, 8H), 6.71 – 6.53 (m, 6H), 4.22 (q, *J* = 7.1 Hz, 1H), 4.05 (q, *J* = 7.1 Hz, 2H), 3.84 (s, 2H), 3.64 (d, *J* = 1.3 Hz, 2H), 1.66 (dd, *J* = 5.0, 2.0 Hz, 11H), 1.27 (t, *J* = 7.1 Hz, 3H), 1.02 (t, *J* = 7.1 Hz, 3H).

General procedure for Corey-Chaykovsky reaction (12, 40, 51–54 and 90): Trimethylsufoxonium iodide (1.2 eq) was added to a suspension of NaH (1.2 eq) in dry DMSO (5 mL/ mmol) stirred under nitrogen atmosphere, and the reaction mixture was stirred at room temperature for 1h. After cooling to 0°C, a solution of the desired acrylate intermediate (1 eq) in dry DMSO (2 mL/ mmol) was added dropwise over 20 min, and the resulting mixture was allowed to stir at room temperature overnight. Water (80 mL) was added and the resulting solution was extracted with ethyl acetate (3 × 30 mL). The organic phases were separated, washed with brine, dried over anhydrous Na_2SO_4, filtered and concentrated under reduced pressure to give a residue that is purified by flash column chromatography to yield the desired intermediate. Yields, purification methods and other analytical data are reported below.

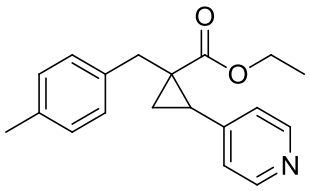

Ethyl-1-(4-methylbenzyl)-2-(pyridin-4-yl)cyclopropane-1-carboxylate (12). Purification by column chromatography eluting Ethyl Acetate/ Petroleum Ether (1:9→3:7) afforded the product as a yellowish oil in 72% yield. ^{1}H NMR (300 MHz, $CDCl_3$) δ: 7.17-7.14 (m, 4H); 7.05-6.99 (m, 4H); 4.19-4.12 (m, 2H); 3.12 (d, J= 15.54, 1H); 2.82 (t, J= 8.1, 1H); 2.30 (s, 3H); 2.07 (d, J= 15.69, 1H); 1.93-1.88 (m, 1H); 1.46 (t, J= 6.72, 1H); 1.24 (t, J= 9.03, 3H).

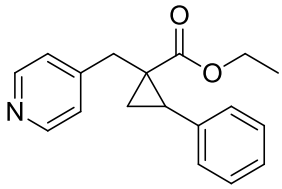

Ethyl 2-phenyl-1-(pyridin-4-ylmethyl)cyclopropane-1-carboxylate (40). Purification by flash column chromatograpy using Ethyl Acetate/ Petroleum Ether (2:8→4:6) allowed the isolation of the desired compound in 48% yield as a yellow oil. ^{1}H NMR (300 MHz, $CDCl_3$) δ 8.42 (s, 2H), 7.41 – 7.14 (m, 5H), 7.08 (d, *J* = 4.5 Hz, 2H), 4.13 (qd, *J* = 7.1, 4.0 Hz, 2H), 3.10 (d, *J* = 16.1 Hz, 1H), 2.90 (dd, *J* = 20.2, 12.7 Hz, 1H), 2.11 (d, *J* = 16.1 Hz, 1H), 1.92 (ddd, *J* = 9.2, 5.0, 1.2 Hz, 1H), 1.42 (dd, *J* = 7.2, 5.0 Hz, 1H), 1.17 (t, *J* = 7.1 Hz, 3H).

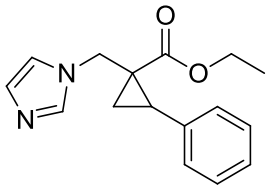

Ethyl 1-((1H-imidazol-1-yl)methyl)-2-phenylcyclopropane-1-carboxylate (51). Purification using Methanol/ Dichloromethane (1:99→5:95) afforded

the product as a brown oil in 64% yield. ^{1}H NMR (400 MHz, $CDCl_3$) δ 7.34 (ddd, *J* = 14.6, 7.7, 6.2 Hz, 3H), 7.25 – 7.16 (m, 3H), 6.93 (s, 1H), 6.73 (s, 1H), 4.34 (dd, *J* = 14.9, 0.6 Hz, 1H), 4.21 (qd, *J* = 7.1, 2.7 Hz, 2H), 3.45 (d, *J* = 14.9 Hz, 1H), 3.13 – 3.01 (m, 1H), 1.82 (ddd, *J* = 9.2, 5.3, 1.0 Hz, 1H), 1.50 (dd, *J* = 7.4, 5.4 Hz, 1H), 1.28 (t, *J* = 7.1 Hz, 3H).

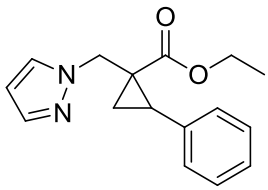

Ethyl 1-((1H-pyrazol-1-yl)methyl)-2-phenylcyclopropane-1-carboxylate (52). Purification using Ethyl Acetate/ Petroleum Ether (5:95→1:9) afforded the product as a colourless oil in 58% yield. ^{1}H NMR (300 MHz, $CDCl_3$) δ 7.46 (dd, *J* = 6.3, 2.0 Hz, 2H), 7.41 – 7.27 (m, 5H), 6.18 (t, *J* = 2.1 Hz, 1H), 4.70 (d, *J* = 14.7 Hz, 1H), 4.31 – 4.11 (m, 2H), 3.43 (d, *J* = 14.8 Hz, 1H), 2.99 (t, *J* = 8.4 Hz, 1H), 1.91 – 1.77 (m, 2H), 1.27 (t, *J* = 7.1 Hz, 3H).

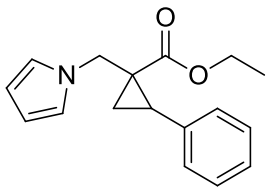

Ethyl 1-((1H-pyrrol-1-yl)methyl)-2-phenylcyclopropane-1-carboxylate (53). Purification using Ethyl Acetate/ Petroleum Ether (0.8:99.2) afforded the product as a slightly yellow solid in 33% yield. ^{1}H NMR (300 MHz, $CDCl_3$) δ 7.31 (ddd, *J* = 18.0, 14.2, 6.7 Hz, 5H), 6.53 (t, *J* = 1.9 Hz, 2H), 6.06 (t, *J* = 1.9 Hz, 2H), 4.48 (d, *J* = 14.9 Hz, 1H), 4.32 – 4.07 (m, 2H), 3.21 (d, *J* = 14.9 Hz, 1H), 3.00 (t, *J* = 8.3 Hz, 1H), 1.83 (dd, *J* = 8.7, 5.4 Hz, 1H), 1.50 (dd, *J* = 7.3, 5.4 Hz, 1H), 1.29 (t, *J* = 7.2 Hz, 3H).

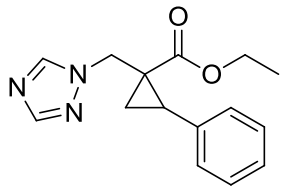

Ethyl 1-((1H-1,2,4-triazol-1-yl)methyl)-2-phenylcyclopropane-1-carboxylate (54). Purification using a gradient of Ethyl Acetate in Petroleum Ether afforded the product as a yellow oil in 38% yield. ^{1}H NMR (300 MHz, $CDCl_3$) δ 8.09 (d, *J* = 13.9 Hz, 1H), 7.86 (s, 1H), 7.42 – 7.25 (m, 5H), 4.71 (d, *J* = 14.7 Hz, 1H), 4.29 – 4.14 (m, 2H), 3.46 (dd, *J* = 14.4, 2.1 Hz, 1H), 3.17 – 3.01 (m, 1H), 1.86 (ddt, *J* = 9.2, 5.4, 3.3 Hz, 2H), 1.28 (t, *J* = 7.1 Hz, 3H).

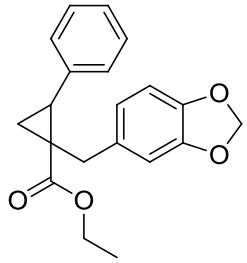

Ethyl 1-(benzo[d][1,3]dioxol-5-ylmethyl)-2-phenylcyclopropanecarboxylate (90). Purification by flash column chromatography using Ethyl Acetate/ Petroleum Ether (2:8) allowed the isolation of the product but it wasn't possible to separate the cis isomer from compound 90. ^{1}H NMR (400 MHz, MeOD) δ 8.95 – 8.67 (m, 8H), 8.35 – 8.23 (m, 3H), 8.18 (t, *J* = 4.9 Hz, 2H), 8.09 (dd, *J* = 7.9, 1.7 Hz, 1H), 7.44 (d, *J* = 2.7 Hz, 1H), 7.40 (s, 2H), 5.77 – 5.61 (m, 2H), 5.57 (q, *J* = 7.1 Hz, 1H), 5.20 (d, *J* = 1.0 Hz, 1H), 4.56 (d, *J* = 15.4 Hz, 1H), 4.35 (dd, *J* = 8.9, 7.5 Hz, 1H), 3.52 (d, *J* = 15.5 Hz, 1H), 3.34 (ddd, *J* = 9.2, 5.0, 1.2 Hz, 1H), 3.04 (dd, *J* = 7.2, 5.0 Hz, 1H), 2.76 (t, *J* = 7.1 Hz, 3H), 2.56 (t, *J* = 7.1 Hz, 2H).

General procedure for the hydrolysis of the esters (13, 16, 18, 20, 23, 41, 55–58, 77a-d and 91): LiOH (4 eq) was added to a solution of the ester (1 eq) in THF/MeOH/H_2O (3:1:1, 1 mL/ mmol) and the reaction mixture was heated in a microwave reactor set with the following parameters: 100 °C, 10 min, 300 W, 250 psi. After concentration of the mixture, 2N HCl aq. solution (10 mL) was added and the resulting slurry was extracted with ethyl acetate (3 × 20 mL). The collected organic phases were washed with brine, dried over anhydrous Na_2SO_4, filtered and concentrated under reduced pressure to give a crude material that is purified by flash column chromatography. Yields, purification methods and other analytical data are reported below.

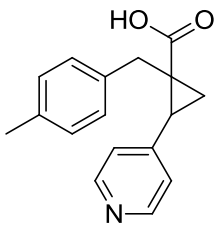

1-(4-methylbenzyl)-2-(pyridin-4-yl)cyclopropane-1-carboxylic acid (13). Purification by column chromatography eluting with Ethyl Acetate/ Petroleum Ether (1:9→3:7) afforded the desired product as a yellowish powder in 64% yield. ^{1}H NMR (300 MHz, $CDCl_3$) δ: 7.23-7.17 (m, 4H); 7.11-7.05 (m, 4H); 3.23 (d, J= 15.54, 1H); 2.87 (t, J= 8.1, 1H); 2.32 (s, 3H); 2.11 (d, J= 15.69, 1H); 1.96-1.92 (m, 1H); 1.53 (t, J= 6.72, 1H).^{13}C NMR (100.6 MHz, $CDCl_3$) δ: 183.64; 142.37; 127.41; 126.71; 126.49; 125.21; 124.23; 122.04; 35.09; 33.69; 30.72; 18.73; 11.45. MS (ESI): m/z: 268.5 [M+H]

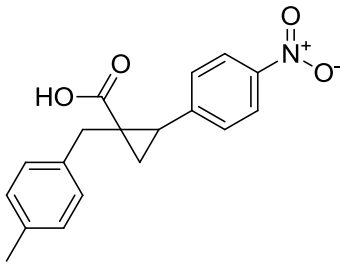

1-(4-methylbenzyl)-2-(4-nitrophenyl)cyclopropane-1-carboxylic acid (16). The product was obtained as a pale yellow oil in 47% yield after purification with Methanol/ Dichloromethane (1:99). ^{1}H NMR (400 MHz, $CDCl_3$) δ 8.20 (dd, *J* = 20.6, 11.5 Hz, 2H), 7.45 (d, *J* = 11.1 Hz, 2H), 7.14 – 6.98 (m, 4H), 3.18 (d, *J* = 15.7 Hz, 1H), 3.05 (t, *J* = 8.1 Hz, 1H), 2.34 (d, *J* = 9.4 Hz, 3H), 2.04 (dd, *J* = 10.8, 7.2 Hz, 2H), 1.63 – 1.53 (m, 1H). ^{13}C NMR (101 MHz, $CDCl_3$) δ 180.10, 147.30, 144.37, 136.17, 136.10, 130.37, 129.29, 128.69, 123.94, 33.23, 32.94, 31.61, 21.29, 19.50. HRMS (ESI): calculated for $C_{18}H_{16}O_4N$ [M-H]310.10738 found 310.10849.

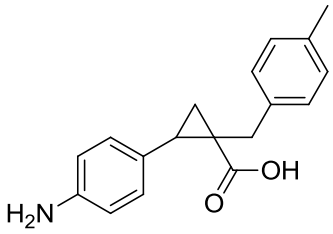

2-(4-aminophenyl)-1-(4-methylbenzyl)cyclopropane-1-carboxylic acid (18). The target compound was obtained as an orange semi-solid compound in 40% yield after purification with Methanol/ Dichloromethane (2:98). ^{1}H NMR (400 MHz, $CDCl_3$) δ 7.10 – 7.00 (m, 6H), 6.68 (d, *J* = 8.4 Hz, 2H), 3.20 (d, *J* = 15.7 Hz, 1H), 2.90 – 2.78 (m, 1H), 2.30 (s, 3H), 1.88 (dd, *J* = 14.5, 9.0 Hz, 2H), 1.36 (dd, *J* = 7.2, 5.0 Hz, 1H). ^{13}C NMR (101 MHz, $CDCl_3$) δ 180.83, 145.21, 137.16, 135.31, 130.25, 128.83, 128.57, 126.23, 115.20, 33.99, 32.64, 30.60, 21.00, 18.56. HRMS (ESI): calculated for $C_{18}H_{19}O_2N$ [M-H] 280.13321 found 280.13467.

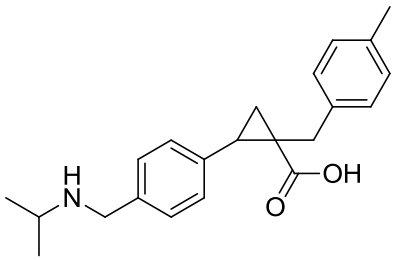

2-(4-((isopropylamino)methyl)phenyl)-1-(4-methylbenzyl)cyclopropane-1-carboxylic acid (20). Purification by flash chromatography on silica gel using Methanol/ Dichloromethane (8:92→1:9) afforded the product as white powder in 55% yield. ^{1}H NMR (400 MHz, MeOD) δ 7.48 (d, *J* = 8.1 Hz, 2H), 7.38 (d, *J* = 8.1 Hz, 2H), 7.00 (q, *J* = 8.1 Hz, 4H), 4.20 (s, 2H), 3.43 (dt, *J* = 13.1, 6.5 Hz, 1H), 3.37 (s, 1H), 3.05 (d, *J* = 15.5 Hz, 1H), 2.93 – 2.79 (m, 1H), 2.25 (s, 3H), 2.04 (d, *J* = 15.6 Hz, 1H), 1.78 (dd, *J* = 8.8, 4.9 Hz, 1H), 1.40 (d, *J* = 6.5 Hz, 7H). ^{13}C NMR (101 MHz, MeOD) δ 180.67, 139.28, 137.33, 134.73, 129.75, 129.71, 129.41, 128.16, 128.13, 50.42, 33.00, 31.66, 31.25, 19.59, 17.86, 16.67. HRMS (ESI): calculated for $C_{22}H_{27}O_2N$ [M-H] 336.19581 found 336.19809.

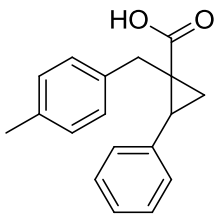

1-(4-methylbenzyl)-2-phenylcyclopropane-1-carboxylic acid (23). Purification by flash chromatography on silica gel using Methanol/ Dichloromethane (1:99) afforded the product as a yellow powder in 80% yield. ^{1}H NMR (400 MHz, $CDCl_3$) δ 7.46 – 7.21 (m, 5H), 7.06 (d, *J* = 13.0 Hz, 4H), 3.20 (d, *J* = 15.8 Hz, 1H), 2.97 (t, *J* = 7.9 Hz, 1H), 2.30 (s, 3H), 1.91 (d, *J* = 16.4 Hz, 2H), 1.47 (s, 1H).

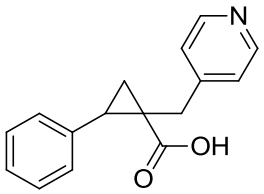

2-phenyl-1-(pyridin-4-ylmethyl)cyclopropane-1-carboxylic acid (41). The Ethyl Acetate organic phase was discarded and the combined organic phases obtained with the Chloroform/ Isopropanol mixture were dried over anhydrous sodium sulphate, filtered and concentrated under reduced pressure to afford 110 mg of the desired compound as a brown solid (25% yield). ^{1}H NMR (400 MHz, MeOD) δ 8.60 (d, *J* = 6.5 Hz, 2H), 7.84 (d, *J* = 6.4 Hz, 2H), 7.36 – 7.19 (m, 5H), 3.24 – 3.14 (m, 1H), 3.09 (dd, *J* = 9.2, 7.4 Hz, 1H), 2.75 (dd, *J* = 18.3, 10.7 Hz, 1H), 2.00 – 1.89 (m, 1H), 1.78 (dd, *J* = 7.3, 5.1 Hz, 1H). ^{13}C NMR (101 MHz, MeOD) δ 177.02, 164.94, 141.92, 137.27, 130.25, 129.54, 128.52, 35.97, 32.96, 30.62, 19.25. HRMS (ESI): calculated for $C_{16}H_{14}O_2N$ [M-H] 252.10191 found 252.10334.

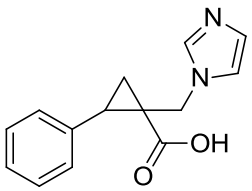

1-((1H-imidazol-1-yl)methyl)-2-phenylcyclopropane-1-carboxylic acid (55). Extractions with Chloroform/Isopropanol of the water phase allowed the isolation of the product as a light brown solid in 65% yield. ^{1}H NMR (400 MHz, MeOD) δ 8.41 (s, 1H), 7.47 – 7.17 (m, 7H), 4.37 (d, *J* = 14.9 Hz, 1H), 4.06 (d, *J* = 14.9 Hz, 1H), 3.14 (dd, *J* = 10.0, 6.7 Hz, 1H), 1.96 (dd, *J* = 7.5, 5.4 Hz, 1H), 1.89 – 1.78 (m, 1H). ^{13}C NMR (101 MHz, MeOD) δ 175.43, 137.00, 135.99, 130.01, 129.99, 128.88, 123.50, 120.37, 50.57, 33.00, 31.02, 19.02. HRMS (ESI): calculated for $C_{14}H_{13}O_2N_2$ [M-H] 241.09715 found 241.09817.

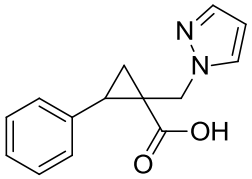

1-((1H-pyrazol-1-yl)methyl)-2-phenylcyclopropane-1-carboxylic acid (56). Purification by flash column chromatography using Methanol/ Dichloromethane (2.5:97.5) with 0.01% formic acid allowed the isolation of the desired product as a light brown powder in 89% yield. ^{1}H NMR (400 MHz, $CDCl_3$) δ 7.51 (s, 1H), 7.40 – 7.21 (m, 5H), 7.17 (s, 1H), 6.16 (s, 1H), 4.53 (d, *J* = 15.0 Hz, 1H), 3.68 (d, *J* = 15.1 Hz, 1H), 3.10 (t, *J* = 8.3 Hz, 1H), 1.92 (dd, *J* = 8.8, 5.4 Hz, 1H), 1.85 – 1.74 (m, 1H). ^{13}C NMR (101 MHz, $CDCl_3$) δ 177.80, 139.03, 135.14, 130.61, 129.26, 128.84, 127.72, 105.46, 50.52, 33.80, 31.01, 18.16. HRMS (ESI): calculated for $C_{14}H_{13}O_2N_2$ [M-H] 241.09715 found 241.09776.

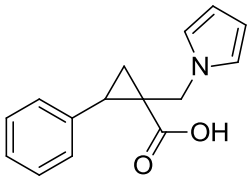

1-((1H-pyrrol-1-yl)methyl)-2-phenylcyclopropane-1-carboxylic acid (57). Purification by flash column chromatography using Methanol/ Dichloromethane (1:99) afforded the product as beige powder in 63% yield. ^{1}H NMR (300 MHz, $CDCl_3$) δ 7.44 – 7.21 (m, 5H), 6.57 (s, 2H), 6.08 (s, 2H), 4.51 (d, *J* = 15.1 Hz, 1H), 3.15 (dd, *J* = 17.8, 11.7 Hz, 2H), 1.92 (dd, *J* = 8.7, 5.6 Hz, 1H), 1.71 – 1.52 (m, 1H). ^{13}C NMR (75 MHz, $CDCl_3$) δ 179.62, 134.74, 128.89, 128.53, 127.48, 120.89, 107.62, 47.06, 33.90, 31.19, 17.50. HRMS (ESI): calculated for $C_{15}H_{14}O_2N$ [M-H] 240.10191 found 240.10257.

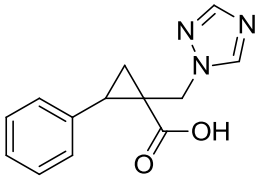

1-((1H-1,2,4-triazol-1-yl)methyl)-2-phenylcyclopropane-1-carboxylic acid (58). Purification by flash column chromatography using Methanol/ Dichloromethane (1:99) with 0.01% formic acid afforded the pure product as a white solid in 53% yield. ^{1}H NMR (400 MHz, $CDCl_3$) δ 8.49 (s, 1H), 7.95 (s, 1H), 7.46 – 7.21 (m, 5H), 4.80 (d, *J* = 14.7 Hz, 1H), 3.48 (d, *J* = 14.7 Hz, 1H), 3.19 (t, *J* = 8.3 Hz, 1H), 1.92 (dd, *J* = 10.6, 5.3 Hz, 2H).^{13}C NMR (101 MHz, $CDCl_3$) δ 176.02, 149.62, 143.90, 134.84, 128.93, 128.66, 127.52, 49.23, 32.94, 30.11, 17.47. HRMS (ESI): calculated for $C_{13}H_{12}O_2N_3$ [M-H] 242.09240 found 242.09300.

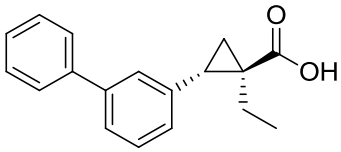

***Trans*-2-([1,1'-biphenyl]-3-yl)-1-ethylcyclopropane-1-carboxylic acid (77a).** Purified by flash cromatography (Methanol/ Dicloromethane 1:99); orange oil; 83% yield. ^{1}H NMR (300 MHz, $CDCl_3$) δ 7.64 – 7.53 (m, 2H), 7.50 – 7.33 (m, 6H), 7.20 (d, *J* = 7.5 Hz, 1H), 3.00 (t, *J* = 8.2 Hz, 1H), 1.84 – 1.73 (m, 1H), 1.73 – 1.63 (m, 1H), 1.28 (ddd, *J* = 20.4, 10.6, 5.9 Hz, 2H), 1.04 – 0.79 (m, 3H). ^{13}C NMR (75 MHz, $CDCl_3$) δ 181.33, 140.94, 140.66, 136.89, 128.50, 128.36, 127.93, 127.88, 127.12, 126.90, 125.49, 33.14, 30.93, 21.34, 18.31, 11.38. HRMS (ESI): calculated for $C_{18}H_{18}O_2$ [M+H] 265.12231 found 265.12341.

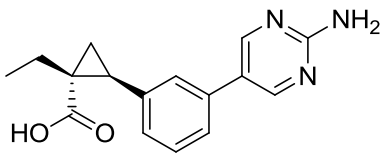

***Trans*-2-(3-(2-aminopyrimidin-5-yl)phenyl)-1-ethylcyclopropane-1-carboxylic acid (77b).** Purified by trituration with Diethyl Ether; white powder; 50% yield. ^{1}H NMR (400 MHz, MeOD) δ 8.83 (s, 2H), 7.50 (d, *J* = 7.7 Hz, 2H), 7.45 (dd, *J* = 18.9, 11.5 Hz, 1H), 7.30 (d, *J* = 7.6 Hz, 1H), 2.97 – 2.81 (m, 1H), 1.70 – 1.58 (m, 1H), 1.54 (dd, *J* = 13.9, 7.0 Hz, 1H), 1.36 (dd, *J* = 6.9, 4.9 Hz, 1H), 1.02 – 0.90 (m, 1H), 0.91 – 0.74 (m, 3H).^{13}C NMR (101 MHz, MeOD) δ 178.20, 156.96, 140.07, 133.28, 130.67, 130.32, 128.16, 125.62, 124.92, 32.98, 32.42, 22.71, 18.22, 11.84. HRMS (ESI): calculated for $C_{16}H_{17}N_3O_2$ [M+H] 282.12370 found 282.12488.

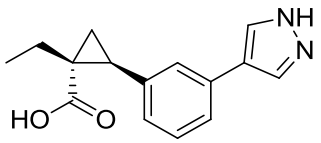

***Trans*-2-(3-(1H-pyrazol-4-yl)phenyl)-1-ethylcyclopropane-1-carboxylic acid (77c).** Purified by flash cromatography (Methanol/ Dicloromethane 1:99 + 0.1% of formic acid); slightly yellow powder; 21% yield. ^{1}H NMR (400 MHz, $CDCl_3$) δ 9.24 (s, 1H), 7.89 (s, 1H), 7.36 (d, *J* = 28.4 Hz, 3H), 7.09 (s, 1H), 2.96 (s, 1H), 1.75 (d, *J* = 23.1 Hz, 2H), 1.25 (dd, *J* = 20.5, 8.0 Hz, 2H), 0.94 (s, 3H).^{13}C NMR (101 MHz, $CDCl_3$) δ 180.49, 147.76, 146.79, 137.77, 133.41, 132.29, 128.94, 127.50, 127.26, 124.50, 33.22, 31.40, 21.92, 18.49, 11.85. HRMS (ESI): calculated for $C_{15}H_{16}N_2O_2$ [M+H] 255.11280 found 255.11413.

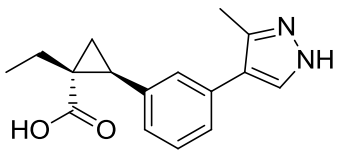

***Trans*-1-ethyl-2-(3-(3-methyl-1H-pyrazol-4-yl)phenyl)cyclopropane-1-carboxylic acid (77d).** Purified by flash chromatography (Methanol/

Dicloromethane 1:99 + 0.1% of formic acid); slightly yellow powder; 25% yield. ^{1}H NMR (300 MHz, $CDCl_3$) δ 7.71 (bs, 1H), 7.35 – 7.23 (m, 3H), 7.15 (d, *J* = 6.5 Hz, 1H), 2.97 – 2.92 (m, 1H), 2.45 (s, 3H) 1.81 – 1.75 (m, 2H), 1.37 – 1.26 (m, 1H), 1.13 (dd, *J* = 7.1, 4.7 Hz, 1H), 0.93 – 0.74 (m, 3H). ^{13}C NMR (101 MHz, $CDCl_3$) δ 181.47, 147.72, 147.65, 138.23, 134.23, 133.49, 128.94, 127.50, 127.26, 122.48, 33.22, 31.40, 21.92, 20.23, 18.49, 11.85. HRMS (ESI): calculated for $C_{16}H_{18}N_2O_2$ [M+H] 270.1368 found 270.3320.

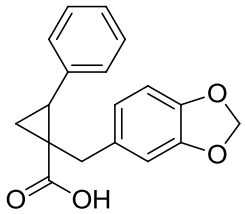

1-(benzo[d][1,3]dioxol-5-ylmethyl)-2-phenylcyclopropanecarboxylic acid (91). Reaction mixture was purified by flash column chromatography on silica gel using Ethyl Acetate/ Petroleum Ether (12.5:87.5) and the product was obtained as a white powder in 41% yield. ^{1}H NMR (300 MHz, $CDCl_3$) δ 7.43 – 7.19 (m, 5H), 6.68 (d, *J* = 7.9 Hz, 2H), 6.57 (d, *J* = 7.9 Hz, 1H), 5.90 (s, 2H), 3.15 (d, *J* = 15.6 Hz, 1H), 2.97 (t, *J* = 8.3 Hz, 1H), 1.97 – 1.79 (m, 2H), 1.46 (dd, *J* = 7.3, 5.2 Hz, 1H).

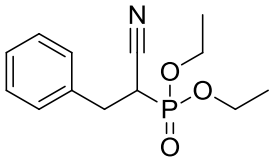

Diethyl (1-cyano-2-phenylethyl)phosphonate (35). Diethyl cyanomethylphosphonate **26** (2.43 mL, 1.5 mmol) was added under nitrogen atmosphere to a suspension of NaH 60% dispersion in mineral oil (900 mg, 2.25 mmol) in dry dimethoxyethane (15 mL) kept at 0 °C. After stirring 2 h at

room temperature, benzyl bromide (2.14 mL, 1.8 mmol) was added and the reaction was heated at 60 °C for 2 h. Water (10 mL) was carefully added and the resulting solution was extracted with ethyl acetate (3 × 10 mL). The organic phases were washed with brine, dried over anhydrous Na_2SO_4, filtered and concentrated under reduced pressure to give a crude material that was purified by flash column chromatography using Ethyl Acetate/ Petroleum Ether (1:9) as the eluent. The product was obtained as an oil in 90% yield. ^{1}H NMR (300 MHz, $CDCl_3$) δ 7.39 – 7.21 (m, 5H), 4.37 – 4.15 (m, 4H), 3.21 (ddt, *J* = 19.2, 11.1, 5.9 Hz, 3H), 1.38 (td, *J* = 7.1, 2.9 Hz, 6H).

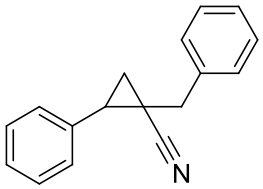

1-benzyl-2-phenylcyclopropanecarbonitrile (36). *n*-BuLi (5.4 mL, 13.48 mmol) was added under nitrogen atmosphere dropwise to a solution of diethyl (1-cyano-2-phenylethyl)phosphonate **27** (3.6 g, 13.48 mmol) in dry dimethoxyethane (15 mL) at room temperature. After stirring for 30 minutes, styrene oxide (1.03 mL, 9 mmol) was added in one portion and the reaction mixture was stirred at 90 °C overnight. After consumption of the starting material, saturated NH_4Cl aq. solution (10 mL) was added and the resulting solution was extracted with ethyl acetate (3 × 100 mL). The organic phases were washed with brine, dried over anhydrous Na_2SO_4, filtered and concentrated under reduced pressure to give a crude material that is purified by flash column chromatography using Ethyl Acetate/ Petroleum Ether (5:95) afforded the title compound as a white solid in 25% yield. ^{1}H NMR (300 MHz, $CDCl_3$) δ 7.46 – 7.25 (m, 8H), 7.09 (dd, *J* = 7.6, 1.6 Hz, 2H), 3.10 – 2.94 (m, 1H), 2.74 (d, *J* = 15.0 Hz, 1H), 2.22 (d, *J* = 15.0 Hz, 1H), 1.74 (ddd, *J* = 9.3, 5.9, 0.7 Hz, 1H), 1.49 (ddd, *J* = 11.6, 5.5, 3.9 Hz, 1H). ^{13}C NMR (75 MHz, $CDCl_3$) δ 137.0,

133.9, 129.2, 129.0, 128.8, 128.7, 128.6, 127.8, 127.2, 123.6, 35.4, 30.6, 17.3. HRMS (ESI): calculated for $C_{17}H_{15}N$ [M+H] 234.1204 found 234.1283.

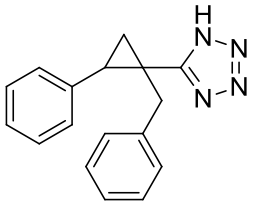

5-(1-benzyl-2-phenylcyclopropyl)-1H-tetrazole (37). Sodium azide (78 mg, 1.56 mmol) and triethylamine (167 µL, 1.2 mmol) were added to a solution of 1-benzyl-2-phenylcyclopropanecarbonitrile **28** (90 mg, 0.39 mmol) in DMF (3 mL) at room temperature. The reaction mixture was stirred under nitrogen atmosphere at 130 °C for 16 h until TLC monitoring revealed complete consumption of the starting material. 1N HCl aq. solution (10 mL) was added and the resulting solution was extracted with ethyl acetate (3 × 10 mL). The organic phases were washed with brine, dried over anhydrous Na_2SO_4, filtered and concentrated under reduced pressure to give a crude material that is purified by flash column chromatography using Ethyl Acetate/ Petroleum Ether (33:67). The product was obtained as an oil in 46% yield. ^{1}H NMR (300 MHz, $CDCl_3$) δ 7.92 (s, 1H), 7.46 – 7.09 (m, 10H), 3.19 (d, *J* = 16.3 Hz, 1H), 2.95 (dt, *J* = 22.9, 11.4 Hz, 1H), 2.49 (d, *J* = 16.3 Hz, 1H), 2.01 (ddd, *J* = 9.1, 5.3, 1.2 Hz, 1H), 1.72 (dd, *J* = 7.0, 5.3 Hz, 1H). ^{13}C NMR (101 MHz, $CDCl_3$) δ 162.74, 139.10, 136.99, 129.30, 128.85, 128.54, 127.03, 126.78, 35.70, 32.41, 25.09, 19.11. MS (ESI): m/z: 275 [M-H]

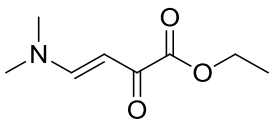

Ethyl (E)-4-(dimethylamino)-2-oxobut-3-enoate (65). Ethyl pyruvate (17.22 mmol, 2g) was solubilized in dichloromethane (34 mL) and to the previous solution was added dropwise dimethylformamide dimethyl acetal (17.22 mmol, 2g). Reaction mixture was stirred at room temperature for 4h and after the volatiles were evaporated under reduced pressure to obtain a dark brown oil that was purified by flash column chromatography using Methanol/ Dichloromethane (1:99) to afford the product as a brown yellowish oil in 54% yield. ^{1}H NMR (300 MHz, Chloroform-*d*) δ 7.83 (d, *J* = 12.5 Hz, 1H), 5.81 (d, *J* = 12.5 Hz, 1H), 4.30 (qd, *J* = 7.1, 0.9 Hz, 2H), 3.18 (s, 3H), 2.95 (s, 3H), 1.36 (td, *J* = 7.1, 0.9 Hz, 3H).

General procedure for the synthesis of ethyl 1R-pyrazole-5-carboxylate (66a-h and 67d-h): To a solution of ethyl (E)-4-(dimethylamino)-2-oxobut-3-enoate (1 eq) in methanol (0.8 mL/ mmol) was added the properly substituted hydrazine (1 eq). Reaction mixture was stirred at 60 °C for 6h. The volatiles were evaporated under reduced pressure and the residue was solubilized in chloroform, treated with a saturated solution of $NaHCO_3$ and then extracted with chloroform (3 x 15 mL). The combined organic layers were washed with brine and dried over anhydrous magnesium sulfate, filtrated and concentrated under reduced pressure. Yields, purification methods and other analytical data are reported below.

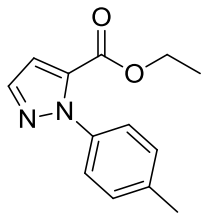

Ethyl 1-(p-tolyl)-1H-pyrazole-5-carboxylate (66a): The product was purified by flash chromatography on silica gel using Ethyl Acetate/ Petroleum Ether (3:97). The product was obtained as a light brown powder in 48% yield. ^{1}H NMR (300 MHz, Chloroform-d) δ 7.67 (d, J = 1.9 Hz, 1H), 7.39 – 7.18 (m, 4H),

7.00 (d, J = 1.9 Hz, 1H), 4.24 (q, J = 7.1 Hz, 2H), 2.42 (s, 3H), 1.26 (t, J = 7.1 Hz, 3H).

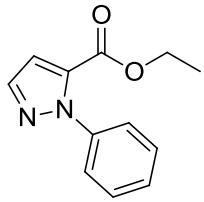

Ethyl 1-phenyl-1H-pyrazole-5-carboxylate (66b): Purification by flash column chromatography on silica gel using Ethyl Acetate/ Petroleum Ether (2:98 with 0.2% triethylamine) afforded the isolation of desired product as a yellow oil in 43% yield. ^{1}H NMR (300 MHz, Chloroform-d) δ 7.69 (d, J = 2.0 Hz, 1H), 7.49 – 7.36 (m, 5H), 7.03 (d, J = 2.0 Hz, 1H), 4.24 (q, J = 7.1 Hz, 2H), 1.24 (t, J = 7.1 Hz, 3H).

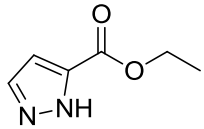

Ethyl 1H-pyrazole-5-carboxylate (66c): The product was obtained as a dark brown solid in 98% yield. ^{1}H NMR (300 MHz, Chloroform-*d*) δ 7.75 (d, *J* = 9.9 Hz, 1H), 6.86 (d, *J* = 2.1 Hz, 1H), 4.42 (qd, *J* = 7.1, 1.0 Hz, 2H), 1.41 (t, *J* = 7.1 Hz, 3H).

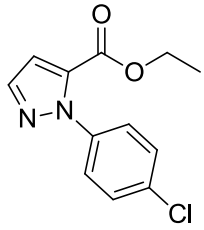

Ethyl 1-(4-chlorophenyl)-1H-pyrazole-5-carboxylate (66d): The product was purified by flash chromatography using Ethyl Acetate/ Petroleum Ether (2:98) and it was obtained as a light yellow powder in 23% yield. ^{1}H NMR (400

MHz, Chloroform-*d*) δ 7.69 (d, *J* = 2.0 Hz, 1H), 7.45 – 7.41 (m, 2H), 7.40 – 7.36 (m, 2H), 7.03 (d, *J* = 2.0 Hz, 1H), 4.26 (q, *J* = 7.1 Hz, 2H), 1.28 (t, *J* = 7.1 Hz, 3H).

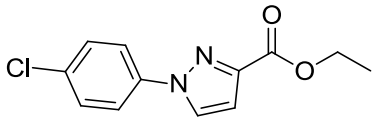

Ethyl 1-(4-chlorophenyl)-1H-pyrazole-3-carboxylate (67d): The product was obtained as a light yellow powder in 10% yield after purification with Ethyl Acetate/ Petroleum Ether (2:98). ^{1}H NMR (400 MHz, $cdcl_3$) δ 7.90 (d, *J* = 2.5 Hz, 1H), 7.70 (d, *J* = 9.0 Hz, 2H), 7.55 – 7.40 (m, 2H), 6.99 (d, *J* = 2.5 Hz, 1H), 4.44 (q, *J* = 7.1 Hz, 2H), 1.42 (t, *J* = 7.1 Hz, 3H).

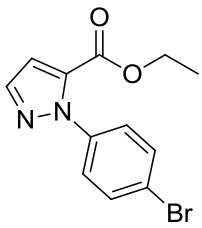

Ethyl 1-(4-bromophenyl)-1H-pyrazole-5-carboxylate (66e): The product was purified by flash column chromatography on silica gel using Ethyl Acetate/ Petroleum Ether (3.5:96.5 with 1.7% triethylamine) and it was obtained as light yellow powder in 35% yield. ^{1}H NMR (300 MHz, Chloroform-d) δ 7.69 (d, J = 2.0 Hz, 1H), 7.64 – 7.53 (m, 2H), 7.38 – 7.26 (m, 2H), 7.03 (d, J = 2.0 Hz, 1H), 4.26 (q, J = 7.2 Hz, 2H), 1.28 (t, J = 7.1 Hz, 3H).

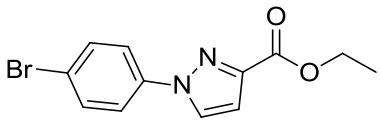

Ethyl 1-(4-bromophenyl)-1H-pyrazole-3-carboxylate (67e): The product was purified by flash column chromatography on silica gel using Ethyl Acetate/ Petroleum Ether (3.5:96.5 with 1.7% triethylamine) and it was obtained as light yellow powder in 23% yield. ^{1}H NMR (300 MHz, Chloroform-*d*) δ 7.91 (dd, *J* = 2.5, 0.6 Hz, 1H), 7.70 – 7.51 (m, 4H), 7.00 (dd, *J* = 2.6, 0.6 Hz, 1H), 4.59 – 4.34 (m, 2H), 1.42 (td, *J* = 7.1, 0.6 Hz, 3H).

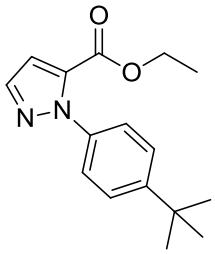

Ethyl 1-(4-(tert-butyl)phenyl)-1H-pyrazole-5-carboxylate (66f): The product was purified by flash column chromatography on silica gel using Ethyl Acetate/ Petroleum Ether (2:98 with 0.2% triethylamine) as eluent. The product was obtained as a yellow oil in 42% yield. ^{1}H NMR (300 MHz, Chloroform-*d*) δ 7.67 (d, *J* = 2.0 Hz, 1H), 7.51 – 7.41 (m, 2H), 7.41 – 7.29 (m, 2H), 7.01 (d, *J* = 2.0 Hz, 1H), 4.24 (q, *J* = 7.2 Hz, 2H), 1.36 (s, 9H), 1.24 (t, *J* = 7.1 Hz, 3H).

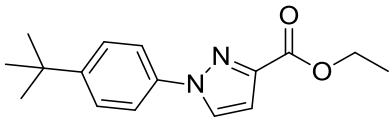

Ethyl 1-(4-(tert-butyl)phenyl)-1H-pyrazole-3-carboxylate (67f): The product was purified by flash column chromatography on silica gel using Ethyl Acetate/ Petroleum Ether (2:98 with 0.2% triethylamine) as eluent. The product was obtained as a yellow oil in 46% yield. ^{1}H NMR (300 MHz, Chloroform-*d*) δ 7.90 (d, *J* = 2.5 Hz, 1H), 7.66 (d, *J* = 8.9 Hz, 2H), 7.47 (d, *J* =

8.8 Hz, 2H), 6.98 (d, *J* = 2.5 Hz, 1H), 4.44 (q, *J* = 7.1 Hz, 2H), 1.42 (t, *J* = 7.1 Hz, 3H), 1.35 (s, 9H).

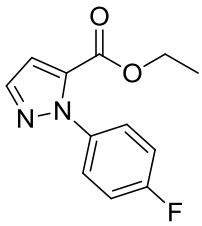

Ethyl 1-(4-fluorophenyl)-1H-pyrazole-5-carboxylate (66g): The product was purified by flash column chromatography on silica gel using Ethyl Acetate/ Petroleum Ether (2:98 with 0.2% triethylamine) as eluent. The product was obtained as a yellow powder in 47% yield. ^{1}H NMR (300 MHz, Chloroform-*d*) δ 7.68 (d, *J* = 2.0 Hz, 1H), 7.50 – 7.34 (m, 2H), 7.21 – 7.07 (m, 2H), 7.02 (d, *J* = 2.0 Hz, 1H), 4.25 (q, *J* = 7.1 Hz, 2H), 1.27 (t, *J* = 7.1 Hz, 3H).

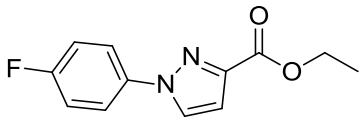

Ethyl 1-(4-fluorophenyl)-1H-pyrazole-3-carboxylate (67g): The product was purified by flash column chromatography on silica gel using Ethyl Acetate/ Petroleum Ether (2:98 with 0.2% triethylamine) as eluent. The product was obtained as a yellow powder in 20% yield. ^{1}H NMR (300 MHz, Chloroform-*d*) δ 7.87 (d, *J* = 2.5 Hz, 1H), 7.82 – 7.62 (m, 2H), 7.23 – 7.10 (m, 2H), 6.99 (d, *J* = 2.5 Hz, 1H), 4.44 (q, *J* = 7.1 Hz, 2H), 1.42 (t, *J* = 7.1 Hz, 3H).

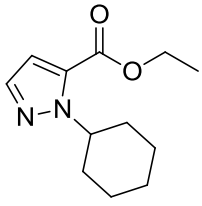

Ethyl 1-cyclohexyl-1H-pyrazole-5-carboxylate (66h): Purification by flash column chromatography on silica gel using Ethyl Acetate/ Petroleum Ether (2:98 with 0.2% triethylamine) allowed the isolation of the desired product in 39% yield as a colourless oil. ^{1}H NMR (300 MHz, Methanol-d_4) δ 7.52 (d, *J* = 2.0 Hz, 1H), 6.86 (d, *J* = 2.0 Hz, 1H), 5.16 (dq, *J* = 10.4, 5.4, 4.1 Hz, 1H), 4.36 (q, *J* = 7.1 Hz, 2H), 2.09 – 1.69 (m, 7H), 1.58 – 1.15 (m, 6H).

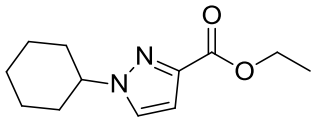

Ethyl 1-cyclohexyl-1H-pyrazole-3-carboxylate (67h): Purification by flash column chromatography on silica gel using Ethyl Acetate/ Petroleum Ether (2:98 with 0.2% triethylamine) allowed the isolation of the desired product as a yellow oil in 39% yield. ^{1}H NMR (300 MHz, Methanol-d_4) δ 7.75 (d, *J* = 2.5 Hz, 1H), 6.78 (d, *J* = 2.4 Hz, 1H), 4.37 (q, *J* = 7.2 Hz, 2H), 4.32 – 4.09 (m, 1H), 2.12 (d, *J* = 14.1 Hz, 2H), 1.99 – 1.63 (m, 8H), 1.39 (t, *J* = 7.2 Hz, 3H).

General procedure for the synthesis of 1-R-pyrazole-5-carboxylic acid (59a-h and 68d-h): To a solution of the proper ethyl 1R-pyrazole-5-carboxylate (1 eq) solubilized in ethanol (3 mL/ mmol) was added sodium hydroxide 6M aq. solution (2 eq). RM was stirred at 80°C for 2h. The solvent was evaporated under reduced pressure, water was added and the residue acidified with HCl 1M until pH 1-2. The precipitate was filtrated and washed with petroleum ether.

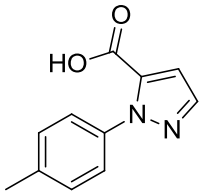

1-(p-tolyl)-1H-pyrazole-5-carboxylic acid (59a): The product was obtained as a white solid in 66% yield. ^{1}H NMR (300 MHz, Methanol-d_4) δ 7.70 (d, J = 2.0 Hz, 1H), 7.29 (s, 4H), 7.04 (d, J = 2.0 Hz, 1H), 2.43 (s, 3H). ^{13}C NMR (101 MHz, Methanol-d_4) δ 161.70, 140.44, 140.01, 139.29, 135.67, 130.15, 126.95, 113.42, 21.17. HRMS (ESI): calculated for $C_{11}H_9O_2N_2$ [M-H] 201.0670 found 201.06691.

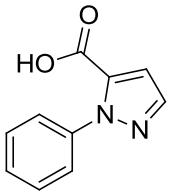

1-phenyl-1H-pyrazole-5-carboxylic acid (59b): The product was obtained as a yellow powder in 78% yield. ^{1}H NMR (300 MHz, Methanol-d_4) δ 7.67 (d, *J* = 2.0 Hz, 1H), 7.50 – 7.33 (m, 5H), 7.02 (d, *J* = 2.0 Hz, 1H). ^{13}C NMR (101 MHz, Methanol-d_4) δ 161.62, 141.73, 140.64, 135.65, 129.74, 129.65, 127.16, 113.60. HRMS (ESI): calculated for $C_{10}H_7O_2N_2$ [M-H] 187.0513found 187.05122.

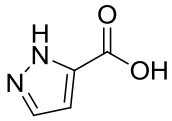

1H-pyrazole-5-carboxylic acid (59c): The product was obtained as a pearl solid in 40% yield. ^{1}H NMR (300 MHz, Methanol-d_4) δ 7.69 (d, J = 2.6 Hz, 1H), 6.81 (d, J = 2.7 Hz, 1H). ^{13}C NMR (101 MHz, Methanol-d_4) δ 164.62, 142.92, 133.87, 109.03. HRMS (ESI): calculated for $C_4H_3O_2N_2$ [M-H] 111.0200 found 111.0200.

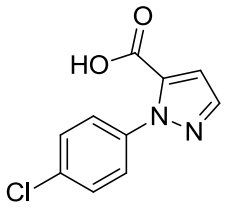

1-(4-chlorophenyl)-1H-pyrazole-5-carboxylic acid (59d): The product was obtained as a white powder in 77% yield. ^{1}H NMR (300 MHz, Methanol-d_4) δ 7.72 (d, J = 2.0 Hz, 1H), 7.54 – 7.37 (m, 4H), 7.05 (d, J = 2.0 Hz, 1H). ^{13}C NMR (101 MHz, Methanol-d_4) δ 161.74, 142.78, 140.98, 140.42, 135.40, 129.72, 128.69, 113.74. HRMS (ESI): calculated for $C_{10}H_6ClO_2N_2$ [M-H] 221.0123 found 221.01221.

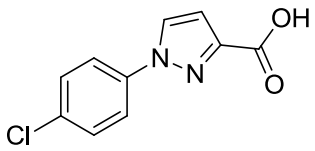

1-(4-chlorophenyl)-1H-pyrazole-3-carboxylic acid (68d): The product was obtained as a white powder in 87% yield. ^{1}H NMR (300 MHz, Methanol-d_4) δ 8.32 (d, *J* = 2.5 Hz, 1H), 7.94 – 7.77 (m, 2H), 7.62 – 7.43 (m, 2H), 6.99 (d, *J* = 2.5 Hz, 1H). ^{13}C NMR (101 MHz, Methanol-d_4) δ 165.07, 146.75, 139.71, 134.20, 130.72, 130.63, 122.22, 111.38. HRMS (ESI): calculated for $C_{10}H_6ClO_2N_2$ [M-H] 221.0123 found 221.01237.

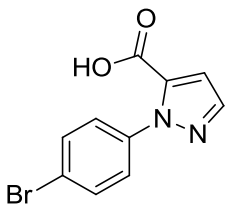

1-(4-bromophenyl)-1H-pyrazole-5-carboxylic acid (59e): The product was obtained as a light yellow powder in 91% yield. ^{1}H NMR (300 MHz, Methanol-d_4) δ 7.73 (d, J = 2.0 Hz, 1H), 7.69 – 7.58 (m, 2H), 7.42 – 7.30 (m, 2H), 7.07 (d,

J = 2.0 Hz, 1H). ^{13}C NMR (101 MHz, Methanol-d_4) δ 161.48, 141.03, 140.85, 135.66, 132.77, 128.99, 123.32, 113.93. HRMS (ESI): calculated for $C_{10}H_6BrO_2N_2$ [M-H] 264.9618 found 264.96170.

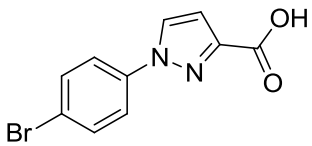

1-(4-bromophenyl)-1H-pyrazole-3-carboxylic acid (68e): The product was obtained as a light yellow powder in 73% yield.^{1}H NMR (300 MHz, Methanol-d_4) δ 8.32 (d, *J* = 2.6 Hz, 1H), 7.84 – 7.75 (m, 2H), 7.71 – 7.63 (m, 2H), 6.99 (d, *J* = 2.6 Hz, 1H). ^{13}C NMR (101 MHz, Methanol-d_4) δ 165.07, 146.79, 140.17, 133.75, 130.59, 122.47, 121.91, 111.41. HRMS (ESI): calculated for $C_{10}H_6BrO_2N_2$ [M-H] 264.9618 found 264.96161.

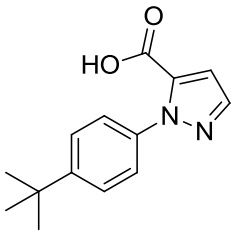

1-(4-(tert-butyl)phenyl)-1H-pyrazole-5-carboxylic acid (59f): The product was obtained as a cream powder in 47% yield. ^{1}H NMR (300 MHz, Methanol-d_4) δ 7.70 (d, *J* = 2.1 Hz, 1H), 7.58 – 7.47 (m, 2H), 7.40 – 7.27 (m, 2H), 7.02 (d, *J* = 2.1 Hz, 1H), 1.38 (s, 9H). ^{13}C NMR (101 MHz, Methanol-d_4) δ 162.45, 153.17, 140.64, 139.45, 136.48, 126.78, 113.34, 111.64, 35.82, 31.95. HRMS (ESI): calculated for $C_{14}H_{15}O_2N_2$ [M-H] 243.1139 found 243.11357.

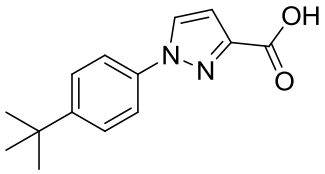

1-(4-(tert-butyl)phenyl)-1H-pyrazole-3-carboxylic acid (68f): The product was obtained as a cream powder in 64% yield. ^{1}H NMR (300 MHz, Methanol-d_4) δ 8.19 (d, *J* = 2.5 Hz, 1H), 7.82 – 7.64 (m, 2H), 7.62 – 7.44 (m, 2H), 6.91 (d, *J* = 2.4 Hz, 1H), 1.36 (d, *J* = 2.3 Hz, 9H). ^{13}C NMR (101 MHz, Methanol-d_4) δ 167.56, 151.63, 149.16, 138.90, 129.94, 127.44, 120.42, 110.52, 35.45, 31.70. HRMS (ESI): calculated for $C_{14}H_{15}O_2N_2$ [M-H] 243.1139 found 243.11377.

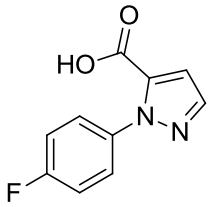

1-(4-fluorophenyl)-1H-pyrazole-5-carboxylic acid (59g): The product was obtained as a yellow powder in 93% yield. ^{1}H NMR (300 MHz, Methanol-d_4) δ 7.67 (d, *J* = 2.0 Hz, 1H), 7.47 – 7.34 (m, 2H), 7.24 – 7.10 (m, 2H), 7.02 (d, *J* = 2.0 Hz, 1H). ^{13}C NMR (101 MHz, Methanol-d_4) δ 165.16, 161.49, 140.73, 137.94, 135.77, 129.37, 129.28, 116.47, 116.24, 113.65. HRMS (ESI): calculated for $C_{10}H_6FO_2N_2$ [M-H] 205.0419 found 205.04185.

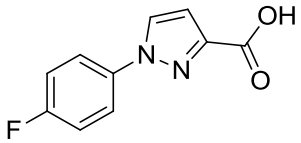

1-(4-fluorophenyl)-1H-pyrazole-3-carboxylic acid (68g): The product was obtained as a yellow powder in 36% yield. ^{1}H NMR (400 MHz, Methanol-d_4) δ 8.25 (d, *J* = 2.6 Hz, 1H), 7.90 – 7.76 (m, 2H), 7.31 – 7.18 (m, 2H), 6.96 (d, *J* = 2.5 Hz, 1H). ^{13}C NMR (101 MHz, Methanol-d_4) δ 164.44, 161.99, 146.52,

137.49, 137.46, 130.78, 123.02, 122.93, 117.44, 117.21, 111.23. HRMS (ESI): calculated for $C_{10}H_6FO_2N_2$ [M-H] 205.0419 found 205.04185.

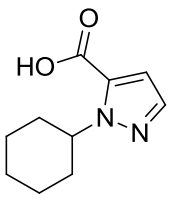

1-cyclohexyl-1H-pyrazole-5-carboxylic acid (59h): The product was obtained as a white powder in 86% yield. ^{1}H NMR (400 MHz, Methanol-d_4) δ 7.49 (dt, *J* = 2.0, 1.0 Hz, 1H), 6.83 (d, *J* = 2.0 Hz, 1H), 5.19 (ddd, *J* = 11.1, 7.6, 4.2 Hz, 1H), 1.92 (dddd, *J* = 21.5, 11.3, 5.6, 2.8 Hz, 6H), 1.78 – 1.70 (m, 1H), 1.53 – 1.39 (m, 2H), 1.35 – 1.18 (m, 1H).^{13}C NMR (101 MHz, Methanol-d_4) δ 162.40, 138.70, 133.53, 112.26, 60.46, 34.22, 26.78, 26.52. HRMS (ESI): calculated for $C_{10}H_{13}O_2N_2$ [M-H] 193.0983 found 193.09834.

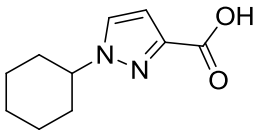

1-cyclohexyl-1H-pyrazole-3-carboxylic acid (68h): The product was obtained as a white powder in 80% yield. ^{1}H NMR (300 MHz, Methanol-d_4) δ 7.72 (d, *J* = 2.4 Hz, 1H), 6.75 (d, *J* = 2.4 Hz, 1H), 4.21 (tt, *J* = 11.5, 3.9 Hz, 1H), 2.16 – 2.01 (m, 2H), 2.00 – 1.63 (m, 6H), 1.60 – 1.17 (m, 2H). ^{13}C NMR (101 MHz, Methanol-d_4) δ 165.44, 144.13, 130.30, 109.26, 63.39, 34.37, 26.41, 26.30. HRMS (ESI): calculated for $C_{10}H_{13}O_2N_2$ [M-H] 193.0983 found 193.09834.

General Procedure for Suzuki-Miyaura Reaction. Method A: Into a flask under argon stirring at room temperature was added a solution of compound **75** (1.0 eq, 0.52 mmol) in a mixture of toluene/methanol/water (80/18/2 v/v, 40mL/mmol), tetrakis(triphenylphosphine)palladium (0.15 eq, 0.08 mmol), the proper boronic acid (3.0 eq, 1.56 mmol), and K_2CO_3 2M (1.6

eq, 0.832 mmol). The reaction mixture was refluxed overnight at 110°C and then filtered through a plug of celite. The filtrate was concentrated under reduced pressure and the residue purified by flash column chromatography on silica gel, as reported herein. Compounds **76a** and **76b** were synthesized according to Method A. **Method B:** A microwave tube was charged with [1,1'-Bis(diphenylphosphino)ferrocene]dichloropalladium(II) (0.02 eq, 0.0134 mmol), the proper boronic acid pinacol ester (2 eq, 0.134 mmol), and cesium carbonate (2 eq, 0.134 mmol). The tube was purged with argon three times and then a solution of compound **75** (1 eq, 0.067 mmol) in a mixture of dimethoxyethane/water 5:1 (175 µL) was injected in the reaction mixture that was then heated in a microwave reactor for 30 min at 140°C using 100 Watts power. Afterwards, reaction mixture was filtered through a plug of celite, the filtrate was concentrated under reduced pressure and the residue purified by flash column chromatography. Compounds **76c** and **76d** were synthesized according to Method B.

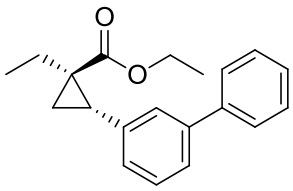

***Trans*-ethyl 2-([1,1'-biphenyl]-3-yl)-1-ethylcyclopropane-1-carboxylate (76a).** Purified by flash column chromatography (Ethyl Acetate/ Petroleum Ether 1:99); colourless oil; 81% yield. ^{1}H NMR (300 MHz, $CDCl_3$) δ 7.66 – 7.54 (m, 2H), 7.51 – 7.29 (m, 6H), 7.18 (d, J = 7.6 Hz, 1H), 4.21 (dq, J = 7.1, 3.7 Hz, 2H), 2.87 (dd, J = 9.1, 7.1 Hz, 1H), 1.81 – 1.54 (m, 2H), 1.30 (t, J = 7.1 Hz, 3H), 1.22 (dd, J = 7.1, 4.6 Hz, 1H), 0.98 – 0.85 (m, 3H).

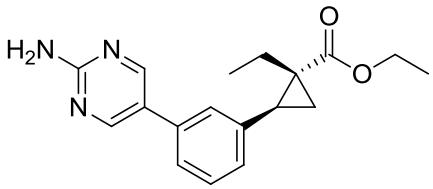

***Trans*-ethyl 2-(3-(2-aminopyrimidin-5-yl)phenyl)-1-ethylcyclopropane-1-carboxylate (76b).** Purified by flash cromatography (Ethyl Acetate/ Petroleum Ether 25:75→1:1 with 0.1% of thriethylamine); slightly yellow powder; 96% yield. ^{1}H NMR (300 MHz, $CDCl_3$) δ 8.52 (s, 2H), 7.54 – 7.28 (m, 3H), 7.19 (d, *J* = 7.0 Hz, 1H), 5.25 (s, 2H), 4.34 – 4.06 (m, 2H), 2.85 (t, *J* = 8.0 Hz, 1H), 1.77 – 1.55 (m, 2H), 1.30 (t, *J* = 7.1 Hz, 3H), 1.19 (dd, *J* = 6.9, 4.8 Hz, 1H), 0.92 – 0.83 (m, 4H).

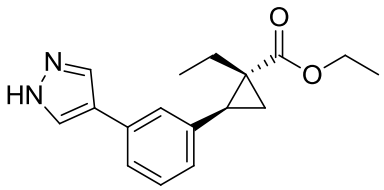

***Trans*-ethyl 2-(3-(1H-pyrazol-4-yl)phenyl)-1-ethylcyclopropane-1-carboxylate (76c).** Purified by flash cromatography (Ethyl Acetate/ Petroleum Ether 25:75→1:1 with 0.1% of thriethylamine); slightly orange oil; 42% yield.

^{1}H NMR (300 MHz, $CDCl_3$) δ 7.67 – 7.28 (m, 5H), 7.04 (d, *J* = 6.5 Hz, 1H), 4.20 (ddd, *J* = 12.7, 7.1, 3.5 Hz, 2H), 2.87 – 2.69 (m, 1H), 1.77 – 1.59 (m, 2H), 1.35 – 1.24 (m, 4H), 1.17 (dd, *J* = 7.1, 4.7 Hz, 1H), 0.95 – 0.77 (m, 3H). HRMS (ESI): calculated for $C_{17}H_{20}N_2O_2$ [M+H] 285.15975 found 285.15948.

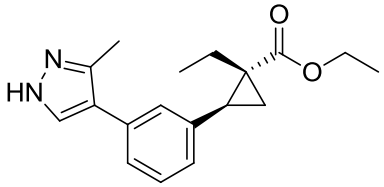

***Trans*-ethyl 1-ethyl-2-(3-(3-methyl-1H-pyrazol-4-yl)phenyl)cyclopropane-1-carboxylate (76d).** Purified by flash cromatography (Ethyl Acetate/ Petroleum Ether 25:75→1:1 with 0.1% of thriethylamine); slightly orange oil; 40% yield. ^{1}H NMR (300 MHz, $CDCl_3$) δ 7.69 (bs, 1H), 7.37 – 7.26 (m, 3H), 7.12 (d, *J* = 6.5 Hz, 1H), 4.20 (ddd, *J* = 12.7, 7.1, 3.5 Hz, 2H), 2.99 – 2.93 (m, 1H), 2.47 (s, 3H) 1.79 – 1.73 (m, 2H), 1.35 – 1.24 (m, 4H), 1.17 (dd, *J* = 7.1, 4.7 Hz, 1H), 0.95 – 0.77 (m, 3H). HRMS (ESI): calculated for $C_{18}H_{22}N_2O_2$ [M+H] 298,1681 found 298,3860.

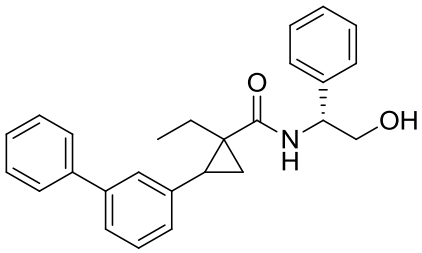

2-([1,1'-biphenyl]-3-yl)-1-ethyl-N-((R)-2-hydroxy-1-phenylethyl)cyclopropane-1-carboxamide (78a and 79a). (R)-(-)-2-Phenylglycinol (1.2 eq), TBTU (1.1 eq), EDC*HCl (1.1 eq) and dry triethylamine (1.5 eq) were added to a solution of compound **77a** (1 eq) in anhydrous dichloromethane, stirring on ice and under nitrogen. Reaction mixture was stirred for 1h at 0°C and about 6h at room temperature until consumption of the starting material as revealed by TLC. Then, a saturated solution of ammonium chloride was carefully added and extractions with dichloromethane were performed. The combined organic layers were dried over anhydrous sodium sulfate, filtered and concentrated under reduced pressure to be purified by flash column chromatography on silica gel using a gradient of Ethyl Acetate in Petroleum Ether (1:9 → 1:1).

78a: White solid (45% yield) ^{1}H NMR (400 MHz, $CDCl_3$) δ 7.60 (d, *J* = 7.4 Hz, 2H), 7.53 – 7.28 (m, 11H), 7.17 (dd, *J* = 26.3, 8.5 Hz, 1H), 6.57 (d, *J* = 6.6 Hz, 1H), 5.14 (dd, *J* = 11.2, 5.0 Hz, 1H), 3.93 (d, *J* = 4.8 Hz, 2H), 3.02 (s, 1H), 2.95 –

2.83 (m, 1H), 1.67 (dt, *J* = 13.9, 7.0 Hz, 1H), 1.56 (ddd, *J* = 15.6, 12.3, 5.5 Hz, 1H), 1.24 – 1.08 (m, 2H), 1.00 – 0.88 (m, 3H).

79a: White solid (16% yield) ^{1}H NMR (400 MHz, $CDCl_3$) δ 7.70 – 7.50 (m, 2H), 7.47 – 7.30 (m, 11H), 7.18 (dd, *J* = 13.3, 4.9 Hz, 1H), 6.55 (d, *J* = 6.6 Hz, 1H), 5.14 (dd, *J* = 11.4, 4.9 Hz, 1H), 3.90 (dd, *J* = 18.1, 5.3 Hz, 2H), 2.92 – 2.82 (m, 1H), 1.69 (dt, *J* = 43.0, 21.5 Hz, 1H), 1.55 (td, *J* = 14.7, 7.1 Hz, 1H), 1.26 – 1.08 (m, 2H), 0.94 (t, *J* = 7.4 Hz, 3H).

General procedure for acidic hydrolysis (80a, 81a): The starting material (7**8a**, 7**9a**) (1 eq, 0.047 mmol) was solubilized in a mixture 1:1 of 3N H_2SO_4/ Dioxane and stirred overnight at 100°C. Water was carefully added to the reaction mixture after cool it down until room temperature. Extractions with dichloromethane were performed and the combined organic layers were dried over anhydrous sodium sulfate, filtered and concentrated under reduced pressure to be purified by flash column chromatography.

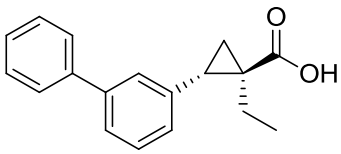

(-)-Trans-2-([1,1'-biphenyl]-3-yl)-1-ethylcyclopropane-1-carboxylic acid (80a). Purified by flash column chromatography using Methanol/ Dichloromethane (1:99); colourless oil; 56% yield. ^{1}H NMR (300 MHz, $CDCl_3$) δ 7.61 (d, *J* = 7.2 Hz, 2H), 7.53 – 7.30 (m, 6H), 7.23 (t, *J* = 8.6 Hz, 1H), 3.02 (t, *J* = 8.1 Hz, 1H), 1.87 – 1.75 (m, 1H), 1.75 – 1.66 (m, 1H), 1.39 – 1.23 (m, 2H), 0.95 (d, *J* = 2.4 Hz, 3H). ^{13}C NMR (101 MHz, $CDCl_3$) δ 182.03, 141.38, 141.10, 137.32, 128.92, 128.78, 128.35, 128.29, 127.54, 127.32, 125.91, 33.58, 31.39, 21.76, 18.74, 11.79. HRMS (ESI): calculated for $C_{18}H_{18}O_2$ [M+H] 265.12231 found 265.12332.

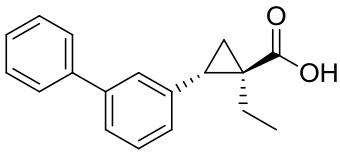

(+)-Trans-2-([1,1'-biphenyl]-3-yl)-1-ethylcyclopropane-1-carboxylic acid (81a). Purified by flash column chromatography with Methanol/ Dichloromethane (1:99); Colourless oil (42% yield). ^{1}H NMR (300 MHz, $CDCl_3$) δ 7.59 (d, *J* = 7.3 Hz, 2H), 7.53 – 7.32 (m, 6H), 7.20 (d, *J* = 7.6 Hz, 1H), 3.00 (t, *J* = 8.1 Hz, 1H), 1.86 – 1.74 (m, 1H), 1.74 – 1.63 (m, 1H), 1.37 – 1.24 (m, 2H), 0.99 – 0.76 (m, 3H). ^{13}C NMR (101 MHz, $CDCl_3$) δ 181.25, 141.07, 140.80, 137.01, 128.61, 128.47, 128.04, 127.99, 127.23, 127.01, 125.60, 33.23, 31.04, 21.47, 18.42, 11.48. HRMS (ESI): calculated for $C_{18}H_{18}O_2$ [M+H] 265.12231 found 265.12346.

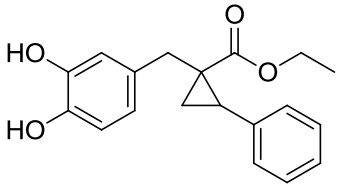

Ethyl 1-(3,4-dihydroxybenzyl)-2-phenylcyclopropanecarboxylate (102). Boron tribromide 1M solution in dichloromethane (165µL, 0.165 mmol) was added to a solution of compound **101** (52.5 mg, 0.15 mmol) stirring in dry dichloromethane (65 µL) under nitrogen. Reaction mixture was allowed to reach room temperature and after 2h TLC monitoring indicated the completion of the reaction. Quenching was performed by carefully addition of water and extractions with dichloromethane were performed. The combined organic layers were dried over anhydrous sodium sulfate, filtered and concentrated under reduced pressure to be purified by flash column chromatography on silica gel using Ethyl Acetate/ Petroleum Ether (12.5:77.5). Purification by flash column chromatography on silica gel using Methanol/ Dichloromethane (1:99) was also attempted but it wasn't possible

to isolate the pure product. The next step was attempted. ^{1}H NMR (400 MHz, MeOD) δ 7.36 – 6.93 (m, 6H), 6.56 (d, *J* = 19.8 Hz, 2H), 6.28 (s, 1H), 6.12 (s, 1H), 4.20 – 4.04 (m, 3H), 3.97 (dd, *J* = 12.0, 5.5 Hz, 1H), 3.00 – 2.71 (m, 4H), 2.36 – 2.26 (m, 1H), 2.24 – 2.07 (m, 1H), 1.86 – 1.72 (m, 1H), 1.29 – 1.10 (m, 6H).

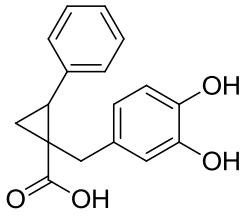

1-(3,4-dihydroxybenzyl)-2-phenylcyclopropanecarboxylic acid (92). To a solution of compound **91** (60 mg, 0.2 mmol) in dry dichloromethane (0.46 mL) stirring under nitrogen and on ice was added dropwise a 1M solution of BBr_3 in dichloromethane (0.26 mL). Reaction mixture was then allowed to reach room temperature and after 4h TLC showed complete consumption of the starting material. RM was then quenched with the addition of NaOH 1M dropwise. Extractions with dichloromethane were performed and then water phase was acidified until pH 1-2, cooled on ice and the precipitate was filtered under vacuum to afford the title compound as a white powder in 10% yield. ^{1}H NMR (400 MHz, Acetone) δ 7.36 – 7.10 (m, 6H), 6.61 (s, 1H), 6.11 (d, *J* = 0.5 Hz, 1H), 3.99 (dd, *J* = 12.0, 5.6 Hz, 1H), 2.97 – 2.83 (m, 3H), 2.81 – 2.69 (m, 1H), 2.32 (ddd, *J* = 12.9, 5.6, 1.6 Hz, 1H), 1.77 (q, *J* = 12.4 Hz, 1H). ^{13}C NMR (101 MHz, Acetone) δ 175.40, 146.24, 142.61, 142.46, 129.24, 127.67, 127.52, 125.74, 125.31, 114.80, 114.05, 44.98, 39.60, 36.13, 31.02. HRMS (ESI) calculated for $C_{17}H_{15}O_4$ 283.09649 found 283.09772.

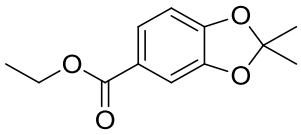

Ethyl 2,2-dimethylbenzo[d][1,3]dioxole-5-carboxylate (94). To a solution of ethyl 3,4-dihydroxibenzoate (300 mg, 1.65 mmol) in acetone (0.73 mL) and benzene (1 mL) was added dropwise PBr_3 (168 µL, 1.77 mmol). Reaction mixture was stirred and capped when bromidic acid release ceased. Reaction mixture was left stirring overnight and TLC monitoring revealed complete consumption of the starting material. A saturated solution of $NaHCO_3$ was added to the reaction dropwise and under ice-cooling conditions. Extractions with ethyl acetate (3 x 15 mL) were performed and the combined organic layers were dried over anhydrous sodium sulfate, filtered and concentrated under reduced pressure to be purified by flash column chromatography using Ethyl Acetate/ Petroleum Ether (4:96). The title compound was obtained as a colourless oil in 76% yield. ^{1}H NMR (300 MHz, $CDCl_3$) δ 7.61 (dd, *J* = 8.2, 1.7 Hz, 1H), 7.39 (d, *J* = 1.5 Hz, 1H), 6.74 (d, *J* = 8.1 Hz, 1H), 4.33 (q, *J* = 7.1 Hz, 2H), 1.69 (s, 6H), 1.36 (t, *J* = 7.1 Hz, 3H).

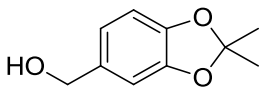

(2,2-dimethylbenzo[d][1,3]dioxol-5-yl)methanol (95). To a solution of compound 94 (363 mg, 1.63 mmol) in dry THF (7 mL) stirring under nitrogen and on ice was added lithium aluminum hydride (247 mg, 6.5 mmol). Reaction mixture was stirred at room temperature overnight and then further 1.63 mmol of lithium aluminum hydride were added to the reaction mixture. After 2h, water was carefully added to the reaction under ice-cooling conditions. Extractions with ethyl acetate (3 x 15 mL) were performed and the combined organic layers were dried over anhydrous

sodium sulfate, filtered and concentrated under reduced pressure. The product was obtained as a colourless oil in 73% yield. ^{1}H NMR (300 MHz, $CDCl_3$) δ 6.77 (m, 2H), 6.69 (d, *J* = 8.0 Hz, 1H), 4.56 (s, 2H), 1.67 (s, 6H).

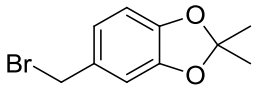

5-(bromomethyl)-2,2-dimethylbenzo[d][1,3]dioxole (96). A solution of PBr3 (29.5 µL, 0.3 mmol) in dry Et_2O (1.4 mL) was added dropwise to a cold solution of compound 95 (143 mg, 0.8 mmol) and pyridine (66.5 µL, 0.8 mmol) in dry Et_2O (1.5 mL) stirring under nitrogen. Reaction mixture was then stirred at room temperature for 2h and further 0.08 mmol of PBr_3 were added to the reaction. After 1h, TLC showed complete consumption of the starting material and reaction was quenched by adding a saturated solution of $NaHCO_3$ under ice cooling conditions dropwise. Extractions with ethyl acetate (3 x 10 mL) were performed and the combined organic layers were dried over anhydrous sodium sulfate, filtered and concentrated under reduced pressure to be used in the next step without further purification. Quantitative yield. ^{1}H NMR (400 MHz, $CDCl_3$) δ 6.80 (tt, *J* = 7.1, 3.6 Hz, 2H), 6.70 – 6.57 (m, 1H), 4.46 (s, 2H), 1.67 (s, 6H).

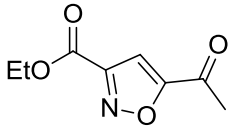

Ethyl 5-acetylisoxazole-3-carboxylate (112). Method A: To a solution of butynone (115 µL, 1.47 mmol) and Ethyl-2-chloro-2-(hydroxyimino)acetate (222.8 mg, 1.47 mmol) in a mixture of H_2O/*t*-BuOH (8.8 mL, 1:1) was added sodium ascorbate (147µL, 0.147 mmol, 1M solution in water). After copper sulfate pentahydrate (7.34 mg, 0.029 mmol) was added as a solution in

147µL of water and finally sodium hidrogenocarbonate (535 mg, 6.37 mmol) was also added to the reaction mixture that was left stirring at room temperature for 1h. Ethyl acetate was added to the reaction mixture and extractions were performed (3 x 15 mL). The combined organic layers were dried over anhydrous sodium sulfate, filtered and concentrated under reduced pressure to be purified by flash column chromatography on silica gel using Ethyl Acetate/ Petroleum Ether (7:93). The product was obtained as a white powder in 19% yield. Method B: To a solution of butynone (2.3 mL, 29 mmol) and Ethyl-2-chloro-2-(hydroxyimino)acetate (4.39 g, 29 mmol) in THF (37.5 mL) was added dropwise a solution of triethylamine (4 mL, 29 mmol) in THF (10 mL). Reaction mixture was left stirring at room temperature for 2.5h and then volatiles were evaporated. Extractions with ethyl acetate were performed (3 x 100 mL) and the combined organic layers were dried over anhydrous sodium sulfate, filtered and concentrated under reduced pressure to be purified by flash column chromatography on silica gel using Ethyl Acetate/ Petroleum Ether (7:93). The product was obtained as a white powder in 50% yield. ^{1}H NMR (400 MHz, $CDCl_3$) δ 7.26 (s, *J* = 2.0 Hz, 1H), 4.47 (q, *J* = 7.1 Hz, 1H), 2.65 (s, 1H), 1.43 (t, *J* = 7.1 Hz, 1H).

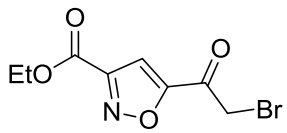

Ethyl 5-(2-bromoacetyl)isoxazole-3-carboxylate (113). To a solution of compound 112 (2.65g, 14.47 mmol) in acetonitrile (26.8 mL) stirring on ice was added *p*-toluenesulfonic acid monohydrate (2.49 g, 14.47 mmol) and N-bromosuccinimide portionwise (2.58 g, 14.47 mmol). Reaction mixture was stirred at reflux for 5h. After volatiles were evaporated and reaction mixture was purified by flash column chromatography on silica gel using a gradient of Ethyl Acetate in Petroleum Ether. The product was obtained as a yellow

powder in 58% yield. ^{1}H NMR (300 MHz, DMSO) δ 7.89 (s, 1H), 4.87 (s, 2H), 4.41 (dt, *J* = 12.4, 4.5 Hz, 2H), 1.34 (t, *J* = 7.1 Hz, 3H).

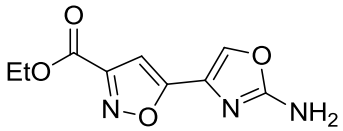

Ethyl 5-(2-aminooxazol-4-yl)isoxazole-3-carboxylate (114). To a mixture of compound ethyl 5-(2-bromoacetyl)isoxazole-3-carboxylate (315 mg, 1.2 mmol) and urea (720.72 mg, 12 mmol) stirring at room temperature and under nitrogen was added dry dimethylformamide (3.14 mL). Reaction mixture was refluxed for 1h30min and then cooled until room temperature. After, a solution of LiCl 5% in water (32 mL) was added to the reaction mixture and extractions with ethyl acetate were performed (4 x 10 mL). The combined organic layers were dried over anhydrous sodium sulfate, filtered and concentrated under reduced pressure to be purified by flash column chromatography on silica gel using Ethyl Acetate/ Petroleum Ether (3:7). The product was obtained as a yellow powder in 77% yield. ^{1}H NMR (300 MHz, DMSO) δ 8.15 (s, 1H), 7.07 (s, 2H), 6.89 (s, 1H), 4.37 (dd, *J* = 13.8, 6.8 Hz, 2H), 1.32 (t, *J* = 6.9 Hz, 3H).

General Procedure for the Buchwald-Hartwig reaction (115a-f): Ethyl 5-(2-aminooxazol-4-yl)isoxazole-3-carboxylate (1 eq), XPhos Pd G2 (0.1 eq) and sodium *tert*-butoxide (1 eq) were placed in a microwave tube and purged with argon 3x. After a mixture of toluene/ *tert*-butanol (1.02 mL, 5:1) and the proper bromophenyl derivative (0.5 eq) were injected in the reaction mixture that was then heated at 130°C on a microwave reactor for 10 min (Power= 100 W, Pressure= 250 psi). Reaction mixture was filtered through a plug of celite and purified by flash column chromatography on silica gel.

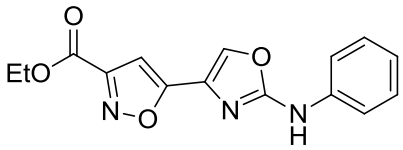

Ethyl 5-(2-(phenylamino)oxazol-4-yl)isoxazole-3-carboxylate (115a). Purification by flash column chromatography using Ethyl Acetate/ Petroleum Ether (1:9) afforded the product as a yellow solid in 24% yield. ^{1}H NMR (400 MHz, Acetone) δ 9.41 (s, 1H), 8.17 (s, 1H), 7.76 (d, *J* = 7.9 Hz, 2H), 7.36 (t, *J* = 7.9 Hz, 2H), 7.12 – 6.75 (m, 2H), 4.43 (q, *J* = 7.1 Hz, 2H), 1.39 (t, *J* = 7.1 Hz, 3H).

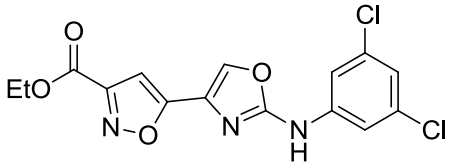

Ethyl 5-(2-((3,5-dichlorophenyl)amino)oxazol-4-yl)isoxazole-3-carboxylate (115b). Purification by flash column chromatography using Ethyl Acetate/ Petroleum Ether (1:9) afforded the product as an orange powder in 30% yield. ^{1}H NMR (300 MHz, $CDCl_3$) δ 7.82 (s, 1H), 7.51 (d, *J* = 1.6 Hz, 2H), 7.07 (s, 1H), 7.02 (s, 2H), 4.48 (q, *J* = 7.1 Hz, 2H), 1.45 (t, *J* = 7.1 Hz, 3H).

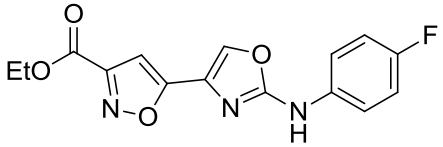

Ethyl 5-(2-((4-fluorophenyl)amino)oxazol-4-yl)isoxazole-3-carboxylate (115c). Purification by flash column chromatography using Ethyl Acetate/ Petroleum Ether (1:9) afforded the product as a slightly orange powder in 8% yield. ^{1}H NMR (300 MHz, $CDCl_3$) δ 7.77 (s, 1H), 7.51 (dd, *J* = 8.4, 4.2 Hz, 2H), 7.07 (t, *J* = 8.5 Hz, 2H), 6.98 (s, 1H), 6.92 (s, 1H), 4.47 (q, *J* = 7.1 Hz, 2H), 1.44 (t, *J* = 7.1 Hz, 3H).

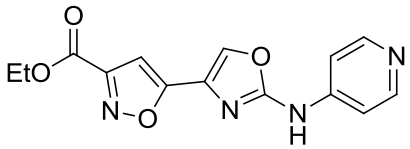

Ethyl 5-(2-(pyridin-4-ylamino)oxazol-4-yl)isoxazole-3-carboxylate (115d). Purification by flash column chromatography using Ethyl Acetate/ Petroleum Ether (1:1→100%) afforded the product as a yellow powder in 15% yield. ^{1}H NMR (400 MHz, Acetone) δ 8.47 (d, *J* = 6.2 Hz, 2H), 8.27 (s, 1H), 7.73 (d, *J* = 6.3 Hz, 2H), 7.07 (s, 1H), 4.44 (q, *J* = 7.1 Hz, 2H), 1.40 (t, *J* = 7.1 Hz, 3H).

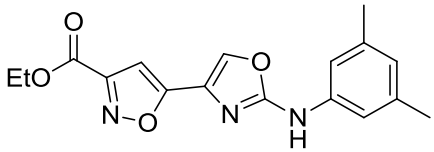

Ethyl 5-(2-((3,5-dimethylphenyl)amino)oxazol-4-yl)isoxazole-3-carboxylate (115e). Purification by flash column chromatography using Ethyl Acetate/ Petroleum Ether (1:9) afforded the desired product as a yellow powder in 35% yield. ^{1}H NMR (300 MHz, DMSO) δ 10.28 (s, 1H), 8.42 (s, 1H), 7.25 (s, 2H), 7.10 (s, 1H), 6.63 (s, 1H), 4.39 (q, *J* = 7.1 Hz, 2H), 2.26 (s, 6H), 1.34 (t, *J* = 7.1 Hz, 3H).

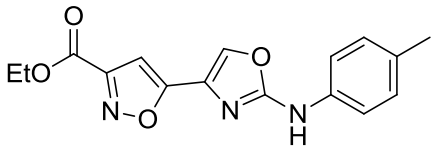

Ethyl 5-(2-(p-tolylamino)oxazol-4-yl)isoxazole-3-carboxylate (115f). Purification by flash column chromatography using Ethyl Acetate/ Petroleum Ether (1:9) afforded the product as a yellow solid in 47% yield. ^{1}H NMR (300 MHz, DMSO) δ 10.32 (s, 1H), 8.41 (s, 1H), 7.53 (d, *J* = 8.5 Hz, 2H), 7.27 – 7.00 (m, 3H), 4.38 (q, *J* = 7.1 Hz, 2H), 2.25 (s, 3H), 1.33 (t, *J* = 7.1 Hz, 3H).

General Procedure for hydrolysis (116a-f): LiOH (4 eq) was added to a solution of compound 115 (1 eq) in a mixture of THF/H_2O (3:1, 3 mL/ mmol). Reaction mixture was stirred at room temperature for 30 min and then volatiles were evaporated. The residue was solubilised with water and acidified with HCl 1N which induced the precipitation of the desired compound, after collected by filtration and washed with petroleum ether.

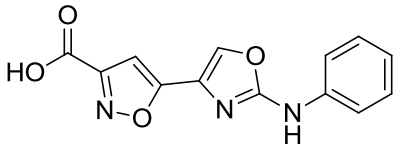

5-(2-(phenylamino)oxazol-4-yl)isoxazole-3-carboxylic acid (116a). Yellow powder (37% yield); ^{1}H NMR (400 MHz, DMSO) δ 10.45 (s, 1H), 8.42 (s, 1H), 7.66 (d, *J* = 7.8 Hz, 2H), 7.34 (t, *J* = 7.9 Hz, 2H), 7.00 (dd, *J* = 15.0, 7.6 Hz, 2H). ^{13}C NMR (101 MHz, DMSO) δ 164.54, 160.60, 157.44, 138.88, 132.16, 129.01, 128.09, 121.69, 116.82, 101.23.

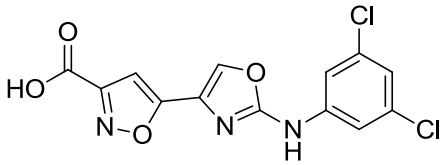

5-(2-((3,5-dichlorophenyl)amino)oxazol-4-yl)isoxazole-3-carboxylic acid (116b). Light yellow powder (60% yield); ^{1}H NMR (400 MHz, DMSO) δ 11.01 (s, 1H), 8.49 (s, 1H), 7.72 (d, *J* = 1.8 Hz, 2H), 7.19 (t, *J* = 1.8 Hz, 1H), 7.03 (s, 1H). ^{13}C NMR (101 MHz, DMSO) δ 160.40, 156.23, 141.01, 134.19, 132.59, 127.91, 123.99, 120.56, 114.75, 101.27.

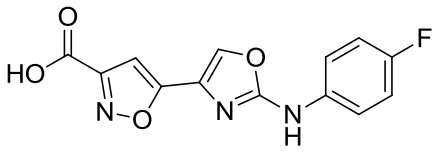

5-(2-((4-fluorophenyl)amino)oxazol-4-yl)isoxazole-3-carboxylic acid (116c). Yellow powder (81% yield); ^{1}H NMR (400 MHz, Acetone) δ 9.48 (s, 1H), 8.18 (s, 1H), 7.85 – 7.77 (m, 2H), 7.19 – 7.11 (m, 2H), 7.01 (s, 1H). ^{13}C NMR (101 MHz, Acetone) δ 166.02, 161.02, 160.16, 158.66, 158.03, 136.34, 132.31, 129.82, 119.64, 119.57, 116.42, 116.20, 102.20.

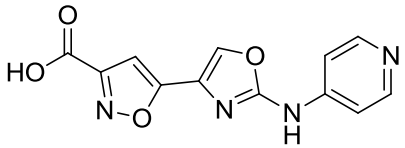

5-(2-(pyridin-4-ylamino)oxazol-4-yl)isoxazole-3-carboxylic acid (116d). Yellow powder (63% yield); ^{1}H NMR (300 MHz, DMSO) δ 12.58 (s, 1H), 8.71 (s, 1H), 8.66 (d, *J* = 7.2 Hz, 2H), 8.12 (d, *J* = 5.6 Hz, 2H), 7.20 (s, 1H). ^{13}C NMR (101 MHz, DMSO) δ 163.69, 160.49, 157.53, 155.05, 143.01, 134.27, 128.23, 112.29, 102.01.

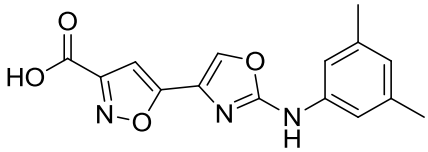

5-(2-((3,5-dimethylphenyl)amino)oxazol-4-yl)isoxazole-3-carboxylic acid (116e). Yellow powder (68% yield); ^{1}H NMR (400 MHz, DMSO) δ 10.28 (s, 1H), 8.41 (s, 1H), 7.26 (s, 2H), 7.04 (s, 1H), 6.64 (s, 1H), 2.27 (s, 6H). ^{13}C NMR (101 MHz, DMSO) δ 165.02, 161.03, 157.93, 157.77, 139.16, 138.44, 132.49, 128.51, 123.82, 115.02, 101.62, 21.63.

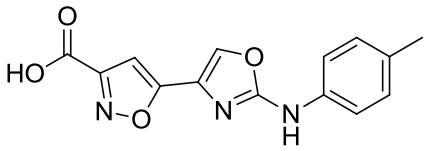

5-(2-(p-tolylamino)oxazol-4-yl)isoxazole-3-carboxylic acid (116f). Yellow powder (38% yield); ^{1}H NMR (400 MHz, Acetone) δ 9.28 (s, 1H), 8.14 (s, 1H), 7.64 (d, *J* = 8.2 Hz, 2H), 7.17 (d, *J* = 8.2 Hz, 2H), 7.00 (s, 1H), 2.29 (s, 3H).

General Procedure to perform amide synthesis (117, 124, 126, 127): To a solution of the carboxylic acid (1 eq) in dry DMF (1.8 mL/ mmol) stirring under nitrogen was added CDI (1.2 eq). Reaction mixture was left stirring for 1h at room temperature and then 5-nitrothiazol-2-amine (1 eq) was added to the reaction. After about 18h further CDI (0.5 eq) was added to the reaction mixture. Since no evolution of the reaction was noticed it was quenched with the addition of brine. Extractions with ethyl acetate (3 x 10 mL) were performed and the combined organic layers were dried over anhydrous sodium sulfate, filtered and concentrated under reduced pressure to be purified by flash column chromatography.

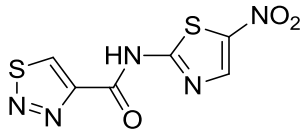

N-(5-nitrothiazol-2-yl)-1,2,3-thiadiazole-4-carboxamide (117). Purification by flash column chromatography using Methanol/ Dichloromethane (0.6:99.4) allowed the isolation of the product as a yellow powder in 13% yield. ^{1}H NMR (400 MHz, DMSO) δ 14.05 (s, 1H), 10.10 (s, 1H), 8.74 (s, 1H). ^{13}C NMR (101 MHz, DMSO) δ 161.86, 158.90, 154.64, 144.95, 142.54, 142.39.

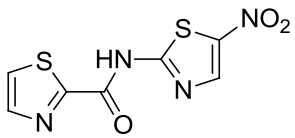

N-(5-nitrothiazol-2-yl)thiazole-2-carboxamide (124). Purification by flash column chromatography using Methanol/ Dichloromethane (0.6:99.4) allowed the isolation of the desired product as a yellow powder in 15% yield. ^{1}H NMR (300 MHz, DMSO) δ 8.71 (s, 1H), 8.30 (d, *J* = 2.2 Hz, 1H), 8.22 (d, *J* = 2.4 Hz, 1H).

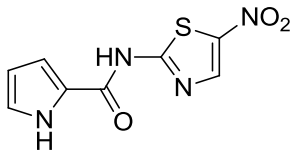

N-(5-nitrothiazol-2-yl)-1H-pyrrole-2-carboxamide (126). Purification by flash column chromatography using Ethyl Acetate/ Petroleum Ether (15:85→3:7) allowed the isolation of the product as a yellow solid in 10% yield. ^{1}H NMR (400 MHz, DMSO) δ 13.17 (s, 1H), 12.13 (s, 1H), 8.66 (s, 1H), 7.42 (ddd, *J* = 3.7, 2.4, 1.4 Hz, 1H), 7.17 (td, *J* = 2.8, 1.5 Hz, 1H), 6.25 (dt, *J* = 4.5, 2.3 Hz, 1H).

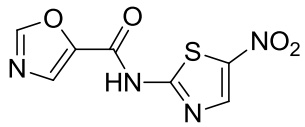

N-(5-nitrothiazol-2-yl)oxazole-5-carboxamide (127). Oxazole-5-carboxylic acid was activated with HATU instead of CDI. Purification by flash column chromatography using Methanol/ Dichloromethane (0.5:99.5) afforded the product as a light orange powder in 15% yield. ^{1}H NMR (300 MHz, DMSO) δ 8.78 (s, 1H), 8.71 (s, 1H), 8.30 (s, 1H). ESI (MS) m/z= 241 [M+H]

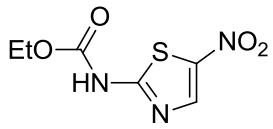

Ethyl (5-nitrothiazol-2-yl)carbamate (125). The product was isolated as a side product of the procedure described below. To a solution of oxazole carboxylic acid (50 mg, 0.44 mmol) in dry THF (1.88 mL) and triehtylamine (92.5 µL, 0.66 mmol) stirring on ice and under nitrogen was added ethyl chloroformate (46 µL, 0.48 mmol). Reaction mixture was left stirring for 1h at room temperature and 5-nitrothiazol-2-amine was added to the reaction that was left stirring at 60°C for 4h. Reaction mixture was quenched with the addition of a saturated solution of $NaHCO_3$ and extractions with ethyl acetate were performed. The combined organic layers were dried over anhydrous sodium sulfate, filtered and concentrated under reduced pressure to be purified by flash column chromatography using Ethyl Acetate/ Petroleum Ether (1:9). The product was obtained as a yellow powder in 6% yield. ^{1}H NMR (300 MHz, $CDCl_3$) δ 11.63 (s, 1H), 8.23 (s, 1H), 4.42 (q, *J* = 7.1 Hz, 2H), 1.43 (t, *J* = 7.1 Hz, 3H).

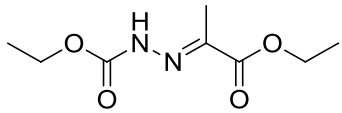

Ethyl 2-(1-ethoxy-1-oxopropan-2-ylidene)hydrazinecarboxylate (129). To a solution of pyruvic acid (789 µL, 11.4 mmol) in dry ethanol (3.3 mL) stirring at -10°C under nitrogen was added dropwise thionyl chloride (896 µL, 12.5 mmol). Reaction mixture was then allowed to warm until room temperature and 1h later it was distilled under reduced pressure. Part of the residue (111.5 mg, 0.96 mmol) was solubilized in ethanol (920 µL) and add dropwise to a solution of ethyl hydrazinecarboxylate (100 mg, 0.96 mmol) in ethanol (1 mL). Reaction mixture was stirred overnight at room temperature and then

volatiles were evaporated. Purification by flash column chromatography using Ethyl Acetate/ Petroleum Ether (7.5:92.5→1:1) afforded the product as an oil in 61% yield. **E:** ^{1}H NMR (300 MHz, $CDCl_3$) δ 11.84 (s, 1H), 4.31 (dt, *J* = 21.4, 7.1 Hz, 4H), 2.18 (s, 3H), 1.43 – 1.16 (m, 6H). ESI (MS) m/z= 203.25 [M+H] **Z:** ^{1}H NMR (300 MHz, $CDCl_3$) δ 7.90 (s, 1H), 4.43 – 4.24 (m, 4H), 2.07 (s, 3H), 1.45 – 1.27 (m, 6H). ESI (MS) m/z= 203.25 [M+H]

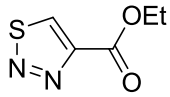

Ethyl 1,2,3-thiadiazole-4-carboxylate (130). To a solution of both E and Z isomers of Ethyl 2-(1-ethoxy-1-oxopropan-2-ylidene)hydrazinecarboxylate (416 mg, 2.1 mmol) in dry dichloromethane (2.1 mL) stirring on ice and under nitrogen was added thionyl chloride (750 µL, 10.3 mmol). Reaction mixture was allowed to warm until room temperature and it was quenched after 16h by adding under ice-cooling conditions a saturated solution of $NaHCO_3$ dropwise. Extractions with dichloromethane were performed (3 x 20 mL) and the combined organic layers were dried over anhydrous sodium sulfate, filtered and concentrated under reduced pressure to be purified by flash column chromatography using Ethyl Acetate/ Petroleum Ether (7.5:92.5→1:9). The product was obtained as a yellow solid in 39% yield. ^{1}H NMR (300 MHz, $CDCl_3$) δ 9.25 (s, 1H), 4.52 (q, *J* = 7.1 Hz, 2H), 1.46 (t, *J* = 7.1 Hz, 3H).

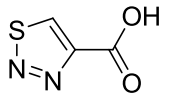

1,2,3-thiadiazole-4-carboxylic acid (131). To a solution of Ethyl 1,2,3-thiadiazole-4-carboxylate (120 mg, 0.8 mmol) in methanol (2.3 mL) was

added a 2M solution of NaOH (1.52 mL, 3 mmol). Reaction mixture was stirred at room temperature for 2h and then the reaction was acidified with HCl 3N until pH 1-2. The precipitate was filtered and washed with ehter. The desired product was obtained as a rose powder in 38% yield. ^{1}H NMR (300 MHz, DMSO) δ 13.83 (s, 1H), 9.79 (s, 1H).

Determination of StSAT inhibition

StSAT inhibitory activity of the commercial acquired 73 compounds was carried out using the the following methodology into 96-well plate format: SAT catalyzes the transfer of the group acetyl from Acetyl CoA to serine, with release of CoASH. After, the thiol group of CoASH reacts with Ellman's reagent (DTNB or 5,5'-dithiobis-(2-nitrobenzoic acid)) producing a yellow product that can be detected spectrophotometrically at 412 nm. The final concentration of DTNB and serine in the assay was 1mM, SAT from *S. typhimurium* was used at a 7 nM concentration and Acetyl CoA final concentration was 0.25 mM. DTNB was dissolved in 20 mM di-sodium hidrogenophosphate buffer (pH 7) containing 85 mM sodium chloride and 2mM EDTA. Serine and Acetyl CoA were dissolved in water and StSAT was dissolved in 20 mM di-sodium hidrogenophosphate buffer (pH 7) containing 85 mM sodium chloride, 2mM EDTA, 100µg/mL bovine serum albumin (BSA) and 15% glycerol. The total volume in each well in96-well plates was 200 µL. The absorbance was read at 412 nm using a Multiskan Go from Thermo Scientific. The plates were measured 12 times: first one background determination and then every 27s during about 5min. The reaction was started with the addition of the substrate Acetyl CoA and % of inhibition for each compound was calculated at time 180s having in mind statistic parameters like S/B, SW and Z' [104].

First the inhibitory potency against StSAT was tested at 100 µM, then compounds with a percentage of inhibition equal or higher than 40% were reassayed at the same concentration. Finally, dose-response curves were performed to determine IC_{50} for all the compounds that showed a percentage of inhibition higher than 50% in the two screenings at 100 µM.

Determination of dissociation constants for OASS

Ligand affinity was measured by direct fluorimetric titrations, monitoring the fluorescence emission spectrum of cofactor PLP upon excitation at 412 nm. 0.1 – 1 µM OASS was titrated by increasing concentrations of ligand in 100 mM HEPES pH 7.0, 1 % DMSO, at 20 ^{o}C. The dependence of fluorescence emission intensity on the concentration of compound was fitted to a binding isotherm:

$$I = I_0 + \frac{\Delta I \cdot [ligand]}{K_d + [ligand]}$$

where I is the fluorescence emission intensity at a given ligand concentration, I_0 is the fluorescence emission intensity in the absence of ligand, I is the amplitude and K_d is the dissociation constant. When the K_d was lower than the concentration of the protein used in the assay the dependence of the fluoresecnce emission intensity on ligand concentration was fitted to a quadratic equation that describes tight binding. [106] A fluorescence competitive binding assay, described elsewhere [77], was used to evaluate whether compounds bind at the active site of the enzyme or to an allosteric site. The assay is based on the formation of a low-affinity, highly fluorescent complex between OASS and 1-ethylcyclopropane-1,2-dicarboxylic acid. Binding of a higher affinity compound to the active site displaces 1-ethylcyclopropane-1,2-dicarboxylic acid and leads to a decrease in the fluorescence emission intensity.

Activity assays OASS

Enzyme activity under steady-state conditions was measured by a discontinuous method as described previously. [106] Briefly, the reaction was carried out in 100 mM HEPES pH 7.0 in the presence of 6 nM OASS, 60 nM BSA to prevent enzyme adhesion to tube wall, 1 mM OAS (equal to the K_m value of this subsrate), 0.6 mM Na_2S (a saturating concentration), 1 % DMSO and variable concentrations of inhibitor. Reaction was stopped at time intervals by the addition of acetic acid and concentration of cysteine was determined by a modification of the ninhydrin assay. [107] The fractional velocity as a function of inhibitor concentration was determined and IC_{50} was calculated by the following equation:

$$\frac{v_i}{v_0} = \frac{1}{1+(\frac{[I]}{IC50})}$$

where v_0 is the reaction velocity in the absence of inhibitor and v_i is reaction velocity in the presence of inhibitor at concentration [I].

For a competitive inhibitor against OAS the IC_{50} measured under these conditions is about $2 \cdot K_d$. [108]

Minimal Inhibitory Concentration

Minimal inhibitory concentration was performed by the broth microdilution assay according to CLSI guidelines. [78] Briefly, *E. coli* ATCC25922 was grown at 37°C on MHB agar plates during 16-24h. A loopful of bacteria was transferred into 5mL saline and the turbidity of the suspension was measure with the DEN-1 densitometer. CFU/mL were determined and a suspension with 10^6 CFU/mL was prepared in the media of the assay.

Compounds were dissolved in DMSO and 2 fold serial diluted 10 times starting from 128 µg/mL. Ciprofloxacin was used as standard antibiotic and each plate contained growth control wells and sterility check wells. The plates were incubated at 37°C during 16h-24h and MIC was determined.

Virtual Screening methodology for the identification of StSAT inhibitors

Receptor Preparation:

SAT enzymes are highly conserved across different bacteria and 6 X-ray crystal structures are reported so far. Among these 6 structure we choose to use those that satisfy the following criteria: (*i*) completeness of the 3D structure; (*ii*) lower resolution; and (*iii*) active site diversity in terms of side chains orientation, so as to take into account protein flexibility. The structure of *Ec*SAT in complex with cysteine (1T3D) and the structure of *Hi*SAT in complex with CoA (1SSM) have been chosen as the most representative.

Both structures were prepared using the Protein Preparation Wizard implemented in the Maestro graphical user interface which assigns bond orders, adds hydrogen atoms, deletes water molecules, and generates appropriate protonation states.

Commercial Library:

Compounds structures were retrieved from the ChemDiv Anti-infective (8523), anti-bacterial (5460), and antiviral (77260) focused library collections, for a total of 91243 compounds. Ligand 3-D structures were prepared along the initial stage of the Schrodinger virtual screening workflow (vsw), where compounds were (*i*) filtered accordingly to Lipinsky's rule, (*ii*) compounds with undefined stereochemistry were removed (*iii*) protonated at pH of 7.4 using epik, and (*iii*) conformers were generated using the enhanced sampling methods. The docking grid boxes for both 1T3D and 1SSM were centred so as to include all the residues into a 4 Å shell around the feedback inhibitor cysteine reported in 1T3D. Indeed, the vsw tool of Schrodinger allows to contemporaneously consider more than one protein structures. Finally the vsw was defined as follows: (*i*) Stage 1, HTVS where one pose per ligand is generated and 25% of compounds is tossed out on the basis of the glide scoring function; (*ii*) Stage II, SP_docking where the compounds are docked

using the classical SP methods, three poses per ligand are generated and 75% of compounds are discharged; (*iii*) Stage III, MM-GBSA rescoring where all the compunds passing Stage II are rescored by using Prime MM-GBSA scoring function.

The final number of compounds was equal to 1409 that were visually inspected and 1391 were selected for further evaluation. PSA and cLogD descriptors were calculated since it has been previously reported that PSA and LogD can affect compound penetration in Gram negative bacteria [20]. 37 compounds displaying a PSA below 200 Å and ClogD lower than 2 were selected to be acquired. The remaining 1354 compounds were evaluated for their chemical diversity using ChemGPS software [24,25]. 3D representation of the principal components describing shape, size and polarizability (xx axis), aromaticity and conjugation (yy axis) and lipophilicity, polarity and H-bond capacity (zz axis) in terms of differences and similarities of scaffolds allowed the selection of further 36 compounds to be purchased.

STD-NMR computational methodologies

The initial *St*OASS-A/inhibitor was obtained by combining the complete relaxation and conformational exchange matrix analysis of saturation transfer (CORCEMA-ST) theory and docking studies. In particular, the 1OAS X-ray crystal structure was used. The complex was prepared by applying the protein preparation protocol available in Maestro9.1. The complex was further minimized using Macromodel, the PRCG method, OPLSS-2005 as force field and water as implicit solvent model.

The system, thus obtained, was parameterized using *ff14SB* and *gaff* as force fields. Inhibitor atomic single charges were computed using Gaussian 09, HF/6-31** as theory level, (http://gaussian.com) and fitted with restrained electrostatic potential (RESP). Atom type and parameters for inhibitor were retrieved from *gaff*. The **PLP** cofactor was simulated in its neutral state as

previously reported, the partial charges of the **PLP** were assigned using Gaussian 09, UB3LYP/6-31G* as theory level, (http://gaussian.com) and fitted with restrained electrostatic potential (RESP). Atom type and parameters for **PLP** were retrieved from *gaff*. The system was solvated using leap and the TIP3P water model.

Plain MD simulations were performed using NAMD2.10 and a relaxation protocol based on six steps. The system was initially equilibrated performing 50ns in the NPT ensemble, after that a production phase of 120 ns was performed in the NVT ensemble.

Random Accelerated Molecular Dynamics simulations (RAMD). For the *St*OASS-A/inhibitor complex the combined RAMD-MD simulations scheme was applied. The starting configuration was represented by the complex generated after the 120 ns of plain MD simulations, the constant force was applied on all the ligand heavy atoms and ten independent RAMD simulations were performed. Each ligand unbinding pathway was drawn by tracing the center of mass of the ligand heavy atoms using VMD1.9.2. The funnel-restrained potential was applied so as to include the most probable unbinding route.

Funnel-metadynamics. The starting configuration for FM was represented by the last frame of the 120ns of the production phase. PLUMED1.3 plugin was used to run metadynamics calculations. Since the funnel-restrained potential is fixed in the space, the *St*OASS-A diffusion was avoided by imposing positional restrains on seven Cα atoms (Ala29, Ile44, Glu153, Val170, Val202, Val246, Ile297). The bias was added on a distance (CV_1) and dihedral angle (CV_2). For CV_1 and CV_2 Gaussian widths of 0.05 Å and 0.09 rad were respectively applied. The Gaussian deposition frequency of 1 Kcal mol^{-1} every 2 ps was initially applied, and gradually decreased on the basis of the adaptive bias with a ΔT of 2700 K. During FM simulations, an upper limit of

31 Å and a lower limit of -3 Å were imposed along the funnel *z* axis, so as to avoid ligand exit from the funnel-restrained potential. Trajectories were analysed with VMD1.9.2.

Absolute binding free energy. In FM simulations when the ligand is inside the cone portion of the restraint potential, no external potential is applied, and the system works under the standard well-tempered metadynamics framework. In this way, the potential does not affect the exploration of the enzyme active site by the ligand. When the ligand is in the unbound state $z > z_{cc}$ a cylindrical restraint potential is applied. Using this protocol the binding constant K_b in presence of the restraint is given by

$$K_b = \pi R_{cyl}^2 \int_{site} dz e^{-\beta[W_{(z)} - W_{ref}]}$$

[**1**]

where πR_{cyl}^2 is the surface of the cylinder used as restraint potential while the potential $W_{(z)}$ and its value in the unbound state, W_{ref} can be obtained from the PMF (Potential Mean Force) obtained from FM calculation. $\beta = (k_b T)^{-1}$ is constant, where k_b is the Boltzman constant and T the temperature of the system. K_b and ΔG_b^0 are directly related through the formula reported below:

$$\Delta G_b^0 = -\frac{1}{\beta} \ln (C^0 K_b)$$

[**2**]

where ΔG_b^0 is the protein-ligand binding free energy, K_b the binding constant and C^0 = 1/1660 $Å^{-3}$ is the standard concentration 1M. As reported in ref. [17] using eq. 1 in FM simulation eq. 2 can be rearranged

$$\Delta G_b^0 = \Delta G - \frac{1}{\beta} ln\left(\pi R_{cyl}^2 C^0\right)$$

[**3**]

$$\Delta G^0 = -RTlnK_{eq}$$

[**4**]

ΔG is the free energy difference between the bound and unbound states, and the absolute protein-ligand binding free energy (ΔG_b^0) is equal to ΔG minus the analytical correction in eq. 3. ΔG^0 was derived from eq. 4 using *RT*=0.57

The reweighting algorithm. To identify the main ligand binding conformations falling into a minima of ≃ 2 kcal/mol we applied a recently developed reweighting procedure. This method allows the reconstruction of the FES using CVs different from those biased during the metadynamics simulations. Once the metadynamics simulation is converged, using the newly computed probability distribution, the FES can be reconstructed as a function of the newly selected CVs. The projection along the main *z* axis of the funnel and the distance from that axis were used as new CVs.

STDc. STDc is an in-house built script able to calculate the STD/G.E.M profile for a given ligand-target complex and to compare it with the experimental one. It is not a standalone script and it works in conjunction with *cpptraj*, *catdcd* and *plumed.*

In the first step a MD trajectory is clustered using cpptraj and user defined parameters. In our case the average-linkage cluster algorithm with a R.M.S.D. cut-off of 1 Å (calculated on the ligand heavy atoms and the Cα atoms of the *St*OASS-A small domain and the flexible loop defined by 215-240 residues)

were used. Cpptraj turns out with representative structures of each cluster obtained. Subsequently, every representative structures generated at the previous step is processed by plumed. For each ligand hydrogen atom the contact with the protein environment are estimated by using eq. 4.

$$s = \sum_j \frac{1-\left(\frac{d_j}{r_0}\right)^n}{1-\left(\frac{d_j}{r_0}\right)^m}$$

[4]

Where n=6, m=12, r_0=3.0 were used. A list, reporting each ligand hydrogen atom with the corresponding total sum of contacts, is then stored and the values are normalized for the hydrogen atom with the highest number of contacts (the ligand proton atom closest to the protein atoms). For each hydrogen atom the R.M.S.E value is calculated with respect to the corresponding experimental value and the representative structures are ranked on the basis of their average R.M.S.E. Finally, STDc turns out with the representative structure having the lowest average R.M.S.E. and with an ensemble of representative structures extrapolated by means of a R.M.S.E. cut-off defined by the users. The ensemble of structures is then used to project a surface representation of the protein binding site where the ligands establishes protein contacts that mostly resemble the experimental STD/G.E.M. profile.

8. Conclusion

The emergence of multidrug resistant (MDR) bacteria across the world is threatening the treatment of common infections and minor injuries both in the community and hospitals.

Antibacterial drug discovery programs haven't been very successful: HTS antibacterial drug discovery programs find few progressable leads to new biochemically validated targets which may be a result of the poor representation, in corporate screening collections, of compounds displaying the molecular properties of antibacterials. Target-based antibacterial drug discovery programs are also very demanding since there is a lack of understanding of the cell permeation rules, therefore render an inhibitor of a purified enzyme into a compound with whole cell activity is a common point of attrition. [97]

De novo cysteine biosynthetic machinery, which is exclusive in prokaryotes, has been associated with the growth, survival and pathogenicity of several bacterial species. Therefore, inhibition of the cysteine synthase complex, the result of the association between O-acetylserine sulfhydrylase (OASS) and serine acetyltransferase (SAT) enzymes, may provide a new therapeutically relevant target against MDR strains. [23] - [25]

The scope of this thesis was to investigate the reason why a nanomolar inhibitor of OASS wasn't able to inhibit bacterial growth in a medium without cysteine, having in mind that mutations in this enzyme result in cysteine auxotrophy. Then, depending of the obtained results the structure of the hit compound should be modified in order to overcome its poor *in vitro* activity. In addition and concerning the regulation of cysteine biosynthesis in bacteria, SAT is the first and rate-limiting step of the biochemical pathway, therefore, it was also the purpose of this work to identify SAT inhibitors.

Permeability emerged as the main reason for the poor *in vitro* activity of the previously identified OASS inhibitor. Thus, the structure of the hit was

modified using medicinal chemistry strategies in order to change the overall physico-chemical properties of the molecule. A scaffold hopping was also performed in order to try to identify a new lead. Funnel-metadynamics and STD NMR were also employed in order to expand the series through the study of the close conformation of the enzyme and in the end a catechol moiety was introduced in the structure of the previously identified hit in order to try to use a trojan horse strategy to promote uptake.

SAT inhibitors were identified by virtual screening of both the in house library and three commercial focused libraries.

As a result of our medicinal chemistry campaign to obtain compounds with different physico-chemical properties of the original hit, nanomolar enzyme binders were identified but in the end none of new synthesized molecules was able to cross Gram negative cell wall. Nevertheless, several OASS inhibitors with different physico-chemical properties were synthesized and they can be used to study permeability in bacteria to obtain a compound with whole cell activity.

Scaffold hopping allowed the identification of a fragment with better pharmacological properties than the original hit. This way, after derivatization new OASS inhibitors can be identified.

Study of the close conformation of the enzyme by employing funnel metadynamics combined with STD NMR allowed the identification of a new pocket that faces the solvent and presents high tolerability towards lipophilic and hydrophilic groups. This way, expansion of the series towards compounds with very different physico-chemical properties can be performed.

The result of inclusion of a siderophore in the parent compound is still under investigation.

Virtual screening of the in house library to obtain the first StSAT inhibitors resulted in the identification of a low a micromolar enzyme binder that once again wasn't able to cross Gram negative cell wall.

Virtual screening of the three commercial focused libraries afforded a compound with whole cell activity that is currently object of study to validate SAT inhibition as a source of antibacterial enhancers.

Through the identification of small molecule inhibitors and the proper conditions to evaluate OASS and SAT inhibition in bacteria, the first steps to validate cysteine biosynthesis inhibition as a new source of antibacterial enhancers are established.

References

[1] R. I. Aminov, “A brief history of the antibiotic era: Lessons learned and challenges for the future,” *Front. Microbiol.*, vol. 1, no. DEC, pp. 1–7, 2010.

[2] S. B. Singh, “Confronting the challenges of discovery of novel antibacterial agents,” *Bioorg. Med. Chem. Lett.*, vol. 24, no. 16, pp. 3683–3689, 2014.

[3] N. C. Lloyd, H. W. Morgan, B. K. Nicholson, and R. S. Ronimus, “The composition of Ehrlich’s Salvarsan: Resolution of a century-old debate,” *Angew. Chemie - Int. Ed.*, vol. 44, no. 6, pp. 941–944, 2005.

[4] K. Reder-Christ and G. Bendas, “Biosensor applications in the field of antibiotic research-a review of recent developments,” *Sensors*, vol. 11, no. 10, pp. 9450–9466, 2011.

[5] S. J. Projan and D. M. Shlaes, “Antibacterial drug discovery: is it all downhill from here?,” *Clin. Microbiol. Infect.*, vol. 10 Suppl 4, no. s4, pp. 18–22, 2004.

[6] K. Lewis, “Platforms for antibiotic discovery,” *Nat. Rev. Drug Discov.*, vol. 12, no. 5, pp. 371–387, 2013.

[7] G. Kaufman, “Antibiotics: mode of action and mechanisms of resistance,” *Nurs. Stand.*, vol. 25, no. 42, pp. 49–55, 2011.

[8] K. M. G. O’Connell, J. T. Hodgkinson, H. F. Sore, M. Welch, G. P. C. Salmond, and D. R. Spring, “Combating multidrug-resistant bacteria: Current strategies for the discovery of novel antibacterials,” *Angew. Chemie - Int. Ed.*, vol. 52, no. 41, pp. 10706–10733, 2013.

[9] J. M. A. Blair, M. A. Webber, A. J. Baylay, D. O. Ogbolu, and L. J. V Piddock, “Molecular mechanisms of antibiotic resistance,” *Nat. Rev. Microbiol.*, vol. 13, no. 1, pp. 42–51, 2015.

[10] E. D. Brown and G. D. Wright, “Antibacterial drug discovery in the resistance era,” *Nature*, vol. 529, no. 7586, pp. 336–343, 2016.

[11] C. L. Ventola, “The antibiotic resistance crisis: part 1: causes and threats.,” *P T A peer-reviewed J. Formul. Manag.*, vol. 40, no. 4, pp. 277–83, 2015.

[12] M. N. Gwynn, A. Portnoy, S. F. Rittenhouse, and D. J. Payne, “Challenges of antibacterial discovery revisited,” *Ann. N. Y. Acad. Sci.*, vol. 1213, no. 1, pp. 5–19, 2010.

[13] J. M. Munita, C. A. Arias, A. R. Unit, and A. De Santiago, “Mechanisms of Antibiotic Resistance,” *Microbiol Spectr.*, vol. 4, no. 2, pp. 1–37, 2016.

[14] P. L. Taylor and G. D. Wright, “Novel approaches to discovery of antibacterial agents.,” *Anim. Health Res. Rev.*, vol. 9, no. 2, pp. 237–246, 2008.

[15] K. et al. Bush, “Tackling Antibiotic Resistance in Nepal,” *Searo*, vol. 9, no. 12, pp. 894–896, 2017.

[16] The Pew Charitable Trusts, “Antibiotics Currently in Clinical Development,” *Antibiot. Resist. Proj.*, no. September, pp. 1–7, 2014.

[17] A. Mullard, “Preclinical antibiotic pipeline gets a pick-me-up,” *Nat. Rev. Drug Discov.*, vol. 16, no. 11, pp. 741–742, 2017.

[18] R. J. Worthington and C. Melander, “NIH Public Access,” *Trends Biotechnol.*, vol. 31, no. 3, pp. 177–184, 2014.

[19] M. N. Alekshun and S. B. Levy, “Targeting virulence to prevent infection: To kill or not to kill?,” *Drug Discov. Today Ther. Strateg.*, vol. 1, no. 4, pp. 483–489, 2004.

[20] M. S. Butler and M. A. Cooper, “Screening Strategies to Identify New Antibiotics,” *Curr. Drug Targets*, vol. 13, no. 3, pp. 373–387, 2012.

[21] D. Becker *et al.*, “Robust Salmonella metabolism limits possibilities for new antimicrobials,” *Nature*, vol. 440, no. 7082, pp. 303–307, 2006.

[22] E. Salsi *et al.*, “Design of O-acetylserine sulfhydrylase inhibitors by mimicking nature,” *J. Med. Chem.*, vol. 53, no. 1, pp. 345–356, 2010.

[23] B. Campanini *et al.*, “Inhibitors of the Sulfur Assimilation Pathway in Bacterial Pathogens as Enhancers of Antibiotic Therapy,” *Curr. Med. Chem.*, vol. 22, pp. 187–213, 2015.

[24] A. L. Tumbull *et al.*, “L -Cysteine is required for induced antibiotic resistance in actively swarming Salmonella enterica serovar Typhimurium,” *Microbiology*, vol. 154, no. 11, pp. 3410–3419, 2008.

[25] A. L. Turnbull and M. G. Surette, “Cysteine biosynthesis, oxidative stress and antibiotic resistance in Salmonella typhimurium,” *Res. Microbiol.*, vol. 161, no. 8, pp. 643–650, 2010.

[26] F. Spyrakis *et al.*, “Fine tuning of the active site modulates specificity in the interaction of O-acetylserine sulfhydrylase isozymes with serine acetyltransferase,” *Biochim. Biophys. Acta - Proteins Proteomics*, vol. 1834, no. 1, pp. 169–181, 2013.

[27] S. K. Inoue K, Noji M, K. Inoue, M. Noji, and K. Saito, “Determination of the sites required for the allosteric inhibition of serine acetyltransferase by L-cysteine in plants,” *Eur. J. Biochem.*, vol. 266, no. 1, pp. 220–227, 1999.

[28] A. M. Francesca Spyrakis , Ratna Singh , Pietro Cozzini, Barbara Campanini , Enea Salsi, Paolo Felici, Samanta Raboni, Paolo Benedetti, Gabriele Cruciani, Glen E. Kellogg, Paul F. Cook *et al.*, “Isozyme-Specific Ligands for O-acetylserine sulfhydrylase, a Novel Antibiotic Target,” *PLoS One*, vol. 8, no. 10, 2013.

[29] N. M. Kredich and G. M. Tomkins, “ENZYMOLOGY : The Enzymic Synthesis of l-Cysteine in Escherichia coli and Salmonella typhimurium and Enzymic Synthesis of L-Cysteine Salmonella typhimurium in Escherichia,” vol. 241, no. 21, pp. 4955–4966, 1966.

[30] K. N. Maclean *et al.*, “Cystathionine protects against endoplasmic reticulum stress-induced lipid accumulation, tissue injury, and apoptotic cell death,” *J. Biol. Chem.*, vol. 287, no. 38, pp. 31994–

32005, 2012.

[31] C.-H. Tai, P. Burkhard, D. Gani, T. Jenn, C. Johnson, and P. F. Cook, “Characterization of the Allosteric Anion-Binding Site of O -Acetylserine Sulfhydrylase †,” *Biochemistry*, vol. 40, no. 25, pp. 7446–7452, 2001.

[32] L. J. Foote and M. Danuta, “Studies on the Mechanism of Inhibition typhimurium of Salmonella,” vol. 250, no. 18, pp. 7324–7331, 1975.

[33] R. Guan, S. L. Roderick, B. Huang, and P. F. Cook, “Roles of histidines 154 and 189 and aspartate 139 in the active site of serine acetyltransferase from Haemophilus influenzae,” vol. 47, no. 24, pp. 6322–6328, 2010.

[34] C. M. Johnson, B. Huang, S. L. Roderick, and P. F. Cook, “Kinetic mechanism of the serine acetyltransferase from Haemophilus influenzae,” *Arch. Biochem. Biophys.*, vol. 429, no. 2, pp. 115–122, 2004.

[35] L. S. Leu and P. F. Cook, “Kinetic Mechanism of Serine Transacetylase from Salmonella typhimurium,” *Biochemistry*, vol. 33, no. 9, pp. 2667–2671, 1994.

[36] V. E. Pye, A. P. Tingey, R. L. Robson, P. C. E. Moody, L. Robert, and P. C. E. Moody, “The structure and mechanism of serine acetyltransferase from Escherichia coli,” *J. Biol. Chem.*, vol. 279, no. 39, pp. 40729–40736, 2004.

[37] V. J. Hindson and W. V. Shaw, “Random-order ternary complex reaction mechanism of serine acetyltransferase from *Escherichia coli*,” *Biochemistry*, vol. 42, no. 10, pp. 3113–3119, 2003.

[38] D. P. Bhave, W. B. Muse Iii, and K. S. Carroll, “Drug Targets in Mycobacterial Sulfur Metabolism,” *Infect Disord Drug Targets*, vol. 7, no. 2, 2007.

[39] D. Schnappinger *et al.*, “Transcriptional Adaptation of *Mycobacterium*

tuberculosis within Macrophages," *J. Exp. Med.*, vol. 198, no. 5, pp. 693–704, 2003.

[40] P. Fontán, V. Aris, S. Ghanny, P. Soteropoulos, and I. Smith, "Global transcriptional profile of Mycobacterium tuberculosis during THP-1 human macrophage infection," *Infect. Immun.*, vol. 76, no. 2, pp. 717–725, 2008.

[41] T. Wang and T. S. Leyh, "Three-stage assembly of the cysteine synthase complex from Escherichia coli," *J. Biol. Chem.*, vol. 287, no. 6, pp. 4360–4367, 2012.

[42] R. Schnell and G. Schneider, "Structural enzymology of sulphur metabolism in Mycobacterium tuberculosis," *Biochem. Biophys. Res. Commun.*, vol. 396, no. 1, pp. 33–38, 2010.

[43] S. K. Hatzios and C. R. Bertozzi, "The regulation of sulfur metabolism in mycobacterium tuberculosis," *PLoS Pathog.*, vol. 7, no. 7, pp. 1–8, 2011.

[44] L. Amori *et al.*, "Design and synthesis of trans-2-substituted-cyclopropane-1-carboxylic acids as the first non-natural small molecule inhibitors of O-acetylserine sulfhydrylase," *Medchemcomm*, vol. 3, no. 9, pp. 1111–1116, 2012.

[45] M. Pieroni *et al.*, "Rational Design, Synthesis, and Preliminary Structure-Activity Relationships of α-Substituted-2-Phenylcyclopropane Carboxylic Acids as Inhibitors of Salmonella typhimurium O-Acetylserine Sulfhydrylase," *J. Med. Chem.*, 2016.

[46] L. A. Nguyen, H. He, and C. Pham-Huy, "Chiral drugs: an overview," *Int. J. Biomed. Sci.*, vol. 2, no. 2, pp. 85–100, 2006.

[47] E. Guédon and I. Matin-Verstraete, "The branched-chain amino acids," *Microbiol Monogr*, vol. 5, pp. 196–218, 2006.

[48] M. F. Hullo *et al.*, "Conversion of methionine to cysteine in Bacillus subtilis and its regulation," *J. Bacteriol.*, vol. 189, no. 1, pp. 187–197,

2007.

[49] S. M. Agarwal, R. Jain, A. Bhattacharya, and A. Azam, “Inhibitors of Escherichia coli serine acetyltransferase block proliferation of Entamoeba histolytica trophozoites,” *Int. J. Parasitol.*, vol. 38, no. 2, pp. 137–141, 2008.

[50] M. F. Richter *et al.*, “Predictive compound accumulation rules yield a broad-spectrum antibiotic,” *Nature*, 2017.

[51] L. Amaral, A. Martins, G. Spengler, and J. Molnar, “Efflux pumps of Gram-negative bacteria: What they do, how they do it, with what and how to deal with them,” *Front. Pharmacol.*, vol. 4 JAN, no. January, pp. 1–11, 2014.

[52] J. Bedard, S. Wong, and L. E. Bryan, “Accumulation of enoxacin by Escherichia coli and Bacillus subtilis,” *Antimicrob. Agents Chemother.*, vol. 31, no. 9, pp. 1348–1354, 1987.

[53] L. J. V Piddock, K. J. Williams, and V. Ricci, “Accumulation of rifampicin by Mycobacterium aurum, Mycobacterium smegmatis and Mycobacterium tuberculosis,” *J. Antimicrob. Chemother.*, pp. 159–165, 2000.

[54] J. M. Zenilman, M. H. Miller, and L. J. Mandel, “In vitro studies simultaneously examining effect of oxacillin on uptake of radiolabeled streptomycin and on associated bacterial lethality in Staphylococcus aureus,” *Antimicrob. Agents Chemother.*, vol. 30, no. 6, pp. 877–882, 1986.

[55] K. Hirai, H. Aoyama, T. Irikura, S. Iyobe, and S. Mitsuhashi, “Differences in susceptibility to quinolones of outer membrane mutants of Salmonella typhimurium and Escherichia coli . Differences in Susceptibility to Quinolones of Outer Membrane Mutants of Salmonella typhimurium and Escherichia coli,” *Antimicrob. Agents Chemother.*, vol. 29, no. 3, pp. 535–538, 1986.

[56] K. Hirai, S. Suzue, T. Irikura, S. Iyobe, and S. Mitsuhashi, “Mutations producing resistance to norfloxacin in Pseudomonas aeruginosa,” *Antimicrob. Agents Chemother.*, vol. 31, no. 4, pp. 582–586, 1987.

[57] B. Joos, B. Ledergerber, M. Flepp, J. D. Bettex, R. Lüthy, and W. Siegenthaler, “Comparison of high-pressure liquid chromatography and bioassay for determination of ciprofloxacin in serum and urine,” *Antimicrob. Agents Chemother.*, 1985.

[58] S. J. Morton, V. H. Shull, and J. D. Dick, “Determination of norfloxacin and ciprofloxacin concentrations in serum and urine by high-pressure liquid chromatography.,” *Antimicrob. Agents Chemother.*, vol. 30, no. 2, pp. 325–327, 1986.

[59] S. Kaščáková, L. Maigre, J. Chevalier, M. Réfrégiers, and J. M. Pagès, “Antibiotic transport in resistant bacteria: Synchrotron UV fluorescence microscopy to determine antibiotic accumulation with single cell resolution,” *PLoS One*, vol. 7, no. 6, 2012.

[60] Y. Zhou *et al.*, “Thinking outside the ‘bug’: A unique assay to measure intracellular drug penetration in Gram-negative bacteria,” *Anal. Chem.*, vol. 87, no. 7, pp. 3579–3584, 2015.

[61] M. Vaara, “Agents that increase the permeability of the outer membrane.,” *Microbiol. Rev.*, vol. 56, no. 3, pp. 395–411, 1992.

[62] P. Viljanen and M. Vaara, “Susceptibility of Gram-Negative Bacteria to Polymyxin B Nonapeptide,” *Antimicrob. Agents Chemother.*, vol. 25, no. 6, pp. 701–705, 1984.

[63] P. A. Lambert, “Cellular impermeability and uptake of biocides and antibiotics in Gram-positive bacteria and mycobacteria,” *J. Appl. Microbiol.*, vol. 92, no. s1, p. 46S–54S, 2002.

[64] J.-Y. Denyer, S.P. and Maillard, “Cellular impermeability and uptake of biocides and antibiotics in Gram-positive bacteria and mycobacteria,” *J. Appl. Microbiol.*, vol. 92, no. s1, p. 35S–45S, 2002.

[65] H. Nikaido, “Molecular basis of bacterial outer membrane permeability revisited.,” *Microbiol. Mol. Biol. Rev.*, vol. 67, no. 4, pp. 593–656, 2003.

[66] A. P. Zavascki, L. Z. Goldani, J. Li, and R. L. Nation, “Polymyxin B for the treatment of multidrug-resistant pathogens: A critical review,” *J. Antimicrob. Chemother.*, vol. 60, no. 6, pp. 1206–1215, 2007.

[67] D. G. Brown, T. L. May-Dracka, M. M. Gagnon, and R. Tommasi, “Trends and Exceptions of Physical Properties on Antibacterial Activity for Gram-Positive and Gram-Negative Pathogens,” *J. Med. Chem.*, 2014.

[68] R. O. Shea and H. E. Moser, “Physicochemical Properties of Antibacterial Compounds : Implications for Drug Discovery Perspecti V e Physicochemical Properties of Antibacterial Compounds : Implications for Drug Discovery,” vol. 51, no. 10, 2008.

[69] D. Benedetto Tiz, D. Kikelj, and N. Zidar, “Overcoming problems of poor drug penetration into bacteria: challenges and strategies for medicinal chemists,” *Expert Opin. Drug Discov.*, vol. 0441, no. 6, pp. 1–11, 2018.

[70] J. Fu, K. Cheng, Z. ming Zhang, R. qin Fang, and H. liang Zhu, “Synthesis, structure and structure-activity relationship analysis of caffeic acid amides as potential antimicrobials,” *Eur. J. Med. Chem.*, vol. 45, no. 6, pp. 2638–2643, Jun. 2010.

[71] A. Huczyński, J. Janczak, J. Stefańska, M. Antoszczak, and B. Brzezinski, “Synthesis and antimicrobial activity of amide derivatives of polyether antibiotic-salinomycin.,” *Bioorg. Med. Chem. Lett.*, vol. 22, no. 14, pp. 4697–4702, Jul. 2012.

[72] G. H. Hitchings, *Inhibition of Folate Metabolism in Chemotherapy: The Origins and Uses of Co-trimoxazole*. Berlin Heidelberg: Springer-Verlag, 1983.

[73] C. D. Bray and F. Minicone, “Stereocontrolled synthesis of quaternary cyclopropyl esters ,” pp. 5867–5869, 2010.

[74] J. Magalhães *et al.*, “Integration of Enhanced Sampling Methods with Saturation Transfer Difference Experiments to Identify Protein Druggable Pockets,” *J. Chem. Inf. Model.*, vol. 58, no. 3, pp. 710–723, 2018.

[75] B. Carlo, M. H. Donna, and L. Amos, B. Smith, “Carboxylic Acid (Bio)Isosteres in Drug Design,” *ChemMedChem*, vol. 8, no. 3, pp. 385–395, 2013.

[76] P. Lassalas *et al.*, “Structure Property Relationships of Carboxylic Acid Isosteres,” *J. Med. Chem.*, vol. 59, no. 7, pp. 3183–3203, 2016.

[77] G. Annunziato *et al.*, “Cyclopropane-1,2-dicarboxylic acids as new tools for the biophysical investigation of O-acetylserine sulfhydrylases by fluorimetric methods and saturation transfer difference (STD) NMR,” *J. Enzyme Inhib. Med. Chem.*, vol. 31, no. September, pp. 78–87, 2016.

[78] *Methods for Dilution Antimicrobial Susceptibility Tests for Bacteria That Grow Aerobically ; Approved Standard — Ninth Edition*, vol. 32, no. 2. 2012.

[79] R. O. Shea, H. E. Moser, R. O’Shea, and H. E. Moser, “Perspecti V e Physicochemical Properties of Antibacterial Compounds : Implications for Drug Discovery,” *J. Med. Chem.*, vol. 51, no. 10, 2008.

[80] S. Andrej, Hanzlowsky , Blanka, Jelenčič, Simon, Rečnik, Jurij, Svete, Amalija, Golobič , Branko, “Regioselective synthesis of ethyl pyrazolecarboxylates from ethyl 3-[(dimethylamino)methylidene]pyruvate and diethyl 3-[(dimethylamino)methylidene]-2-oxosuccinate. Isolation of ethyl 4,5-dihydro-1-heteroaryl-5-hydroxy-1H-pyrazole-5-carboxylates as stable,” *J. Heterocycl. Chem.*, vol. 40, no. 3, pp. 487–498, 2009.

[81] A. Bruno, L. Amori, and G. Costantino, “Computational insights into the mechanism of inhibition of OASS-A by a small molecule inhibitor,” *Mol. Inform.*, vol. 32, no. 5–6, pp. 447–457, 2013.

[82] S. Schultes, C. De Graaf, E. E. J. Haaksma, I. J. P. De Esch, R. Leurs, and O. Krämer, “Ligand efficiency as a guide in fragment hit selection and optimization,” *Drug Discov. Today Technol.*, vol. 7, no. 3, pp. 157–162, 2010.

[83] A. L. Hopkins, G. M. Keserü, P. D. Leeson, D. C. Rees, and C. H. Reynolds, “The role of ligand efficiency metrics in drug discovery,” *Nat. Rev. Drug Discov.*, vol. 13, no. 2, pp. 105–121, 2014.

[84] B. C. Doak, R. S. Norton, and M. J. Scanlon, “The ways and means of fragment-based drug design,” *Pharmacol. Ther.*, vol. S0163-7258, no. 16, pp. 30123–1, 2016.

[85] F. Scheraga, Harold A, Ni, “Use of the Transferred Nuclear Overhauser Effect To Determine the Conformations of Ligands Bound to Proteins,” *Acc. Chem. Res.*, vol. 27, no. 9, pp. 4017–4018, 1994.

[86] V. Limongelli, M. Bonomi, and M. Parrinello, “Funnel metadynamics as accurate binding free-energy method,” *Proc. Natl. Acad. Sci.*, vol. 110, no. 16, pp. 6358–6363, 2013.

[87] N. M. Maier, P. Franco, and W. Lindner, *Separation of enantiomers : needs , challenges , perspectives q*, vol. 906. 2001.

[88] C. Roussel, P. Piras, and I. Heitmann, “An approach to discriminating 25 commercial chiral stationary phases from structural data sets extracted from a molecular database,” *Biomed. Chromatogr.*, vol. 11, no. 5, pp. 311–316, 1997.

[89] V. Andrushko and N. Andrushko, “Principles, Concepts and Strategies of Stereoselective Synthesis,” *Stereoselective Synth. Drugs Nat. Prod.*, no. OCTOBER 2013, pp. 2–44, 2013.

[90] E. Baco, F. Hoegy, I. J. Schalk, and G. L. A. Mislin, “Diphenyl-

benzo[1,3]dioxole-4-carboxylic acid pentafluorophenyl ester: A convenient catechol precursor in the synthesis of siderophore vectors suitable for antibiotic Trojan horse strategies," *Org. Biomol. Chem.*, vol. 12, no. 5, pp. 749–757, 2014.

[91] K. D. Krewulak and H. J. Vogel, "Structural biology of bacterial iron uptake," *Biochim. Biophys. Acta - Biomembr.*, vol. 1778, no. 9, pp. 1781–1804, 2008.

[92] J. Starr *et al.*, "Siderophore receptor-mediated uptake of lactivicin analogues in gram-negative bacteria," *J. Med. Chem.*, vol. 57, no. 9, pp. 3845–3855, 2014.

[93] U. Bilitewski *et al.*, "Chemical and Biological Aspects of Nutritional Immunity—Perspectives for New Anti-Infectives that Target Iron Uptake Systems," *Angew. Chemie - Int. Ed.*, vol. 56, no. 46, pp. 14360–14382, 2017.

[94] C. Carvalho and FernandesPedro, "Siderophores as 'Trojan Horses': tackling multidrug resistance?," *Front. Microbiol.*, vol. 5, pp. 1–3, 2014.

[95] E. Azzali *et al.*, "Substituted N-Phenyl-5-(2-(phenylamino)thiazol-4-yl)isoxazole-3-carboxamides Are Valuable Antitubercular Candidates that Evade Innate Efflux Machinery," *J. Med. Chem.*, vol. 60, no. 16, pp. 7108–7122, 2017.

[96] R. H. Wiley, "The chemistry of oxazoles," *Chem. Rev.*, vol. 37, no. 3, pp. 401–442, 1945.

[97] R. Tommasi, D. G. Brown, G. K. Walkup, J. I. Manchester, and A. A. Miller, "ESKAPEing the labyrinth of antibacterial discovery," *Nat. Rev. Drug Discov.*, vol. 14, no. 8, pp. 529–542, 2015.

[98] D. G. Brown, T. L. May-Dracka, M. M. Gagnon, and R. Tommasi, "Trends and Exceptions of Physical Properties on Antibacterial Activity for Gram Positive and Gram Negative Pathogens.," *J. Med. Chem.*,

2014.

[99] Æ. A. Lo, “ChemGPS-NP Web : chemical space navigation online,” pp. 253–259, 2009.

[100] J. Larsson, J. Gottfries, S. Muresan, and A. Backlund, “ChemGPS-NP: Tuned for Navigation in Biologically Relevant Chemical Space,” pp. 789–794, 2007.

[101] J. Y. Yeon, S. J. Yoo, H. Takagi, and H. A. Kang, “A Novel Mitochondrial Serine O - Acetyltransferase , OpSAT1 , Plays a Critical Role in Sulfur Metabolism in the Thermotolerant Methylotrophic Yeast Ogataea parapolymorpha,” no. January, pp. 1–12, 2018.

[102] H. Takagi, “Role of Saccharomyces cerevisiae serine O - acetyltransferase in cysteine biosynthesis,” vol. 218, 2003.

[103] J. R. Winther and C. Thorpe, “Quantification of thiols and disul fides,” *Biochim. Biophys. Acta*, vol. 1840, pp. 838–846, 2014.

[104] J. Inglese, C. E. Shamu, and R. K. Guy, “C O M M E N TA RY Reporting data from high-throughput screening of small-molecule libraries,” vol. 3, no. 8, pp. 438–441, 2007.

[105] P. W. Iversen, B. J. Eastwood, G. S. Sittampalam, and K. L. Cox, “A Comparison of Assay Performance Measures in Screening Assays: Signal Window , Z ’ Factor , and Assay Variability Ratio,” pp. 247–252, 2006.

[106] R. Benoni *et al.*, “Activation of an anti-bacterial toxin by the biosynthetic enzyme CysK: Mechanism of binding, interaction specificity and competition with cysteine synthase,” *Sci. Rep.*, vol. 7, no. 1, pp. 1–16, 2017.

[107] M. K. Gaitonde, “A spectrophotometric method for the direct determination of cysteine in the presence of other naturally occurring amino acids.,” *Biochem. J.*, vol. 104, no. 2, pp. 627–633, 1967.

[108] Y. Cheng and W. H. Prusoff, “Relationship between the inhibition

constant (K1) and the concentration of inhibitor which causes 50 per cent inhibition (I50) of an enzymatic reaction," *Biochem. Pharmacol.*, vol. 22, no. 23, pp. 3099–3108, 1973.